

AUS DEM HELMHOLTZ ZENTRUM MÜNCHEN

VORSTAND: PROF. DR. W. HAMMERSCHMIDT

# THE CONTRIBUTION OF GAMMA-HERPES VIRUSES ON THE DEVELOPMENT OF CD30+ B CELL LYMPHOMAS: RESEARCH AND INVESTIGATION IN A MOUSE MODEL

Dissertation

zum Erwerb des Doktorgrades der Medizin

an der Medizinischen Fakultät der

Ludwig-Maximilians-Universität München

vorgelegt von

ZAKIR HASSAN CHEW

aus

SINGAPUR

Jahr

2023

MIT GENEHMIGUNG DER MEDIZINISCHEN FAKULTÄT  
DER UNIVERSITÄT MÜNCHEN

Berichterstatter:	Priv. Doz. Dr. Ursula Zimber-Strobl (LHI/CPC, Helmholtz Zentrum München)
	Prof. Dr. Heiko. Adler (Institut für Asthma- und Allergieprävention, Helmholtz Zentrum München)
Mitberichterstatter:	Prof. Dr. Tobias Herold
	Prof. Dr. Ralf Schmidmaier
Dekan:	Prof. Dr. med. Thomas Gudermann
Tag der mündlichen Prüfung:	30.03.2023

Die Dissertation wurde im Jahr 2023 bei der Ludwig-Maximilians-Universität München eingereicht.

## ABSTRACT

EBV and KSHV are two gammaherpesviruses that are known to be highly associated with CD30-positive lymphomas, such as Hodgkin lymphomas. Whether deregulated CD30-signaling cooperates with herpes viral infections in tumorigenesis is not well understood. Thus, the aim of the thesis was to establish a system allowing for the investigation of the interplay between a dysregulated CD30 expression and EBV infection in lymphomagenesis in a mouse model. EBV does not infect murine B cells, thus, we used the murine gammaherpesvirus 68 (MHV68) as a tool to propagate infection in mice. To make MHV68 much more similar to EBV, the EBV protein LMP2a was inserted into the MHV68. To this end, LMP2a was cloned into MHV68 to obtain MHV68-LMP2a, enabling the analysis of the effects of LMP2a in vivo after infection of mice. Thus, the potential contribution of the EBV protein LMP2a to lymphomagenesis could be investigated in mice. To induce the dysregulated constitutive CD30 expression in B cells upon MHV68 infection, LMP1/CD30 $\gamma$ 1cre (LC30) mice were used. These mice contain a LMP1/CD30 fusion protein in the R26 locus together with a loxP flanked stop cassette. B cells responding to the MHV68 infection express Cre, resulting in deletion of the stop-cassette followed by expression of the LMP1/CD30 fusion protein (LC30) together with the reporter hCD2. After generating a MHV68-LMP2a, the recombinant virus was first tested for fitness in wild-type C57BL/6 mice, in comparison to wild-type MHV68. MHV68-LMP2a was similar to wild-type MHV68 regarding lytic replication in the lung but established less latency in the spleen when compared to wild-type MHV68. Next, MHV68-LMP2a was used to infect LMP1/CD30 $\gamma$ 1cre (LC30) mice. As control virus, MHV68-NGF-R was used, which expresses a truncated Nerve-growth factor receptor (NGF-R) instead of LMP2a. As control mice, we infected R26 CAR $\gamma$ 1cre mice, which express the reporter gene CAR instead of LC30/hCD2. Virus infection in LC30 mice led to a higher percentage of reporter positive B cells when compared to control CAR mice. Moreover, two months after infection, the splenomegaly was increased in LC30 in comparison to control mice, suggesting an expansion of LC30 expressing B cells. From acute infections at 14 days to chronic infections of 2 months, constitutive CD30 expression forced germinal center B cells to leave the germinal center, evident from the reduced percentage of reporter positive GCB cells at 2 months post infection in CD30 mice compared to controls. Instead, more reporter positive B cells with a B1 cell phenotype and plasma cells were detected in LC30 compared to control CAR mice. The expanded reporter positive B1 cell population was detected in the spleen and in the peritoneal cavity. Currently, it is still unclear whether these reporter positive cells are derived from GC B cells. The LMP2a protein, on the other hand, did not significantly affect the phenotype and expansion of LMP1/CD30 express-

ing B cells. The only difference which we could detect between MHV68-LMP2a and MHV68-NGF-R was a slightly enhanced GC formation after infection of CAR mice. Enhanced germinal center B cell formation and proliferation by LMP2a expression could play a role in formation of lymphomas. In summary, most of the differences observed in the experiments were due to the constitutive signaling of the CD30 in LMP1/CD30 $\gamma$ 1cre when infected with the two viruses, and not to the expression of LMP2a. A potential reason for the latter might be that LMP2A is switched off during latency. Though further studies need to be conducted, the data shown here suggest that dysregulated CD30 expression, combined with gammaherpesvirus infection, might be associated with accelerated tumorigenesis. To answer the question whether infection with MHV68-LMP2a, when compared to infection with MHV68-NGFR, leads to further enhancement of lymphoma development in LMP1/CD30 $\gamma$ 1cre mice, more investigations and studies need to be done in the future.

## DAS ABSTRAKT

EBV und KSHV sind zwei Gammaherpesviren, von denen bekannt ist, dass sie stark mit CD30-positiven Lymphomen wie Hodgkin-Lymphomen assoziiert sind. Ob eine fehlregulierte CD30-Signaltransduktion mit herpesviralen Infektionen bei der Tumorentstehung zusammenwirkt, ist noch nicht vollständig verstanden. Ziel dieser Arbeit war es daher, ein System zu etablieren, mit dem das Zusammenspiel zwischen einer fehlregulierten CD30-Expression und einer EBV-Infektion bei der Lymphomagenese im Mausmodell untersucht werden kann. EBV infiziert keine Maus-B-Zellen, daher wurde das Murine Gammaherpesvirus 68 (MHV68) als Modell verwendet. Um die Rolle des EBV-Proteins LMP2a in vivo zu untersuchen, wurde LMP2a in MHV68 eingefügt. Zu diesem Zweck wurde LMP2a in MHV68 kloniert, um MHV68-LMP2a zu erhalten. Somit konnte der potenzielle Beitrag des EBV-Proteins LMP2a zur Lymphomagenese bei Mäusen untersucht werden. Um die fehlregulierte konstitutive CD30-Expression in B-Zellen nach einer MHV68-Infektion zu induzieren, wurden LMP1/CD30 $\gamma$ 1cre (LC30) Mäuse verwendet. Diese Mäuse enthalten ein LMP1/CD30-Fusionsprotein im R26-Lokus zusammen mit einer loxP-flankierten Stoppkassette. B-Zellen, die auf die MHV68-Infektion reagieren, exprimieren Cre, was zur Deletion der Stoppkassette und damit zur Expression des LMP1/CD30-Fusionsproteins (LC30) sowie des Reporters hCD2 führt. Nach der Generierung eines MHV68-LMP2a wurde das rekombinante Virus zunächst in Wildtyp-C57BL/6-Mäusen auf seine Fitness im Vergleich zu Wildtyp-MHV68 getestet. MHV68-LMP2a ähnelte dem Wildtyp-MHV68 in Bezug auf die lytische Replikation in der Lunge, führte jedoch im Vergleich zum Wildtyp-MHV68 zu einer geringeren Latenz in der Milz. Als nächstes wurde MHV68-LMP2a verwendet, um LMP1/CD30 $\gamma$ 1cre (LC30) Mäuse zu infizieren. Als Kontrollvirus wurde MHV68-NGFR verwendet, das anstelle von LMP2a einen verkürzten Nervenwachstumsfaktor-Rezeptor (NGFR) exprimiert. Als Kontrollmäuse infizierten wir R26-CAR $\gamma$ 1cre Mäuse, die anstelle von LC30/hCD2 das Reportergen CAR exprimieren. Die Virusinfektion bei LC30-Mäusen führte im Vergleich zu CAR-Kontrollmäusen zu einem höheren Prozentsatz an Reporter-positiven B-Zellen. Darüber hinaus war die Splenomegalie zwei Monate nach der Infektion bei LC30 im Vergleich zu Kontrollmäusen erhöht, was auf eine Expansion von LC30-exprimierenden B-Zellen schließen lässt. Innerhalb des Zeitraums von 14 Tagen (akute Phase) bis zu zwei Monaten (chronische Phase) nach Infektion führte die konstitutive CD30-Expression dazu, dass die Keimzentrums-B-Zellen das Keimzentrum verlassen, was aus dem reduzierten Prozentsatz an Reporter-positiven Keimzentrums-B-Zellen zwei Monate nach der Infektion bei CD30-Mäusen im Vergleich zu Kontrollen ersichtlich ist. Stattdessen wurden in LC30 im Vergleich zu Kontroll-CAR-Mäusen mehr Reporter-positive B-Zellen mit einem B1-Zellphänotyp

und Plasmazellen nachgewiesen. Die expandierte Reporter-positive B1-Zellpopulation wurde in der Milz und in der Peritonealhöhle nachgewiesen. Derzeit ist noch unklar, ob diese Reporter-positiven Zellen von Keimzentrums-B-Zellen abgeleitet sind. Andererseits beeinflusste das LMP2a Protein den Phänotyp und die Expansion von LMP1/CD30-exprimierenden B Zellen nicht signifikant. Der einzige Unterschied, den wir zwischen MHV68-LMP2a und MHV68-NGFR feststellen konnten, war eine leicht erhöhte Keimzentrums-Bildung nach Infektion von CAR-Mäusen. Eine verstärkte Keimzentrums-B Zellbildung und -Proliferation durch die LMP2a-Expression könnte eine Rolle bei der Entstehung von Lymphomen spielen. Zusammenfassend waren die meisten in den Experimenten beobachteten Unterschiede auf die konstitutive Signaltransduktion des CD30 in LMP1/CD30 $\gamma$ 1cre-Mäusen bei Infektion mit den beiden Viren zurückzuführen und nicht auf die Expression von LMP2a. Ein möglicher Grund für Letzteres könnte sein, dass LMP2A während der Latenzzeit ausgeschaltet wird. Obwohl weitere Studien durchgeführt werden müssen, legen die hier gezeigten Daten nahe, dass eine fehlregulierte CD30-Expression in Kombination mit einer Gammaherpesvirus-Infektion mit einer beschleunigten Tumorentstehung assoziiert sein könnte. Ob eine Infektion mit MHV68-LMP2a im Vergleich zur Infektion mit MHV68-NGFR zu einer weiteren beschleunigten Entwicklung der Lymphome bei LMP1/CD30 $\gamma$ 1cre-Mäusen führt, muss in Zukunft in weiteren Studien untersucht werden.

## ACKNOWLEDGMENTS

I am deeply grateful to all those who have played a pivotal role in my journey towards completing my doctoral thesis. This accomplishment would not have been possible without the unwavering support, guidance, and encouragement of numerous individuals and institutions.

First and foremost, I would like to express my sincere appreciation to my dissertation advisors Prof. Dr. Heiko Adler and Priv. Doz. Dr. Ursula Zimber-Strobl and their team. Their mentorship, expertise, and dedication to my research have been invaluable. I am fortunate to have had the opportunity to learn from their wisdom and guidance throughout my entire journey.

I am grateful to Helmholtz-Zentrum Munich and Ludwig Maximilian University of Munich for providing an intellectually stimulating and supportive environment for pursuing my doctoral studies. The resources, facilities, and academic community at this institution have been instrumental in the successful completion of this research.

I owe a special debt of gratitude to my friends for their unwavering belief in me. Their encouragement and moral support sustained me during the challenging phases of this journey, through the successes and failures that I experienced.

Last but certainly not least, I want to express my deepest appreciation to my family. Their patience, love, and understanding have been my rock throughout this long and arduous process.

This dissertation is a testament to the collective effort, encouragement, and support of these wonderful individuals and institutions. Thank you all for being an integral part of this significant chapter in my academic life.

## LIST OF FIGURES

1.1 **SCHEMATIC DIAGRAM SHOWING THE DIFFERENT CELL SURFACE RECEPTORS TOGETHER WITH THE CLASSICAL CANONICAL AND ALTERNATIVE NON-CANONICAL NF- $\kappa$ B SIGNALLING CASCADES.** THE PRIMARY B CELL FOLLICLES IN THE SECONDARY LYMPHOID ORGANS, FOR EXAMPLE, IN THE SPLEEN AND LYMPH NODES, BECOME ACTIVATED GERMINAL CENTERS AFTER RECEIVING ANTI-GENS AND T CELL HELP. THEY UNDERGO SHM AND CSR PRODUCING PLASMA CELLS AND MEMORY B CELLS THAT ARE ABLE TO SECRETE ANTIBODIES / IMMUNOGLOBULIN OF HIGH AFFINITY AS PART OF THE ADAPTIVE IMMUNESYSTEM TO FIGHT OFF CHRONIC INFECTIONS. DURING THE PROCESS OF CLONAL EXPANSION AND PROLIFERATION IN THE GERMINAL CENTER, NAIVE B CELLS ARE DISPLACED INTO THE MANTLE ZONE. MAJORITY OF THE MUTATIONS DURING CLONAL EXPANSION ARE DISADVANTAGEOUS FOR THE CELL CONFERRING REDUCED AFFINITIES. THESE DISADVANTAGED CELLS ARE REMOVED BY APOPTOSIS. MARGINAL ZONES WITH PREDOMINANT B CELL RICH POPULATIONS IN BETWEEN THE B CELL FOLLICLES AND T CELL AREA ARE FOUND MAINLY IN THE SPLEENS AND NOT USUALLY IN THE LYMPH NODES. (ADAPTED FROM KLEIN & DALLA-FAVERA (2008) AND KÜPPERS (2005)).

8

1.2 **SCHEMATIC DIAGRAM SHOWING THE DIFFERENT CELL SURFACE RECEPTORS TOGETHER WITH THE CLASSICAL CANONICAL AND ALTERNATIVE NON-CANONICAL NF $\kappa$ B SIGNALLING CASCADES.** ACTIVATION OF THE CANONICAL AND NON-CANONICAL PATHWAYS THROUGH ONE OF SEVERAL CELL SURFACE RECEPTORS LEADS TO EXPRESSION OF PROTEINS THAT IN TURN CONTRIBUTE TO CELL SURVIVAL, PROLIFERATION AND EITHER RESPONSES TO PROMOTE INNATE AND ADAPTIVE IMMUNITY RESPECTIVELY. BOTH THE CD30 AND CD40 CELL SURFACE RECEPTORS ARE ABLE TO ACTIVATE BOTH PATHWAYS, WHEREAS THE TCR OR BCR ACTIVATE ONLY THE CANONICAL PATHWAY. THE BAFF, ON THE OTHER HAND, ACTIVATES ONLY THE NON-CANONICAL PATHWAY. WHILE LMP2A MIMICS THAT OF THE BCR, THE LMP1 TRANSMEMBRANE PROTEIN MIMICS CD40 (ADAPTED FROM CANCRO (2009) AND JOST & JURGEN (2006)).

11

1.3 **SCHEMATIC DIAGRAM SHOWING THE TRANSMEMBRANE PROTEIN LMP2A AND THE VARIOUS SIGNALLING PATHWAYS AND CASCADES THAT IT TRIGGERS.** WHILE THE NEDD4 PATHWAYS LEAD TO SELF DEGRADATION OF THE LMP2A AND ASSOCIATED PROTEINS, THAT OF THE STAT, NF- $\kappa$ B, PI3K/AKT AND MAPK PATHWAYS ARE RESPONSIBLE FOR CELL GROWTH AND PROLIFERATION, PROMOTION OF CELL TRANSFORMATION AS WELL AS ANTI-APOPTOTIC EFFECTS ON THE CELLS. (ADAPTED FROM KNIPE & HOWLEY (2013))

13

1.4 **SCHEMATIC DIAGRAM SHOWING THE GENERATION OF LMP1/CD30 $\gamma$ 1CRE MICE.** THE LMP1/CD30 $\gamma$ 1CRE MICE CONTAIN THE CRE GENE ON THE Ig LOCUS WHILE THE LMP1/CD30 GENE ON THE R26 LOCUS. IMMUNIZATION IN THE FORM OF VIRAL INFECTION LEADS TO THE EXPRESSION OF Ig LOCUS THUS TRANSCRIBING AND EXPRESSING THE CRE RECOMBINASE. THIS WOULD IN TURN LEAD TO THE ACTIVATION AND EXPRESSION OF THE GENES ON THE R26 LOCUS AND THE SUBSEQUENT EXPRESSION OF THE LMP1/CD30 PROTEIN LEADING TO THE CONSTITUTIVE EXPRESSION OF CD30 (ADAPTED FROM CASOLA ET AL. (2006). 15

4.1 **SCHEMATIC ILLUSTRATION OF THE WESTERN BLOT SETUP FOR BLOTTING AND TRANSFER OF PROTEINS FROM THE GEL TO THE MEMBRANE.** 34

5.1 **SIMPLIFIED ILLUSTRATION OF THE PROCESS OF BAC SHUTTLE MUTAGENESIS IN *E. coli*.** THE SHUTTLE PLASMID CONTAINS THE GENE OF INTEREST (PCMV-LMP2A) THAT IS TO BE INSERTED BETWEEN THE HOMOLOGOUS GENE SEGMENTS (LIGHT BLUE RECTANGLES) INTO THE MHV68 GENOME. THE MHV68 GENOME WAS CLONED AS A BAC IN *E. coli*. IN ADDITION TO THE BAC SEQUENCE, SEVERAL OTHER SEQUENCES ARE CONTAINED IN THE BAC CASSETTE; GPT (GUANOSINE PHOSPHORIBOSYL TRANSFERASE) AND GFP (GREEN FLUORESCENT PROTEIN) FLANKED BY LOXP SEQUENCES THAT SERVE AS SITES FOR EXCISION OF THE BAC CASSETTE BY CRE RECOMBINASE LATER ON. AFTER SHUTTLE MUTAGENESIS, A RECOMBINANT BAC-MHV68 PLASMID CONTAINING THE PCMV-LMP2A GENE OF INTEREST IS CREATED. 49

5.2 **(A) PCR<sup>TM</sup>3 PLASMID CIRCULAR AND LINEARIZED.** THE PCR<sup>TM</sup>3 PLASMID IS LINEARIZED BY DIGESTION WITH BAMHI AND HINDIII. **(B) PEBNA-G-LMP2A PLASMID CIRCULAR AND LINEARIZED.** THE GENE OF INTEREST LMP2A TETR IN THE PEBNA-G-LMP2A PLASMID IS CUT OUT BY RESTRICTION ENZYMES HINDIII AND BGLII TO GIVE THE LINEAR LMP2A-TETR. THE CIRCULAR PCR<sup>TM</sup>3-LMP2A-TETR PLASMID ENCOMPASSING BOTH THE PCMV AND BGH POLY A TAIL, AND THE TETR-LMP2A GENE OF INTEREST IS OBTAINED BY LIGATION OF BOTH THE LINEARIZED SEGMENTS OBTAINED. 50

5.3 **(A) PLASMID PCR<sup>TM</sup>3-LMP2A-TETR IS RESTRICTION ENZYME DIGESTED WITH NDEI TO GIVE RISE TO TWO FRAGMENTS OF 6.10KB AND 1.55KB IN LENGTH. (B) GEL ELECTROPHORESIS SHOWING RESTRICTION DIGESTION ANALYSIS WITH NDEI TO SELECT FOR THE RECOMBINANT PCR<sup>TM</sup>3-LMP2A-TETR PLASMID.** THE DESIRED RECOMBINANT PLASMID WITH NDEI IS OBSERVED IN SAMPLES 1 AND 20. 51

5.4 **REMOVAL OF THE TETR SEQUENCE TO OBTAIN A PLASMID CONTAINING THE PCMV PROMOTER FOLLOWED BY THE LMP2A GENE AND POLY A TAIL.** REMOVAL OF THE ROUGHLY 500BP TETR SEQUENCE BY RESTRICTION DIGESTION WITH SACII ENZYME. 51

**5.5 INSERTION OF THE PCMV-LMP2A EXPRESSION CASSETTE INTO THE SHUTTLE VECTOR PST76K-SR.** RESTRICTION DIGESTION OF THE SHUTTLE PLASMID AT THE MCS WITH SMAI AND OF THE PCMV-LMP2A WITH SspI AND AFLIII FOLLOWED BY THE DNA POLYMERASE KLENOW TO GENERATE BLUNT ENDS IS PERFORMED TO OBTAIN LINEAR DNA STRANDS. LIGATION AND SUBSEQUENT CONTROL DIGESTION IS PERFORMED TO IDENTIFY THE CORRECT RECOMBINANT PLASMID OF PCMV-LMP2A IN PST76K-SR. THE SHUTTLE VECTOR CONTAINS A REC A GENE THAT IS NEEDED FOR RECOMBINATION DURING THE SHUTTLE-MUTAGENESIS WHILE SAC B IS A SELECTION MARKER.

52

**5.6 RESTRICTION ENZYME ANALYSIS OF BAC DNA OF MHV68-LMP2A IN COMPARISON TO MHV68-WT TO DETERMINE AND SELECT FOR THE DESIRED RECOMBINANT.** **(A)** THE INITIAL TEN PROBES WERE SUBJECTED TO RESTRICTION DIGESTION WITH BglII AND RESULTS COMPARED TO THE CONTROL CONTAINING MHV68-WT. THE LOSS OF A 4578BP BAND WITH THE GAIN OF A 7761BP BAND, ILLUSTRATED WITH WHITE ARROWS AND DOTS, SIGNIFIES THE CORRECT AND SUCCESSFUL INSERTION OF THE LMP2A GENE CONSTRUCT THROUGH HOMOLOGOUS RECOMBINATION (SAMPLES 2, 7, 9 AND 10). **(B)** A SELECTED CLONE (CLONE 2) WAS FURTHER RESTRICTION DIGESTED SEPARATELY WITH HpaI, EcoRI AND HindIII FOR FURTHER CONFIRMATION OF THE DESIRED RECOMBINANT, GIVING RISE TO EXPECTED BAND PATTERNS SHOWN. THE TABLES SUMMARIZE THE DIGESTION WITH THE DIFFERENT RESTRICTION ENZYMES USED SHOWING FRAGMENTS WITHOUT THE INSERT, AND FRAGMENTS WITH THE INSERT SUCCESSFULLY INSERTED. (YELLOW ARROWS MARKING OUT THE SELECTED GAIN OR LOSS OF BANDS WHEN DIGESTION WITH HpaI WAS DONE, RED ARROWS FOR DIGESTION WITH EcoRI, ORANGE ARROWS FOR DIGESTION WITH HindIII).

54

**5.7 SCHEMATIC DIAGRAM SHOWING HOW VIRUS PARTICLES ARE GENERATED FROM THE CLONED MHV68-LMP2A VIRAL GENOME.** BAC CASSETTE IS REMOVED AND VIRUS WITHOUT BAC IS GENERATED WITH SUBSEQUENT DETERMINATION OF VIRUS TITER.

55

**5.8 CHARACTERIZATION OF THE RECOMBINANT VIRUS BY LEFT END GENOME PCR.** **(A)** SCHEMATIC ILLUSTRATION OF THE LEFT END GENOME OF MHV68-WT. PRIMER PAIRS SPECIFIC FOR THE LEFT END GENOME OF MHV68-WT WERE USED, PRODUCING PCR PRODUCTS OF 124BP (M1) AND 1543BP (M1-M2) WHICH CAN BE VISUALISED BY GEL ELECTROPHORESIS. **(B)** LEFT END GENOME PCR GEL ELECTROPHORESIS. THE BANDS OBSERVED FROM MHV68-WT AND MHV68-LMP2A SHOW THE SAME BAND PATTERNS INDICATING THAT LEFT END GENOME DELETION HAD NOT OCCURRED.

56

**5.9 DETECTION OF LMP2A AND TUBULIN PROTEIN BY WESTERN BLOT ANALYSIS.** MHV68-WT OR MHV68-LMP2A INFECTED NIH3T3 CELLS AND A LYMPHOBLASTIC CELL LINE LCL2098 SERVING AS THE POSITIVE CONTROL WERE HARVESTED AND PREPARED FOR WESTERN BLOTH ANALYSIS. LMP2A PROTEIN WAS DETECTED IN MHV68-LMP2A INFECTED CELLS AND THE LCL2098 CONTROLS. DETECTION OF TUBULIN SERVED AS A POSITIVE LOADING CONTROL.

57

5.10 **GROWTH CURVES SHOWING LYtic REPLICATION IN NIH3T3 CELLS.** NIH3T3 CELLS ARE INFECTED WITH MHV68-WT OR MHV68-LMP2A AND HARVESTED AFTER VARIOUS TIMEPOINTS WITH THE RESPECTIVE VIRUS TITER DETERMINED. A MULTIPLICITY OF INFECTION (MOI) OF 0.1 WAS USED. AFTER 96 HOURS, BOTH THE MHV68-WT AND THE RECOMBINANT MHV68-LMP2A REACHES COMPARABLE TITERS. EXPERIMENT WAS REPEATED THREE TIMES (N=3) WITH EACH POINT REPRESENTING THE *mean*  $\pm$  *SE*.

57

5.11 **VIRAL LYtic REPLICATION.** VIRAL TITERS, PLOTTED LOGARITHMICALLY, AS A REPRESENTATIVE OF THE TOTAL VIRAL LYtic REPLICATION ARE DETERMINED FROM THE HOMOGENIZED LUNG TISSUE OF THE MHV68-WT AND MHV68-LMP2A INFECTED C57BL/6 MICE 6 OR 7 DAYS POST-INFECTION, WHERE THE MEAN (REPRESENTED BY THE HORIZONTAL LINE) WAS DETERMINED. C57BL/6 MICE WERE I.N INFECTED WITH  $5 \times 10^4$  PFU. (N=6) WHERE N= NUMBER OF MICE USED AND EACH POINT ON THE GRAPH REPRESENTS VIRUS TITER OF A MOUSE. EXPERIMENT WAS REPEATED TWICE, EACH WITH 6 MICE (3 WITH MHV68-WT AND 3 WITH MHV68-LMPA) FOR A TOTAL OF 12 MICE. 58

5.12 **WEIGHT OF SPLEEN AFTER INTRANASAL INFECTION.** C57BL/6 MICE WERE I.N INFECTED WITH  $5 \times 10^4$  PFU. SPLENIC WEIGHTS OF MHV68-LMP2A AND MHV68-WT INFECTED C57BL/6 MICE WERE DETERMINED AFTER 10 DAYS (N=12), 14 DAYS (N=12), AND 17 DAYS (N=16) OF INFECTION, TOGETHER WITH THE NON-INFECTED CONTROLS (N=6). N= NUMBER OF MICE USED AND EACH POINT ON THE GRAPH REPRESENTS THE SPLENIC WEIGHT OF ONE MOUSE WITH MEANS BEING TABULATED AND REPRESENTED BY THE HORIZONTAL LINE ON THE GRAPH.

58

5.13 **EX-VIVO REACTIVATION OF SPLENOCYTES AFTER I.N INFECTION OF C57BL/6 MICE WITH MHV68-WT AND RECOMBINANT MHV68-LMP2A AT 10, 14 AND 17 DAYS POST INFECTION.** C57BL/6 MICE WERE I.N INFECTED WITH  $5 \times 10^4$  PFU OF VIRUS. AFTER 10, 14 AND 17 DAYS POST INFECTION, THE INCUBATION OF THREE FOLD DILUTIONS OF THE SPLENOCYTES WITH NIH3T3 CELLS WAS DONE TO OBTAIN A SET OF 8 VALUES. EXPERIMENT WAS REPEATED TWICE FOR DAY 10 AND 14 POST-INFECTION (N=3 FOR EACH VIRUS AND EXPERIMENT) AND THREE TIMES FOR DAY 17 POST-INFECTION (N=3 FOR EACH VIRUS AND EXPERIMENT TWICE FOLLOWED BY AN EXPERIMENT WITH N=2). EACH POINT ON THE GRAPH REPRESENTS THE MEAN  $\pm$  SD.

59

**5.14 VIRAL GENOMIC LOAD IN SPLEEN.** THE QUOTIENT OF COPY NUMBER OF THE GB GENE TO THE COPY NUMBER OF THE L8 GENE MULTIPLIED BY 1000 WAS USED AS A SUITABLE INDEX FOR VIRAL GENOMIC LOAD DETERMINATION, SO THAT QUANTITIES COULD BE EFFECTIVELY COMPARED BETWEEN THE EXPERIMENTAL GROUPS. GRAPH SHOWS VIRAL GENOMIC LOAD IN SPLEENS, THAT WERE PREVIOUSLY WEIGHED. EXPERIMENT WAS REPEATED TWICE FOR DAY 10 AND 14 POST-INFECTION (N=3 FOR EACH VIRUS AND EXPERIMENT) AND THREE TIMES FOR DAY 17 POST-INFECTION (N=3 FOR EACH VIRUS AND EXPERIMENT TWICE FOLLOWED BY AN EXPERIMENT WITH N=2) WHERE N= NUMBER OF MICE USED. EACH POINT ON THE GRAPH REPRESENTS VIRAL GENOMIC LOAD OF A MOUSE WITH MEANS BEING TABULATED AND REPRESENTED BY THE SHORT HORIZONTAL LINE ON THE GRAPH. A DASHED HORIZONTAL LINE NEAR THE BOTTOM OF THE GRAPH REPRESENTS THE DETECTION LIMIT OF THE PCR, WITH POINTS BELOW IT REPRESENTING VIRAL GENOMIC LOADS THAT REMAIN UNDETECTED.

60

**5.15 TOTAL B CELL NUMBERS WERE SLIGHTLY HIGHER IN MHV68-WT INFECTED MICE WITH HIGHER B CELL ACTIVATION AT DAY 17 POST INFECTION IN COMPARISON TO MHV68-LMP2A. (A) TOTAL B CELL NUMBERS.** LIVING LYMPHOCYTES WERE GATED AND CELLS THAT WERE CD19<sup>+</sup>THY1.2<sup>-</sup> WERE GATED AS B CELLS. TOTAL B CELL NUMBERS WERE CALCULATED WITH RESPECT TO TOTAL SPLENOCYTES TALLIED. **(B) TOTAL NUMBER OF CD86<sup>+</sup> B CELLS.** LYMPHOCYTES WERE GATED FOLLOWED BY GATING OF B220<sup>+</sup> CELLS. NEXT, CD86<sup>+</sup> CELLS WERE GATED AND TOTAL NUMBERS WERE CALCULATED WITH RESPECT TO TOTAL SPLENOCYTES TALLIED.

61

**5.16 TOTAL T CELL NUMBERS OF MHV68-WT INFECTED MICE WERE HIGHER COMPARED TO MHV68-LMP2A INFECTED MICE.** LIVING LYMPHOCYTES WERE GATED AND CELLS THAT WERE CD19<sup>-</sup>THY1.2<sup>+</sup> WERE GATED AS T CELLS. TOTAL T CELL NUMBERS WERE CALCULATED IN RELATION TO TOTAL SPLENOCYTES TALLIED.

61

**5.17 HIGHER CD4<sup>+</sup> AND CD8<sup>+</sup> T CELL ACTIVATION (CD69<sup>+</sup>) IN MHV68-WT INFECTED MICE THAN MHV68-LMP2A INFECTED MICE. (A) CD69 EXPRESSION ON CD4<sup>+</sup> T CELLS.** LYMPHOCYTES WERE GATED AND CD69<sup>+</sup> WAS GATED AFTER CD4<sup>+</sup> T CELLS (CD4<sup>+</sup> CD8<sup>-</sup>) AND TOTAL NUMBERS OF CD69<sup>+</sup> CD4<sup>+</sup> T CELLS WERE CALCULATED WITH RESPECT TO TOTAL SPLENOCYTES. **(B) CD69 EXPRESSION ON CD8<sup>+</sup> T CELLS.** LYMPHOCYTES WERE GATED AND CD69<sup>+</sup> WAS GATED AFTER CD8<sup>+</sup> T CELLS (CD4<sup>-</sup> CD8<sup>+</sup>) AND TOTAL NUMBERS OF CD69<sup>+</sup> CD8<sup>+</sup> T CELLS WERE CALCULATED WITH RESPECT TO TOTAL SPLENOCYTES. A SIGNIFICANT DIFFERENCE WAS OBSERVED BETWEEN MHV68-WT AND MHV68-LMP2A INFECTED MICE GROUPS AT DAY 10 POST INFECTION (P= 0.033).

62

**5.18 COMPARABLE GCB CELL FORMATION AFTER INFECTION WITH MHV68-LMP2A AND MHV68-WT. (A) FACS DIAGRAM SHOWING THE PERCENTAGES OF GCB CELLS (CD95<sup>+</sup> CD19<sup>+</sup>) IN SPLEENS. (B) PERCENTAGE OF GCB CELLS IN SPLEENS.** THE PLOTS ARE GATED ON LYMPHOCYTES AND B CELLS (CD19<sup>+</sup>). **(C) TOTAL GCB CELL NUMBERS IN SPLEENS.** TOTAL GCB CELL NUMBERS WERE CALCULATED WITH RESPECT TO TOTAL SPLENOCYTES TALLIED.

63

5.19 PERCENTAGE OF GCB CELLS IN THE CERVICAL LYMPH NODES SHOWED NO DIFFERENCE BETWEEN THE VIRUSES USED. GCB CELLS (CD95<sup>+</sup> CD19<sup>+</sup>) WERE GATED IN A SIMILAR MANNER AS THAT OF GCB CELLS IN SPLEENS.

64

5.20 NO DIFFERENCES BETWEEN PERCENTAGES OF PLASMA CELLS AS WELL AS TOTAL PLASMA CELL NUMBERS BETWEEN BOTH VIRUSES USED. (A) FACS DIAGRAM SHOWING THE PERCENTAGES OF PLASMA CELLS (CD138<sup>+</sup> B220<sup>-</sup>). (B) PERCENTAGE OF PLASMA CELLS. THE PLOTS WERE GATED ON LYMPHOCYTES FOLLOWED BY CD3<sup>-</sup> AND CD11b<sup>-</sup>. (C) TOTAL PLASMA CELL NUMBERS.

TOTAL PLASMA CELL NUMBERS WERE CALCULATED WITH RESPECT TO TOTAL SPLENOCYTES TALLIED. 65

5.21 SPLENIC WEIGHT. LC30 AND CAR MICE WERE INTRAPERITONEALLY (I.P) INFECTED WITH A CONCENTRATION OF  $1 \times 10^5$  PFU OF VIRUS. SPLENIC WEIGHT OF MHV68-NGFR AND MHV68-LMP2A INFECTED LC30 AND CAR MICE WERE DETERMINED AFTER 14 DAYS AND 2 MONTHS OF INFECTION, TOGETHER WITH NON-INFECTED CONTROLS. DECREASED SPLENOMEGLY OBSERVED 2 MONTHS POST INFECTION THAN 14 DAYS POST INFECTION IN VIRUS INFECTED MICE.

67

5.22 VIRUS REACTIVATION FROM LATENCY IN SPLEENS AT 14 DAYS POST INFECTION. LC30 AND CAR MICE WERE INTRAPERITONEALLY (I.P) INFECTED WITH A CONCENTRATION OF  $1 \times 10^5$  PFU OF VIRUS. AFTER 14 DAYS AND 2 MONTHS POST INFECTION, THE INCUBATION OF THREE FOLD DILUTIONS OF THE SPLENOCYTES WITH NIH3T3 CELLS WAS DONE TO OBTAIN A SET OF 8 VALUES. VIRUS REACTIVATION FROM LATENCY WAS SIMILAR ACROSS THE FOUR DIFFERENT EXPERIMENTAL GROUPS WITH NO DIFFERENCES OBSERVED BETWEEN THE TWO RECOMBINANT VIRUSES USED.

68

5.23 VIRAL GENOMIC LOAD IN SPLEEN AT 14 DAYS POST INFECTION. THE QUOTIENT OF COPY NUMBER OF THE GB GENE TO THE COPY NUMBER OF THE L8 GENE MULTIPLIED BY 1000 WAS USED AS A SUITABLE INDEX FOR VIRAL GENOMIC LOAD DETERMINATION, SO THAT QUANTITIES COULD BE EFFECTIVELY COMPARED BETWEEN THE EXPERIMENTAL GROUPS. GRAPH SHOWS VIRAL GENOMIC LOAD IN SPLEENS, THAT WERE PREVIOUSLY WEIGHED. VIRUS INFECTED LC30 MICE HAVE LOWER VIRAL GENOMIC LOADS THAN THEIR VIRUS INFECTED CAR MICE COUNTERPARTS. EACH POINT ON THE GRAPH REPRESENTS VIRAL GENOMIC LOAD OF A MOUSE WITH MEANS BEING TABULATED AND REPRESENTED BY THE SHORT HORIZONTAL LINE ON THE GRAPH. A DASHED HORIZONTAL LINE NEAR THE BOTTOM OF THE GRAPH REPRESENTS THE DETECTION LIMIT OF THE PCR, WITH POINTS BELOW IT REPRESENTING VIRAL GENOMIC LOADS THAT REMAIN UNDETECTED.

69

5.24 TOTAL B CELL NUMBERS WERE HIGHER 14 DAYS POST INFECTION COMPARED TO 2 MONTHS POST INFECTION WITH NO DIFFERENCES OBSERVED BETWEEN THE VIRUSES USED. LIVING LYMPHOCYTES WERE FIRST GATED FOLLOWED BY THE B CELLS (CD19<sup>+</sup> THY1.2<sup>-</sup>).

70

5.25 **VIRUS INFECTED LC30 MICE SHOW LARGER EXPANSION OF REPORTER POSITIVE CELLS WITHIN B CELLS AT 14 DAYS AND 2 MONTHS POST INFECTION. (A) PERCENTAGE REPORTER POSITIVE CELLS WITHIN B CELLS IN SPLEENS.** LYMPHOCYTES WERE GATED FOLLOWED BY B CELLS ( $B220^+CD19^+$ ) AND FINALLY REPORTER POSITIVE CELLS ( $HCD2^+$  OR  $CAR^+$ ) WERE GATED TO OBTAIN THE PERCENTAGES OF REPORTER POSITIVE CELLS WITHIN B CELLS. **(B) TOTAL REPORTER POSITIVE B CELLS IN SPLEENS.** AFTER REPORTER POSITIVE CELLS WITHIN THE B CELLS WERE GATED, TOTAL NUMBER OF REPORTER POSITIVE CELLS WERE CALCULATED WITH RESPECT TO THE TOTAL SPLENOCYTES TALLIED.

71

5.26 **VIRUS DEPENDENT DIFFERENCES WERE OBSERVED WITH MHV68-LMP2A INFECTED MICE SHOWING A GREATER PERCENTAGE OF DECREASE IN TERMS OF TOTAL NUMBER OF REPORTER POSITIVE CELLS WITHIN B CELLS MEASURED MOVING FROM 14 DAYS TO 2 MONTHS POST INFECTION WHEN COMPARING WITH MHV68-NGFR INFECTED MICE. (A) PERCENTAGE CHANGE AMONG VIRUS INFECTED CAR MICE. (B) PERCENTAGE CHANGE AMONG VIRUS INFECTED LC30 MICE.**

71

5.27 **TOTAL T CELL NUMBERS WERE HIGHER 14 DAYS POST INFECTION COMPARED TO 2 MONTHS POST INFECTION WITH NO DIFFERENCES OBSERVED BETWEEN THE MICE TYPE OR VIRUS STRAINS USED.** LIVING LYMPHOCYTES WERE GATED AND CELLS THAT WERE  $CD19^-Thy1.2^+$  WERE GATED AS T CELLS. TOTAL T CELL NUMBERS WERE CALCULATED IN RELATION TO TOTAL SPLENOCYTES TALLIED.

72

5.28 **LMP2A ENHANCES THE GENERATION OF GC REACTIONS. (A) FACS DIAGRAM SHOWING GATINGS OF GCB CELLS ( $GL7^+ CD95^+ B220^+$ ) FROM SPLEENS OF VIRUS INFECTED LC30 MICE AND CAR MICE.** THE FACS DIAGRAM DEPICTS HOW GCB GATINGS WERE DONE AND OBSERVED IN VIRUS INFECTED LC30 OR CAR MICE AND DOES NOT DIFFERENTIATE BETWEEN WHICH RECOMBINANT VIRUS WAS USED. **(B) PERCENTAGE OF GCB CELLS IN SPLEENS.** PLOTS WERE GATED ON LYMPHOCYTES FOLLOWED BY B CELLS ( $B220^+$ ) AND GCB CELLS ( $GL7^+ CD95^+$ ). **(C) TOTAL GCB CELLS IN SPLEEN.** TOTAL GCB CELL NUMBERS WERE CALCULATED WITH RESPECT TO TOTAL SPLENOCYTES TALLIED.

73

5.29 **LC30 MICE HAD LOWER PERCENTAGES AND TOTAL NUMBERS OF REPORTER POSITIVE CELLS WITHIN GCB CELLS IN COMPARISON TO CAR MICE. (A) PERCENTAGE REPORTER POSITIVE CELLS WITHIN GCB CELLS IN SPLEENS.** REPORTER POSITIVE CELLS ( $HCD2^+$  OR  $CAR^+$ ) WERE GATED FROM GCB CELLS ( $GL7^+ CD95^+ B220^+$ ). **(B) TOTAL NUMBER OF REPORTER POSITIVE CELLS WITHIN GCB CELLS IN SPLEEN.** TOTAL NUMBER OF REPORTER POSITIVE CELLS WERE CALCULATED WITH RESPECT TO THE TOTAL SPLENOCYTES TALLIED.

73

5.30 **LC30 MICE HAD LOWER PERCENTAGES OF GCB CELLS WITHIN REPORTER POSITIVE CELLS IN COMPARISON TO CAR MICE AT BOTH TIME POINTS, WITH MHV68-LMP2A INFECTED CAR MICE SHOWING THE LARGEST PERCENTAGES AT 14 DAYS POST INFECTION. (A) FACS DIAGRAM SHOWING GATINGS OF GCB CELLS WITHIN THE FRACTION OF REPORTER POSITIVE CELLS FROM SPLEENS OF VIRUS INFECTED LC30 MICE AND CAR MICE.** THE FACS DIAGRAM DEPICTS HOW GCB GATINGS WERE DONE AND OBSERVED IN VIRUS INFECTED LC30 OR CAR MICE AND DOES NOT DIFFERENTIATE BETWEEN WHICH RECOMBINANT VIRUS WAS USED. **(B) PERCENTAGE OF GCB CELLS WITIN REPORTER POSITIVE CELLS.** GCB CELLS ( $GL7^+ CD95^+$ ) WERE GATED FROM REPORTER POSITIVE B CELLS ( $HCD2^+ B220^+$  OR  $CAR^+ B220^+$ ).

74

5.31 **NO CLEAR VIRUS DEPENDENT DIFFERENCES WERE OBSERVED BETWEEN THE RECOMBINANT VIRUSES USED. (A) FACS DIAGRAM SHOWING GATINGS OF GCB CELLS FROM CERVICAL LYMPH NODES OF VIRUS INFECTED LC30 MICE AND CAR MICE.** THE FACS DIAGRAM DEPICTS HOW GCB GATINGS WERE DONE AND OBSERVED IN VIRUS INFECTED LC30 OR CAR MICE AND DOES NOT DIFFERENTIATE BETWEEN WHICH RECOMBINANT VIRUS WAS USED. **(B) PERCENTAGE OF GCB CELLS IN CERVICAL LYMPH NODES.** GCB CELLS ( $GL7^+ CD95^+ B220^+$ ) WERE GATED IN A SIMILAR MANNER AS THAT OF SPLEENS.

76

5.32 **MICE DEPENDENT DIFFERENCES WERE OBSERVED WITH VIRUS INFECTED LC30 MICE HAVING LOWER PERCENTAGES OF REPORTER POSITIVE CELLS WITHIN GCB IN THE CERVICAL LYMPH NODES AND HIGHER PERCENTAGES BEING OBSERVED IN COMPARISON TO CAR MICE AT 2 MONTHS THAN 14 DAYS POST INFECTION.** PERCENTAGE OF REPORTER POSITIVE CELLS WITHIN GCB CELLS WERE GATED IN A SIMILAR MANNER AS THAT OF SPLEENS.

76

5.33 **MICE DEPENDENT DIFFERENCES WERE OBSERVED WITH MHV68-NGFR AND MHV68-LMP2A INFECTED CAR MICE HAVING HIGHER PERCENTAGES OF GCB CELLS WITHIN REPORTER POSITIVE CELLS WHEN COMPARED TO VIRUS INFECTED LC30 MICE AT 2 MONTHS POST INFECTION. (A) FACS DIAGRAM SHOWING GATINGS GCB CELLS WITHIN REPORTER POSITIVE CELLS FROM CERVICAL LYMPH NODES BETWEEN VIRUS INFECTED LC30 MICE AND CAR MICE.** THE FACS DIAGRAM DEPICTS HOW GCB CELL GATINGS WERE DONE AND OBSERVED IN VIRUS INFECTED LC30 OR CAR MICE AND DOES NOT DIFFERENTIATE BETWEEN WHICH RECOMBINANT VIRUS WAS USED. **(B) PERCENTAGE OF GCB CELLS WITHIN THE REPORTER POSITIVE CELLS IN CERVICAL LYMPH NODES.** PERCENTAGE OF GCB CELLS WITHIN THE REPORTER POSITIVE CELLS IN THE CERVICAL LYMPH NODES WERE GATED IN A SIMILAR MANNER AS THAT OF SPLEENS.

77

**5.34 (A) FACS DIAGRAM SHOWING GATINGS OF B1A, B1B AND B2 CELLS IN SPLEENS BETWEEN VIRUS INFECTED LC30 MICE AND CAR MICE.** THE FACS DIAGRAM DEPICTS HOW THE B CELL GATINGS WERE DONE AND OBSERVED IN VIRUS INFECTED LC30 OR CAR MICE AND DOES NOT DIFFERENTIATE BETWEEN WHICH RECOMBINANT VIRUS WAS USED. LYMPHOCYTES WERE CD19<sup>+</sup> B220<sup>+</sup> GATED AND THE SUBSEQUENT B1A CELL (CD5<sup>+</sup> B220<sup>low</sup> CD19<sup>+</sup>), B1B CELL (CD5<sup>low</sup> B220<sup>low</sup> CD19<sup>+</sup>) AND B2 CELL (B220<sup>high</sup> CD19<sup>+</sup>) POPULATIONS GATED. **(B) FACS DIAGRAM SHOWING GATINGS OF B1A, B1B AND B2 CELLS WITHIN REPORTER POSITIVE CELLS IN SPLEENS OF VIRUS INFECTED LC30 MICE AND CAR MICE.** THE FACS DIAGRAM DEPICTS HOW THE B CELL GATINGS WERE DONE AND OBSERVED IN VIRUS INFECTED LC30 OR CAR MICE AND DOES NOT DIFFERENTIATE BETWEEN WHICH RECOMBINANT VIRUS WAS USED. REPORTER POSITIVE B220<sup>+</sup> CD19<sup>+</sup> B CELLS WERE GATED FROM LYMPHOCYTES AND SUBSEQUENTLY B1A CELL (CD5<sup>+</sup> B220<sup>low</sup> CD19<sup>+</sup>), B1B CELL (CD5<sup>low</sup> B220<sup>low</sup> CD19<sup>+</sup>) AND B2 CELL (B220<sup>high</sup> CD19<sup>+</sup>) POPULATIONS GATED.

78

**5.35 MICE DEPENDENT DIFFERENCES WERE OBSERVED AT 2 MONTHS POST INFECTION WITH VIRUS INFECTED LC30 MICE HAVING HIGHER PERCENTAGES OF REPORTER POSITIVE CELLS WITHIN B1A CELLS AS WELL AS TOTAL NUMBER OF REPORTER POSITIVE CELLS WITHIN B1A CELLS THAN VIRUS INFECTED CAR MICE. (A) PERCENTAGE REPORTER POSITIVE CELLS WITHIN B1A CELLS IN SPLEENS.** REPORTER POSITIVE CELLS (HCD2<sup>+</sup> OR CAR<sup>+</sup>) WERE GATED FROM B1A CELLS (CD5<sup>+</sup> B220<sup>low</sup> CD19<sup>+</sup>). **(B) TOTAL NUMBER OF REPORTER POSITIVE CELLS WITHIN B1A CELLS IN SPLEENS.** TOTAL NUMBER OF REPORTER POSITIVE CELLS WITHIN B1A CELLS WERE CALCULATED WITH RESPECT TO THE TOTAL SPLENOCYTES TALLIED.

78

**5.36 PERCENTAGE OF B1A CELLS WITHIN REPORTER POSITIVE CELLS.** REPORTER POSITIVE B220<sup>+</sup> CD19<sup>+</sup> B CELLS WERE GATED FROM LYMPHOCYTES AND SUBSEQUENTLY B1A CELL POPULATION (CD5<sup>+</sup> B220<sup>low</sup> CD19<sup>+</sup>) GATED FROM THE REPORTER POSITIVE CELLS. MICE DEPENDENT DIFFERENCES WERE OBSERVED WITH VIRUS INFECTED LC30 MICE HAVING HIGHER PERCENTAGES THAN VIRUS INFECTED CAR MICE. HIGHER PERCENTAGES WERE OBSERVED AT 2 MONTHS POST INFECTION THAN AT 14 DAYS POST INFECTION.

79

**5.37 MICE DEPENDENT DIFFERENCES WERE OBSERVED WITH VIRUS INFECTED LC30 MICE HAVING HIGHER PERCENTAGES AND TOTAL NUMBERS OF REPORTER POSITIVE CELLS WITHIN B1B CELLS IN COMPARISON TO VIRUS INFECTED CAR MICE AT 14 DAYS AND 2 MONTHS POST INFECTION. (A) PERCENTAGE REPORTER POSITIVE CELLS WITHIN B1B CELLS IN SPLEENS.** B1B CELLS (CD5<sup>low</sup> B220<sup>low</sup> CD19<sup>+</sup>) WERE GATED FROM REPORTER POSITIVE CELLS (HCD2<sup>+</sup> OR CAR<sup>+</sup>). **(B) TOTAL REPORTER POSITIVE CELLS WITHIN B1B CELLS IN SPLEENS.** TOTAL NUMBER OF REPORTER POSITIVE CELLS WITHIN B1B CELLS WERE CALCULATED WITH RESPECT TO THE TOTAL SPLENOCYTES TALLIED.

80

5.38 **PERCENTAGE OF B1B CELLS WITHIN REPORTER POSITIVE CELLS IN SPLEENS.** B1B CELLS ( $CD5^{low}$   $B220^{low}$   $CD19^+$ ) WERE GATED FROM REPORTER POSITIVE CELLS (HCD2 $^+$  OR CAR $^+$ ). MICE DEPENDENT DIFFERENCES WERE OBSERVED WITH VIRUS INFECTED LC30 MICE HAVING HIGHER PERCENTAGES THAN VIRUS INFECTED CAR MICE. HIGHER PERCENTAGES WERE OBSERVED AT 2 MONTHS POST INFECTION THAN AT 14 DAYS POST INFECTION.

80

5.39 **MICE DEPENDENT DIFFERENCES WERE OBSERVED WITH VIRUS INFECTED LC30 MICE HAVING HIGHER PERCENTAGES AND TOTAL NUMBERS OF REPORTER POSITIVE CELLS WITHIN B2 CELLS IN COMPARISON TO VIRUS INFECTED CAR MICE. PERCENTAGES DECREASED AT 14 DAYS TO 2 MONTHS POST INFECTION.** (A) **PERCENTAGE REPORTER POSITIVE CELLS WITHIN B2 CELLS IN SPLEENS.** REPORTER POSITIVE CELLS (HCD2 $^+$  OR CAR $^+$ ) WERE GATED FROM B2 CELLS ( $B220^{high}$   $CD19^+$ ). (B) **TOTAL NUMBER OF REPORTER POSITIVE CELLS WITHIN B2 CELLS IN SPLEENS.** TOTAL NUMBER OF REPORTER POSITIVE CELLS WITHIN B2 CELLS WERE CALCULATED WITH RESPECT TO THE TOTAL SPLENOCYTES TALLIED.

81

5.40 **PERCENTAGE OF B2 CELLS WITHIN REPORTER POSITIVE CELLS IN SPLEENS.** B2 CELLS ( $B220^{high}$   $CD19^+$ ) WERE GATED FROM REPORTER POSITIVE CELLS (HCD2 $^+$  OR CAR $^+$ ). MICE DEPENDENT DIFFERENCES WERE OBSERVED WITH VIRUS INFECTED LC30 MICE HAVING LOWER PERCENTAGES THAN VIRUS INFECTED CAR MICE. LOWER PERCENTAGES WERE OBSERVED AT 2 MONTHS POST INFECTION THAN AT 14 DAYS POST INFECTION.

81

5.41 (A) **PERCENTAGE REPORTER POSITIVE CELLS WITHIN B1A CELLS IN THE PERITONEAL CAVITY.** REPORTER POSITIVE CELLS (HCD2 $^+$  OR CAR $^+$ ) WERE GATED FROM B1A CELLS ( $CD5^{high}$   $B220^{low}$   $CD19^+$ ) SIMILAR TO THAT OF SPLEENS. MICE DEPENDENT DIFFERENCES WERE OBSERVED WITH VIRUS INFECTED LC30 MICE HAVING HIGHER PERCENTAGES THAN VIRUS INFECTED CAR MICE. ONLY MHV68-LMP2A INFECTED LC30 MICE HAD LOWER PERCENTAGES AT 2 MONTHS THAN AT 14 DAYS POST INFECTION. (B) **PERCENTAGE OF B1A CELLS IN REPORTER POSITIVE CELLS IN THE PERITONEAL CAVITY.** B1A CELLS ( $CD5^{high}$   $B220^{high}$   $CD19^+$ ) WERE GATED FROM REPORTER POSITIVE CELLS (HCD2 $^+$  OR CAR $^+$ ) IN A SIMILAR MANNER AS THAT OF SPLEENS. HIGHEST PERCENTAGES OBSERVED IN MHV68-NGFR INFECTED LC30 MICE AT 2 MONTHS POST INFECTION.

82

**5.42 (A) PERCENTAGE REPORTER POSITIVE CELLS WITHIN B1B CELLS IN THE PERITONEAL CAVITY.** REPORTER POSITIVE CELLS (HCD2<sup>+</sup> OR CAR<sup>+</sup>) WERE GATED FROM B1B CELLS (CD5<sup>low</sup> B220<sup>low</sup> CD19<sup>+</sup>) SIMILAR TO THAT OF SPLEENS. MICE DEPENDENT DIFFERENCES WERE OBSERVED WITH VIRUS INFECTED LC30 MICE HAVING HIGHER PERCENTAGES THAN VIRUS INFECTED CAR MICE. MHV68-LMP2A INFECTED CAR MICE HAD HIGHER PERCENTAGES AT 2 MONTHS POST INFECTION THAN AT 14 DAYS POST INFECTION. **(B) PERCENTAGE OF B1B CELLS WITHIN REPORTER POSITIVE CELLS IN THE PERITONEAL CAVITY.** B1B CELLS (CD5<sup>low</sup> B220<sup>high</sup> CD19<sup>+</sup>) WERE GATED FROM REPORTER POSITIVE CELLS (HCD2<sup>+</sup> OR CAR<sup>+</sup>) IN A SIMILAR MANNER AS THAT OF SPLEENS. VIRUS INFECTED LC30 MICE HAD HIGHER PERCENTAGES THAN VIRUS INFECTED CAR MICE AT BOTH TIME POINTS. HIGHER PERCENTAGES WERE OBSERVED 2 MONTHS POST INFECTION THAN AT 14 DAYS POST INFECTION.

83

**5.43 (A) FACS DIAGRAM SHOWING GATINGS OF PLASMA CELLS FROM SPLEENS OF VIRUS INFECTED LC30 MICE AND CAR MICE AT 14 DAYS AND 2 MONTHS POST INFECTION.** THE FACS DIAGRAM DEPICTS HOW PLASMA CELL GATINGS WERE DONE AND OBSERVED IN VIRUS INFECTED LC30 OR CAR MICE AND DOES NOT DIFFERENTIATE BETWEEN WHICH RECOMBINANT VIRUS WAS USED. PLOTS WERE GATED ON LYMPHOCYTES AND SUBSEQUENTLY PLASMA CELLS (CD138<sup>+</sup> B220<sup>low</sup>). **(B) PERCENTAGE OF PLASMA CELLS IN SPLEENS.** NO SIGNIFICANT DIFFERENCES WERE OBSERVED BETWEEN THE DIFFERENT EXPERIMENTAL GROUPS IN TERMS OF PERCENTAGE OF PLASMA CELLS GENERATED IN THE SPLEEN, AT 14 DAYS OR 2 MONTHS POST INFECTION.

84

**5.44 MICE DEPENDENT DIFFERENCES WERE OBSERVED WITH VIRUS INFECTED LC30 MICE HAVING HIGHER PERCENTAGES AND TOTAL NUMBER OF REPORTER POSITIVE CELLS WITHIN PLASMA CELLS IN SPLEENS. PERCENTAGES AT 2 MONTHS POST INFECTION WERE LOWER THAN THOSE AT 14 DAYS POST INFECTION.** **(A) PERCENTAGE REPORTER POSITIVE CELLS WITHIN PLASMA CELLS IN SPLEENS.** REPORTER POSITIVE CELLS (HCD2<sup>+</sup> OR CAR<sup>+</sup>) WERE GATED FROM PLASMA CELLS (CD138<sup>+</sup> B220<sup>low</sup>). **(B) TOTAL NUMBER OF REPORTER POSITIVE CELLS WITHIN PLASMA CELLS IN SPLEENS.** TOTAL NUMBER OF REPORTER POSITIVE CELLS WITHIN PLASMA CELLS WERE CALCULATED WITH RESPECT TO TOTAL SPLENOCYTES TALLIED.

84

**5.45 MICE DEPENDENT DIFFERENCES WERE OBSERVED WITH LOWER PERCENTAGES OF PLASMA CELLS WITHIN REPORTER POSITIVE CELLS BEING OBSERVED IN VIRUS INFECTED CAR MICE COMPARED TO VIRUS INFECTED LC30 MICE. (A) FACS DIAGRAM SHOWING GATINGS OF PLASMA CELLS WITHIN THE REPORTER POSITIVE CELLS FROM SPLEENS BETWEEN VIRUS INFECTED LC30 MICE AND CAR MICE.** THE FACS DIAGRAM DEPICTS HOW PLASMA CELL GATINGS WERE DONE AND OBSERVED IN VIRUS INFECTED LC30 OR CAR MICE, AND DOES NOT DIFFERENTIATE BETWEEN WHICH RECOMBINANT VIRUS WAS USED. REPORTER POSITIVE CELLS (HCD2<sup>+</sup> OR CAR<sup>+</sup>) WERE FIRST GATED, FOLLOWED BY THE SUBSEQUENT GATINGS OF PLASMA CELLS (C138<sup>+</sup> B220<sup>low</sup>) FROM THESE REPORTER POSITIVE CELLS (HCD2<sup>+</sup> OR CAR<sup>+</sup>). **(B) PERCENTAGE OF PLASMA CELLS WITHIN REPORTER POSITIVE CELLS.** LOWER PERCENTAGES OF PLASMA CELLS WITHIN THE FRACTION OF REPORTER POSITIVE CELLS WERE OBSERVED IN VIRUS INFECTED CAR MICE WHEN COMPARED TO VIRUS INFECTED LC30 MICE AT BOTH TIME POINTS. AT 14 DAYS POST INFECTION, VIRUS DEPENDENT DIFFERENCES WERE OBSERVED WITH MHV68-NGFR INFECTED CAR MICE HAVING HIGHER PERCENTAGES THAN MHV68-LMP2A INFECTED CAR MICE.

85

**5.46 LOWEST PERCENTAGES AND TOTAL NUMBER OF REPORTER POSITIVE CELLS WITHIN IgG1 MEMORY CELLS WERE OBSERVED IN MHV68-LMP2A INFECTED CAR MICE AT 14 DAYS POST INFECTION. PERCENTAGES AT 2 MONTHS POST INFECTION WERE LOWER THAN THOSE AT 14 DAYS POST INFECTION. (A) PERCENTAGE REPORTER POSITIVE CELLS WITHIN IgG1 MEMORY CELLS IN SPLEENS.** IgG1 MEMORY CELLS PLOTS (IGM<sup>low</sup> IgG<sup>+</sup>) WERE GATED FROM LYMPHOCYTES AND B CELLS (B220<sup>+</sup>). SUBSEQUENTLY, REPORTER POSITIVE CELLS (HCD2<sup>+</sup> OR CAR<sup>+</sup>) WERE GATED FROM IgG1 MEMORY CELLS. **(B) TOTAL REPORTER POSITIVE CELLS WITHIN IgG1 MEMORY CELLS IN SPLEENS.** TOTAL NUMBER OF REPORTER POSITIVE CELLS WITHIN IgG1 MEMORY CELLS WERE CALCULATED WITH RESPECT TO TOTAL SPLENOCYTES TALLIED.

86

**5.47 MICE DEPENDENT DIFFERENCES WERE OBSERVED AT DAY 14 WITH LOWER PERCENTAGES OF IgG1 CELLS WITHIN REPORTER POSITIVE CELLS BEING OBSERVED IN VIRUS INFECTED LC30 MICE COMPARED TO VIRUS INFECTED CAR MICE. HIGHER PERCENTAGES WERE OBSERVED 14 DAYS POST INFECTION COMPARED TO 2 MONTHS POST INFECTION. (A) FACS DIAGRAM SHOWING GATINGS OF IgG1 MEMORY CELL WITHIN THE REPORTER POSITIVE CELLS FROM SPLEENS BETWEEN VIRUS INFECTED LC30 MICE AND CAR MICE.** FACS DIAGRAM DEPICTS HOW IgG1 MEMORY CELL GATINGS WERE DONE AND OBSERVED IN VIRUS INFECTED LC30 OR CAR MICE, AND DOES NOT DIFFERENTIATE BETWEEN WHICH RECOMBINANT VIRUS WAS USED. **(B) PERCENTAGE OF IgG1 MEMORY CELLS WITHIN REPORTER POSITIVE CELLS.** PLOTS WERE GATED TO LYMPHOCYTES AND B CELLS (B220<sup>+</sup>). SUBSEQUENTLY, REPORTER POSITIVE CELLS (HCD2<sup>+</sup> OR CAR<sup>+</sup>) WERE GATED FOLLOWED BY IgG1 MEMORY CELLS (IGM<sup>low</sup> IgG<sup>+</sup>). SIGNIFICANT DIFFERENCES WERE OBSERVED BETWEEN THE VIRUS INFECTED LC30 MICE AND CAR MICE AT 14 DAYS POST INFECTION (P= 0.0286).

87

## LIST OF TABLES

3.1 PRIMERS USED FOR THE ANALYSIS OF THE LEFT END OF THE MHV68 GENOME	21
3.2 PRIMERS USED FOR GENOTYPING	21
3.3 PRIMERS AND PROBES USED FOR QUANTITATIVE PCR	22
3.4 LIST OF ANTIBODIES USED FOR WESTERN BLOT Antibodies were obtained from Christine Bogl	22
3.5 LIST OF ANTIBODIES USED FOR IMMUNOHISTOHEMISTRY	22
3.6 LIST OF INSTRUMENTS AND DEVICES	23
3.7 LIST OF CHEMICALS AND REAGENTS	24
4.1 TABLE SHOWING PREPARATION OF 1xTAE	26
4.2 TABLE SHOWING PREPARATION OF 1xTBE	26
4.3 TABLE SHOWING LEFT GENOME END PCR PROGRAMME	27
4.4 TABLE SHOWING LEFT GENOME END PCR REACTION PROCEDURE	27
4.5 TABLE SHOWING TAQMAN PCR PROGRAMME	28
4.6 TABLE SHOWING TAQMAN PCR REACTION PROCEDURE	28
4.7 TABLE SHOWING CD30FLSTOP PCR PROGRAMME	29
4.8 TABLE SHOWING CD30FLSTOP PCR REACTION PROCEDURE	29
4.9 TABLE SHOWING PREPARATION OF 2xLAEMMLI BUFFER	32
4.10 TABLE SHOWING PREPARATION OF STACKING GEL	33
4.11 TABLE SHOWING PREPARATION OF 10% SEPARATION GEL	33
4.12 TABLE SHOWING PREPARATION OF RUNNING BUFFER	33
4.13 TABLE SHOWING PREPARATION OF BLOTTING BUFFER	33
4.14 TABLE SHOWING PREPARATION OF MILK BLOCKING SOLUTION	34
4.15 TABLE SHOWING PREPARATION OF TBST	35
4.16 TABLE SHOWING PREPARATION OF THE ERYTHROCYTE LYSIS BUFFER	44
A.1 LIST OF RESTRICTION ENZYMES AND OTHER ENZYMES USED WITH THEIR CONDITIONS	102

# NOMENCLATURE

## LIST OF SYMBOLS

$\alpha$	Alpha
$\beta$	Beta
$C$	Constant
$D$	Diversity
$\gamma$	Gamma
$J$	Joining
$\kappa$	Kappa
$\lambda$	Lambda
$\Omega$	Ohms
$V$	Variable
$^{\circ}\text{C}$	Degrees Celsius
$mg$	Milligram
$mL$	Milliliter
$ mM$	Millimolar
$ng$	Nanogram
$s$	Seconds
$\mu g$	Microgram
$\mu L$	Microliter
$\mu F$	Microfarad

## LIST OF ACRONYMS

AID	Activation induced cytidine deaminase
APC	Antigen presenting cell
ATP	Adenosine triphosphate
BAC	Bacterial artificial chromosome
BAFF	B cell activating factor
BHK	Baby hamster kidney (cells)
bp	Base pairs
BSA	Bovine serum albumin

CAR	R26-Car $\gamma$ 1cre (Mice)
CD	Cluster of differentiation
CSR	Class switch recombination
CTL	Cytotoxic T cell
CTP	Cytidine triphosphate
dd	Deionized
DLBCL	Diffuse large B cell lymphoma
dNTPs	Deoxyribonucleotidetriphosphates
EBV	Epstein-Barr Virus
ECL	Enhances chemiluminescence
EDTA	Ethylenediaminetetraacetic acid
FDC	Follicular dendritic cells
FCS	Fetal calf serum
FO	Follicular (cells)
GC	Germinal center
GCB	Germinal center B (cells)
GFP	Green fluorescence protein
GHV	Gammaherpesvirus
GMEM	Glasgow minimum essential medium
GPT	Glutamate pyruvate transaminase
GTP	Guanosine triphosphate
HL	Hodgkin Lymphoma
HRS	Hodgkin Reed Sternberg (cells)
IDC	Interdigitating dendritic cells
IFN	Interferon
Ig	Immunoglobulin
i.n	Intranasal
IRES	Internal ribosome entry site
i.p	Intraperitoneal
kbp	Kilo base pairs
KSHV	Kaposi's sarcoma-associated Herpesvirus
LB	Lysogeny broth
LCL	Lymphoblastoid cell line
LC30	LMP1/CD30 $\gamma$ 1cre (Mice)
LMP	Latent membrane protein
LPS	Lipopolysaccharide

MHC	Major histocompatibility complex
MHV68	Murine herpesvirus 68
MOI	Multiplicity of infection
MZ	Marginal zone (cells)
NGFR	Nerve growth factor receptor
NHL	Non-hodgkin lymphoma
n.i	Non-infected (controls)
NK	Natural killer (cells)
OCT	Optimal cutting temperature (gel)
PAL	Periarteriolar lymphoid sheaths
PAMP	Pathogen associated molecular patterns
PBS	Phosphate-buffered saline
PCR	Polymerase chain reaction
PCMV	Promoter of the human cytomegaly virus
PEL	Primary effusion lymphoma
PFA	Paraformaldehyde
PFU	Plaque forming units
p.i	Post infection
Ref/cre	Rat embryo-fibroblast/ cre recombinase
R26	Rosa 26 gene locus
rpm	Revolutions per minutes
RT	Room temperature
SDS	Sodium dodecyl sulfate
SHM	Somatic hypermutation
S.O.C	Super optimal broth with catabolite repression medium
S1P	Sphingosine 1-phosphate receptor
TBS	Tris-buffered saline
TBST	Tris-buffered saline + Tween
TCR	T cell receptor
TD	Thymus dependent
TI	Thymus independent
TNF	Tumor necrosis factor
TPB	Tryptose phosphate broth
TPP	Thymidine triphosphate
UV	Ultraviolet
WHO	World Health Organisation



# CONTENTS

<b>ABSTRACT - ENGLISH</b>	i
<b>ABSTRAKT - DEUTSCH</b>	iii
<b>LIST OF FIGURES</b>	xvii
<b>LIST OF TABLES</b>	xviii
<b>NOMENCLATURE</b>	xix
<b>1 INTRODUCTION</b>	1
1.1 THE IMMUNE SYSTEM	1
1.2 B LYMPHOCYTE CELLS	2
1.2.1 DEVELOPMENT OF B CELLS	2
1.2.2 MARGINAL ZONE B CELLS AND FOLLICULAR B CELLS	4
1.2.3 B1 CELLS	5
1.2.4 B CELL ACTIVATION, SOMATIC HYPERMUTATION AND CLASS-SWITCHING	5
1.3 B CELL LYMPHOMAS	8
1.3.1 HODGKIN AND NON-HODGKIN LYMPHOMA (NHL)	9
1.3.2 CD30 AND NF- $\kappa$ B SIGNALLING IN B CELL LYMPHOMAS	9
1.4 GAMMAHERPESVIRUSES: EBV AND KSHV	12
1.4.1 ROLE OF THE VIRAL LMP1 AND LMP2A PROTEINS OF EBV	12
1.5 MHV68 MODEL AND BAC MUTAGENESIS	14
1.6 CD30 DEREGLULATION IN MICE	14
<b>2 AIM OF THESIS</b>	16
<b>3 MATERIALS</b>	18
3.1 BACTERIA	18
3.2 VIRUSES	18

3.3 EUKARYOTIC CELL LINES	19
3.4 PLASMIDS	19
3.5 ANTIBIOTICS	19
3.6 MEDIUM	20
3.7 MICE STRAINS	21
3.8 OLIGONUCLEOTIDES	21
3.9 ANTIBODIES	22
3.10 INSTRUMENTS, DEVICES, CHEMICALS AND REAGENTS	22
<b>4 METHODS</b>	25
4.1 MOLECULAR BIOLOGY METHODS	25
4.1.1 GEL ELECTROPHORESIS	25
4.1.2 PCR	26
4.1.3 ISOLATION OF DNA	29
4.1.4 NUCLEIC ACID CONCENTRATION DETERMINATION	31
4.1.5 RESTRICTION ENZYME ANALYSIS	31
4.1.6 WESTERN BLOT	31
4.1.7 MOLECULAR CLONING	35
4.2 CELL CULTURE METHODS	37
4.2.1 GENERAL CELL CULTURE TECHNIQUES	37
4.2.2 DISRUPTION OF CELLS BY FREEZING AND THAWING	38
4.3 BACTERIOLOGICAL METHODS	38
4.3.1 CULTIVATION OF BACTERIA	38
4.3.2 ESTABLISHMENT OF ELECTROCOMPETENT BACTERIA	38
4.3.3 ELECTROPORATION	38
4.3.4 CHEMICAL COMPETENT BACTERIA	39
4.3.5 BAC SHUTTLE MUTAGENESIS	39
4.4 VIROLOGY METHODS	40
4.4.1 TRANSFECTION OF BAC-MHV68-LMP2A DNA IN BHK-21 EUKARYOTIC CELLS FOR VIRUS RECONSTRUCTION	40
4.4.2 BAC SEQUENCE REMOVAL BY INFECTION OF REF/CRE CELLS	40
4.4.3 LIMITING DILUTION FOR SELECTION OF VIRUS WITHOUT THE BAC CASSETTE	41
4.4.4 GENERATION OF VIRUS STOCK SOLUTION	41
4.4.5 VIRAL GROWTH CURVES FOR VIRUS KINETICS ANALYSIS	42
4.4.6 PLAQUE ASSAY TO DETERMINE VIRAL TITER	42
4.5 ANIMAL EXPERIMENTS (IN VIVO)	43
4.5.1 INFECTION OF MICE	43

4.5.2 PREPARATION OF ORGANS; LUNGS, CERVICAL LYMPH NODES, SPLEEN AND PERITONEAL CAVITY	43
4.5.3 DETERMINATION OF THE VIRAL GENOMIC LOAD	45
4.5.4 VIRAL LATENCY DETERMINATION AND EX VIVO REACTIVATION ASSAY	45
4.5.5 FACS ANALYSIS (FLOW CYTOMETRY)	45
4.5.6 IMMUNOHISTOCHEMISTRY	46
<b>5 RESULTS</b>	48
5.1 GENERATION OF RECOMBINANT VIRUS MHV68-LMP2A	48
5.1.1 CLONING OF LMP2A CONSTRUCT WITH THE PCMV PROMOTER IN A SHUTTLE VECTOR	49
5.1.2 GENERATION OF THE MHV68-LMP2A VIRAL CONSTRUCTS	52
5.2 MHV68-LMP2A VIRUS CHARACTERIZATION AND PHENOTYPIC ANALYSIS	53
5.2.1 CHARACTERIZATION OF RECOMBINANT MHV68-LMP2A BY LEFT END GENOME PCR	53
5.2.2 IN VITRO ANALYSIS OF RECOMBINANT MHV68-LMP2A SHOWED LMP2A EXPRESSION AND UNAFFECTED VIRAL REPLICATION	55
5.2.3 IN VIVO ANALYSIS OF RECOMBINANT MHV68-LMP2A AFTER INTRANASAL INFECTION.	56
5.2.4 FACS ANALYSIS OF MHV68-LMP2A IN INFECTED WILD TYPE C57BL/6 MICE	60
5.3 EFFECT OF RECOMBINANT MHV68-LMP2A IN LMP1/CD30 $\gamma$ 1CRE MICE	66
5.3.1 SPLENIC WEIGHT AND FREQUENCY OF REACTIVATION	67
5.3.2 NO DIFFERENCES IN THE VIRAL GENOMIC LOAD IN MICE INFECTED WITH THE TWO RECOMBINANT VIRUSES	68
5.3.3 FACS ANALYSIS OF MHV68-NGFR AND MHV68-LMP2A IN CAR AND LC30 MICE	70
<b>6 DISCUSSION</b>	89
6.1 INFLUENCE OF MHV68 INFECTION IN MICE	89
6.2 GENERATION AND CHARACTERIZATION OF RECOMBINANT MHV68-LMP2A	90
6.2.1 IN VITRO ANALYSIS OF RECOMBINANT MHV68-LMP2A	90
6.2.2 IN VIVO ANALYSIS OF RECOMBINANT MHV68-LMP2A AFTER INTRANASAL INFECTION OF C57BL6 WILD TYPE MICE	91
6.3 INFECTION OF MHV68-LMP2A AND MHV68-NGFR IN CAR AND LC30 MICE	92
6.3.1 LOWER VIRAL GENOMIC LOAD LEVELS OF RECOMBINANT VIRUS COULD LIMIT EFFECTS STUDIED IN CHRONIC INFECTIONS	92
6.3.2 LMP2A LEADS TO ENHANCED GCB CELL FORMATION AND PROLIFERATION	93
6.3.3 REPORTER POSITIVE CELLS REPRESENT CELLS THAT ORIGINATE FROM THE GCB CELL REACTION	93
6.3.4 CD30 DYSREGULATION IN LYMPHOMA DEVELOPMENT	94
6.3.5 CONSTITUTIVE CD30 SIGNAL LEADS TO LARGER DIFFERENTIATION OF GCB CELLS TO B1 CELLS, ESPECIALLY THAT OF B1B IN PERITONEAL CAVITY, AS WELL AS PLASMA CELLS.	95

6.3.6 CONSTITUTIVE CD30 SIGNAL BLOCKS THE GC REACTION.	96
<b>7 CONCLUSION &amp; OUTLOOK</b>	<b>98</b>
<b>APPENDIX A RESTRICTION ENZYMES AND ADDITIONAL ENZYMES</b>	<b>101</b>
<b>REFERENCES</b>	<b>112</b>

# 1

## INTRODUCTION

### 1.1 THE IMMUNE SYSTEM

The purpose of the immune system is to defend the host organism against various infections and a wide range of pathogens, such as bacteria, parasites and viruses. The immune system is made up of the innate immunity and the adaptive immunity, both consisting of various specialized cells and mechanisms that allow the host to remove or contain the pathogens and infections effectively. The innate immunity serves as the first line of defence, inducing a rapid but relatively unspecific general response that detects and targets many different pathogens using similar defence mechanisms, such as that of the epithelial barriers, mucus, anti-bacterial and microbial enzymes and peptides. Receptors such as that of the TLR, intracellular NOD-like receptors and RIG-like helicases detect antigens on pathogens, thus activating signalling cascades such as that of the Nf- $\kappa$ B and MAPK, that lead to expression of pro-inflammatory substances and anti-viral cytokines (Interferons) that contain the infection. The innate immunity also helps in the initiation of adaptive immunity. While the innate immunity on one hand targets all pathogens unspecifically, the adaptive immunity brings about a highly specific response with the help of its wide spectrum of antigen

receptors, each enabling the targeting of specific pathogens that manage to survive the innate responses. Hence, it provides a form of specific protective immunity that will help in preventing re-infection. Cells of the immune system originate from pluripotent haematopoietic stem cells of the bone marrow, giving rise to two possible groups that of the myeloid progenitor cells consisting of granulocytes, mast cells and monocytes, and that of the lymphoid progenitor cells consisting of the B and T lymphocytes, and the natural killer (NK) cells. Another group of very important cells are the dendritic cells, which may develop from either the lymphoid or the myeloid progenitor cells and play a very important role in phagocytosis and in acting as a bridge between the innate and adaptive immunity. While the NK cells, granulocytes and the monocytes play a role in the innate immunity, the B and T lymphocyte are responsible for the adaptive immunity responses. Due to the differentiation and selection processes that these cells undergo, each lymphocyte possesses antigen specificity targeting a particular pathogen for elimination. The adaptive immunity can be further divided into the cell mediated immunity, played mainly by the T cells such as that of the cytotoxic T cells, which target intracellular pathogens such as viruses or even tumor cells, and that of the humoral immune responses played mainly by the activated B cells and their secreted antibodies [Murphy et al. \(2017\)](#).

## 1.2 B LYMPHOCYTE CELLS

### 1.2.1 DEVELOPMENT OF B CELLS

B cells develop from the haematopoietic stem cells in the bone marrow and migrate to the peripheral lymphoid organs where they can be activated by antigens. During their development in the bone marrow, they undergo a series of stages with the help of the different signals and cytokines, that enable them to finally exit the bone marrow as immature naive B cells with IgM and IgD transmembrane immunoglobulin as B cell receptors (BCR). The B cell receptor consists of a heavy chain and a light chain, either Kappa ( $\kappa$ ) or Lambda ( $\lambda$ ), with both having variable and constant regions. While the variable regions play a role in the antigen specificity of the immunoglobulin, the constant regions gives the immunoglobulin various different important effector functions in an immune response. The respective chains are located on different chromosomes with the heavy chain gene locus on chromosome 14, and the  $\kappa$  and  $\lambda$  light chain locus on chromosome 2 and 22 respectively. In the generation of the initial primary repertoire of the variable (V) region, somatic recombination plays a very important role in the light chain V-regions that are generated from 2 gene segments, variable (V) and joining (J) segments, whereas that of the heavy chain is generated from 3 gene segments, variable (V), diversity (D) and joining (J) gene segments. There are many different V, (D) and J segments and it is their random selection that creates the large diversity of V regions among immunoglobulins. Hence, the entire process generates each a V-region exon for the light chain

and heavy chain. The subsequent pairing of different light to heavy chain V regions in generating the antigen-binding site of the immunoglobulin later on, further diversifies the primary repertoire of the BCR and immunoglobulin specificities. The B cell moves through various stages starting as an early pro B-cell, that becomes the late-pro B-cell, and then the pre-B cell, small pre-B cell and finally an immature naive B cell is generated [Murphy et al. \(2017\)](#). In generating the B cell from the common lymphoid progenitor cells, the heavy chain is first generated before the light chain. Once a successful VDJ recombination occurs generating a productive heavy chain, allelic exclusion inhibits the rearrangement on the second chromosome ensuring only one functional heavy chain is produced [Roth \(2014\)](#). If non-functional, rearrangement begins on the second chromosome and if again is non-productive, the cell will undergo clonal deletion. This productive V region is paired together with the C region and they are assembled in a pre BCR complex, which consists of two invariant surrogate proteins resembling the light chains and also that of the Ig $\alpha$  and Ig $\beta$ , that are expressed from the pro B cell stage till death or till a plasma cell capable of secreting antibodies is formed. This assembly signifies a checkpoint where positive selection occurs to identify B cells with a functional heavy chain and hence pre-BCR. This induces a signal to expand the population producing many small pre-B cells and hence progression from the pro-B cells stage. Here, rearrangements of the light chain gene locus begins starting on the  $\kappa$  locus, with the V to J joining, followed by the  $\lambda$  locus only if rearrangement on both alleles of the  $\kappa$  locus fails to produce something productive, similar as that of the heavy chain VDJ rearrangement. The assembly of the light and heavy chains completes the formation of an immature B cell with the IgM as the BCR. Before the B cell leaves the bone marrow, a process of negative selection occurs to check for auto-reactivity. If the B cells bind strongly to self-antigen, it will undergo receptor editing to correct the self-reactive receptor or failing to do so, undergo apoptosis or remain inactivated in a state of anergy [Meffre & Wardemann \(2008\)](#) and [Melchers \(2006\)](#). Hence, the immature naive B cells that leave the bone marrow through the blood travel to the periphery and the peripheral lymphoid organs where they may be presented with antigens and be activated. More than 50% of early immature B cells are autoreactive but with correction or deletion, less than 10% exiting the bone marrow are reactive [Rowland et al. \(2010\)](#) and [Wardemann \(2003\)](#). Hence, only a small amount of immature B cells that leave the bone marrow end up as mature naive B cells [Srivastava et al. \(2005\)](#). Leaving the bone marrow, the immature B cells go through transitional stages before becoming a fully mature naïve B cell with both transmembrane IgM and IgD immunoglobulin [Bemark \(2015\)](#). The peripheral lymphoid organs, the spleen, lymph nodes and the mucosa associated lymphoid tissues are important areas that provide these newly formed immature B cells and transitional cells with signals for survival. A BAFF (B cell activating Factor) receptor, which is found on immature B cells receives such signals and together with the tonic BCR signalling, it aids in the selection of non-autoreactive immature B cells from the bone marrow and their transition to

transitional T1 cells and subsequently to T2 cells in the spleen [Rowland et al. \(2010\)](#). Hence, the B cell receptor plays a very important role in the maturation and recirculation of peripheral B cells because without the B cell receptor, the B cells will not receive survival signals and will die. The transitional 2 (T2) cells can then become either the follicular B cell or the marginal zone B cell in the spleen. Even in the development of B1 cells, the BCR has been shown to be important in B cell development and proliferation [Macias-Garcia et al. \(2016\)](#).

### 1.2.2 MARGINAL ZONE B CELLS AND FOLLICULAR B CELLS

The development of the B cells as explained earlier, may be referred to as the conventional B cell development or that of B2 cells. They are developed in the bone marrow and undergo maturation in follicles in the peripheral lymphoid organs. As mentioned, they have various fates. (i) They may leave the spleen to the peripheral blood, (ii) enter the follicles becoming follicular B cells which make up the main population of B cells in the body or (iii) remain in the marginal zone as marginal zone B cells of the spleen. The repertoire of the BCR and the strength of its signal plays a role in deciding whether a T2 cell in the spleen becomes a follicular B cell or a marginal zone B cell [Pillai & Cariappa \(2009\)](#) and [Carey et al. \(2008\)](#). The Marginal zone B cells and the B1 cells, discussed later, are different in a way because they do not reside in such B cell follicles. The spleen is made up of the white pulp that is supplied by a central artery. In mice, the branches of the arterial supply terminate in the marginal sinus, which is the space between the white pulp and the marginal zone, or passes through the sinus and marginal zone to end in the red pulps venous system. In humans, part of the supply ends in the perifollicular zone which surrounds the entire white pulp. The white pulp resembles lymph nodes and consists of the periarteriolar lymphoid sheaths (PALS), which is the T cell zone that surrounds the arterial vessels, and the B cell follicles, which are the B cell zones where clonal expansion, somatic hypermutation (SHM) and isotype switching (CSR) of activated B cells occur. It is in these follicles where the germinal center reaction occurs and the follicular B cells receive signals from the follicular dendritic cells, together with the subsequent help from the T cells (T cell dependent activation) at the borders, thus differentiating into memory B cells or long-lived plasma cells. Hence, while marginal zone B cells remain in the spleen, the follicular B cells that make up the largest B cell population maybe be found in the both in spleen and lymph nodes and may circulate the body [Carey et al. \(2008\)](#). Marginal zone B cells are not the only cells that reside in the marginal zone as resident macrophages and dendritic cells may also be found here when they enter the white pulp from the red pulp during blood flow across the marginal sinus. Transitional cells (T1, T2, T3) that end up as marginal zone B cells differ from the follicular B cells in that they receive certain special signals such as that of the Notch2 signal, and they posses Sphingosine-1-phosphate(S1P) receptors which respond to S1P enabling them to remain in the marginal zone instead of traversing into the follicles to become follicular B cells

Mebius & Kraal (2005) and Pillai & Cariappa (2009). Some of these signals are thought to arise as the B cells get lodged in this marginal zone. Their location around the marginal sinus enables the marginal zone B cells, the macrophages and dendritic cells to come into contact with common pathogens in blood and play a role in innate immunity Martin et al. (2001). As such, the marginal zone B cells can be induced to secrete IgM antibodies after differentiation to short-lived plasma blasts. Marginal zone B cells may also pick up antigen and function as APCs, subsequently shuttling these antigens from the blood to the follicle area, thus presenting these antigens to the follicular area and the follicular dendritic cells Arnon et al. (2012). In addition, marginal zone B cells may be involved in T-dependent B cell responses indirectly by activating naïve CD4 T cells present at the borders of the follicles and play a role in initiating the adaptive immune system Allman & Pillai (2008) and Attanavanich & Kearney (2004). T1 cells may also differentiate directly to the marginal zone B cells directly Carey et al. (2008).

### 1.2.3 B1 CELLS

While the conventional B2 cells and hence FO B cells and MZ B cells are first produced after birth predominantly in adult life, another group of cells found also in mice, the B1 cells, are found mainly in the peritoneal and pleural cavities and only seldom in the spleen and lymph nodes and are fetally derived. B1 cells are different from the conventional B2 cells as they do not express CD21 or CD23, but only express low levels of B220 and IgD and high levels of IgM. B1 cells from the peritoneal cavity differ from those in the spleen in expressing the Mac-1 surface marker, and two sub-populations B1a (CD19+, CD11b+, CD5high) and B1b (CD19, CD11b+, CD5low) exist and making up of about only 5% of all B cells (in both mice and humans) Kantor (1993). B1 cells, similar to the marginal zone B cells, may play a role in innate immunity in a thymus cell independent manner. B1a cells, being partly activated, constitutively produce the natural antibodies to protect against infection thus lowering of bacterial burden. On the other hand, the B1b cells produce the antibodies after antigen activation, clearing bacteria and permitting survival in generating long-lasting IgM memory cells also in a thymus cell independent manner Alugupalli & Gerstein (2005) and Haas et al. (2005). Thus B1-cells contribute to the large portion of the IgM that circulates in the blood of mice even in the absence of infection Macias-Garcia et al. (2016).

### 1.2.4 B CELL ACTIVATION, SOMATIC HYPERMUTATION AND CLASS-SWITCHING

B cells play a very important role in secreting antibodies that serve to protect the host organism from pathogens in the adaptive immune response. In order to do this, the mature B cells consisting of the subsets of B cells described earlier, the MZ B cells, FO B cells, and B1b cells will have to bind antigens and be activated first. Only B1a cells do not need to be antigen activated and are able to secrete natural antibodies continuously Alugupalli & Gerstein (2005). Out of the 3 sub-

set of B cells, the FO B2 cells are able to form secondary follicles and form the germinal center undergoing somatic hypermutation and class-switch recombination. In the B cell activation process, some pathogenic antigens, however are able to bind to B cells and induce responses in them without the need of T cell help. Such non-protein antigens like bacterial polysaccharide LPS and flagellins, are called thymus-independent antigens. The Marginal zone B cells and B1 cell are able to bind to various TI antigens inducing differentiation to form mainly short-lived IgM secreting plasmablasts [Fairfax et al. \(2008\)](#). They differentiate much more rapidly in comparison to B2 cells initially hence providing immediate immunity [Martin et al. \(2001\)](#). TI mechanisms can be divided into categories of TI1 antigens such as that of LPS or CpG that induce TLRs, and TI2 antigens that are relatively multivalent resulting in extensive BCR cross-linking [Bemark \(2015\)](#). FO B cells, however, may be activated by either TI mechanisms producing mainly plasmablasts that are short lived, or by TD (Thymus dependent) mechanisms with the help of T helper cells in their differentiation to plasma cells or memory B cells, which are relatively long-lived, conferring live long immunity for subsequent infections with the pathogen. The TD response is thought to be the response that generates high affinity somatic hypermutated antibodies and germinal center reactions, although the TI2 mechanism has been shown to generate rapid but shorter germinal centers and subsequently memory (during immunization or vaccinations) [Lentz & Manser \(2001\)](#). B1b cells for instance have been shown to produce long lived IgM memory B cells [Alugupalli et al. \(2004\)](#) and [Obukhanych & Nussenzweig \(2006\)](#). The TD response is said to be a two part response. In the first part, antigens enter the follicle with the help of dendritic cells; the follicular and interdigitating dendritic cells. The follicular dendritic cells (FDC) which are found mainly in the follicles present the antigens to the B cells while the interdigitating dendritic cells (IDC) present the antigens to the T cells, thus priming the T cells. In the spleen, the marginal zone B cells as mentioned may also play a role in presenting these antigens to the follicle areas. On binding of the antigens to the BCR and TCR of the B and T cell respectively, both subsets undergo clonal expansion together and move to the borders of the follicles from their respective zones where they may be able to interact better with one another. After antigen processing, epitopes of the digested antigens are presented on the MHC II of the B cell. Only CD4+ T helper 2 cells that were earlier primed by the same antigen will recognise the MHCII-antigen complex, thus binding to the B cell. This process called linked recognition induces B cell activation. The B cell co-receptor complex consisting of surface markers such as CD19, CD21 and CD81 may co-ligate with the BCR increasing the BCR signalling strength thus amplifying this B cell activation process. Various other receptors on both the B and T cell play important roles in B cell activation. CD40L found on T cells binds to CD40 on B cells increasing their proliferation and up-regulating several other co-stimulatory molecules such as that of the B7 markers. In the presence of the co-stimulatory molecules, T cells secrete cytokines that further regulate B cell proliferation and immunoglobulin secretion. CD30L expressed on T cells and the BAFF cytokine secreted by

dendritic cells also play a part in B cell proliferation. On doing so, the stimulated B cells proliferate further, some migrating out of the follicles into the extrafollicular areas (for the spleen between the T zone and red pulp and for the lymph nodes in the medullary cords) establishing the primary focus, and differentiating to the short-lived plasmablasts that secrete IgM antibodies which are effective in the primary infection. Thus, this concludes the first step of the TD extrafollicular response. The second step further prepares the host for a chronic infection, which is the task of the long living plasma cells and memory cells. Some activated B cells from the primary focus migrate back into the follicles, proliferating and forming the secondary follicle with a germinal center. The germinal center is made up of the dark zone densely packed with rapidly proliferating centroblasts and the light zone with loosely packed centrocytes. In the dark zone, as the centroblasts proliferate and rapidly divide, an enzyme, the Activation induced cytidine deaminase (AID), adds mutations at a high rate [Murphy et al. \(2017\)](#) to the V regions of the light and heavy chains of the Ig receptor. The mutations generate new combinations that may be functional but are often non-functional. This generates the secondary repertoire of variability on the BCR. The newly formed centrocytes, now in the light zone, interact with the FDCs. After somatic hypermutation, the centrocytes with BCR that bind stronger to the antigens presented by the FDCs will be selected and undergo further expansion. Hence, this process of affinity maturation selects the B cells with BCRs that recognize the antigens better so that memory cells producing high affinity antibodies may be produced. Another process of equal importance is the class switch recombination or class switching. Each BCR or immunoglobulin has a V region and a C region. While the V region is responsible for specificity to the antigen, the C region is important in deciding what immunoglobulin type is produced. The constant region on the DNA is made of several important genes and with the help of the AID enzyme again, the removal of these genes may occur leading to the switching from the IgM isotype to the other isotypes such as to the IgG, playing important effector functions.

Hence, while the plasmablasts form the primary focus and are mainly short-lived cells that secrete IgM antibodies that serve to immediately protect the infected individual, the T-dependent germinal center reaction with somatic hypermutation and class switch recombination gives rise to memory cells and plasma cells which secrete higher affinity immunoglobulin antibodies that provide a more effective and specific long lasting humoral immunity for the individual. This protects the organism against chronic infections if they were to persist.

While the B cell activation process and germinal center reactions are important in conferring immunity to the organism, several problems may arise during B cell proliferation, differentiation and the regulation processes which may lead to tumors and lymphoma formation.

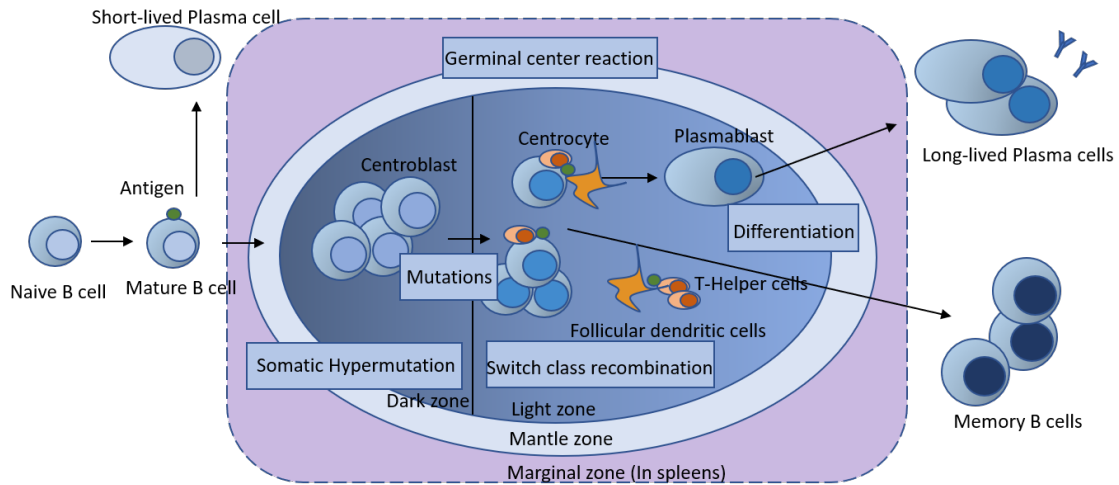


**Figure 1.1: Schematic diagram showing the different cell surface receptors together with the classical canonical and alternative non-canonical NF- $\kappa$ B signalling cascades.** The primary B cell follicles in the secondary lymphoid organs, for example, in the spleen and lymph nodes, become activated germinal centers after receiving antigens and T cell help. They undergo SHM and CSR producing plasma cells and memory B cells that are able to secrete antibodies / immunoglobulin of high affinity as part of the adaptive immune system to fight off chronic infections. During the process of clonal expansion and proliferation in the germinal center, naive B cells are displaced into the mantle zone. Majority of the mutations during clonal expansion are disadvantageous for the cell conferring reduced affinities. These disadvantaged cells are removed by apoptosis. Marginal zones with predominant B cell rich populations in between the B cell follicles and T cell area are found mainly in the spleens and not usually in the lymph nodes. (Adapted from Klein & Dalla-Favera (2008) and Küppers (2005)).

### 1.3 B CELL LYMPHOMAS

Lymphomas are cancers derived from the immune system and can be classified into the hodgkin lymphoma (HL) or the non-hodgkin lymphoma (NHL). While lymphomas may have origins from T cells or NK cells, the majority of lymphomas are, however, B cell lymphomas that arise from the different stages of development and maturation of the B cells. Most of these take place during the germinal center reaction or the post-germinal center reactions because it is during these phases, where somatic hypermutation (SHM) and class switch recombination (CSR) occur in which modifications of the nucleotides and double strand breaks arise, favouring translocations Küppers (2009). The translocation of an Ig locus to a locus where an oncogene is located, generates a proto-oncogene, and this process is a trademark of B cell lymphomas Küppers (2005). Apart from these mutations and translocations, other signalling pathways such as the NF- $\kappa$ B activation pathway play a part in the multi-step transformation of the B cell. These pathways contribute additionally to the proliferation of cells and dysregulation of tumor suppressor genes, which in turn lead to the prevention of apoptosis and subsequent lymphoma formation Jost & Jurgen (2006).

### 1.3.1 HODGKIN AND NON-HODGKIN LYMPHOMA (NHL)

The NHL make up 75% of all lymphomas, and consist of T and NK cell lymphomas but the majority of the NHL, about 85%, have B cells origins. The tumors of the NHL can be slow growing or aggressive with prognosis being very heterogenous. NHL are usually related to translocations in which a protooncogene is generated, promoting proliferation. Several other alterations that promote cell immortality and hinder apoptosis may also be present. For example, in the case of Burkitt lymphoma, chromosomal translocation of t(8:14) leads to a translocation of a cMYC oncogene to a Ig heavy chain locus, generating a protooncogene that transforms the B cells [Klein & Dalla-Favera \(2008\)](#) and [Evans & Hancock \(2003\)](#). The Primary Effusion lymphoma (PEL) on the other hand, which is a subtype of the DLBCL, undergoes NF- $\kappa$ B activation and an inhibition of additional anti-apoptotic pathways. One such anti-apoptotic pathways is the the fas-mediated caspase activation, which is responsible for the immortalisation of the PEL post GC- B cells; the plasmablasts [Chen et al. \(2007\)](#) and [Küppers \(2005\)](#). While the NHL are tumors that are of various origins, either B cell, T cell or natural killer cells, the malignant cells of the HL are derived from lymphocytes of the B cell lineage. The key feature of the HL is the presence of pathogenic Hodgkin Reed-Sternberg (HRS) cells, which are of B cell lineage [Küppers et al. \(1996\)](#). One may recognise two separate groups, one being that of the nodular lymphocyte-predominant HL and the other, that of the classical HL, which in turn may be categorized based on histology, into the nodular sclerosis, mixed cellularity, lymphocyte rich and lymphocyte depleted classical hodgkin lymphoma. The HRS cells that characterize the (classical) HL, although derived from lymphocytes of B cell lineage, no longer resemble B cells due to the loss of most of the usual B cell gene expression and hence do not posses a BCR. As mentioned, the BCR is essential for the survival of the B cells and thus, without the BCR, the cell will undergo apoptosis. However, the HRS cells are able to avoid apoptosis due to several other factors that activate pathways such as that of the Jak-Stat, p53 and NF- $\kappa$ B pathways, which in turn activate anti-apoptotic processes or genes. Some of the genes that are altered and later converge to these pathways include that of the REL gene, NF- $\kappa$ BIA and NF- $\kappa$ BIE genes, and the MDM2 alterations [Küppers \(2009\)](#). HRS cells also posses a high expression of the TNFR superfamily of surface markers (CD40 and CD30) which lead to the constitutive activation of these NF- $\kappa$ B pathways as well, hence preventing apoptosis of these BCR deficient GC cells

### 1.3.2 CD30 AND NF- $\kappa$ B SIGNALLING IN B CELL LYMPHOMAS

CD30 is a surface marker found on various cells, particularly those of activated lymphoid B and T cells, and it belongs to the tumor necrosis factor receptor superfamily, which consists of many other members such as the CD40 [Sotomayor et al. \(2014\)](#). CD30 plays a role in several malignancies including that of malignant lymphomas. For example, around 15-20% of B cell lymphomas

are CD30+ and its expression has been observed in more than 95% of classical HL and even other lymphomas in the NHL such as that of the PEL subtype of the DLBCL [Leval & Gaulard \(2010\)](#) and [Sotomayor et al. \(2014\)](#). Such lymphomas belong to the family of CD30+ lymphoproliferative disorders, in which antibodies that target these CD30 molecules have been used in their therapy. In mice, it has been shown that stimulation of the CD30 receptors lead to proliferation and production of antibodies. In the case of human B cells, activation of the CD30 together with the CD40 blocks class switching and antibody production [Chiarle et al. \(1999\)](#) and [Cerutti et al. \(1998\)](#). A deregulated CD30 expression also drives B cells in expressing a HL or PEL like phenotype [Fiedler \(2011\)](#) and [Sperling et al. \(2019\)](#). Various factors play a role in the driving of these phenotypes as CD30 is known to involve many interactions and even activate many pathways such that of the JNK, p38, MAPK and the NF- $\kappa$ B pathways but, whether it activates the former or latter is dependent on cell conditions, type and signals [Schneider & Hübinger \(2002\)](#) and [Kennedy et al. \(2006\)](#). CD30 downregulation is brought about when anti-CD40 and germinal center / activated B cells interact. Furthermore, not only is CD30 expression reduced, but class-switching of those germinal center/ activated B cells occur. This was the case when CD40 was solely engaged. However, in cases in which both CD40 and CD30 are involved, class switching was inhibited [Chiarle et al. \(1999\)](#). Apart from CD30, another important pathway, which activates anti-apoptotic mechanisms is that of the NF- $\kappa$ B activation pathway as mentioned.

NF- $\kappa$ B consists of a small group of transcription factors of a family namely the RelA (p65), c-Rel, RelB, NF- $\kappa$ B1 (p50 with precursor 105) and NF- $\kappa$ B2 (p52 with precursor100), which play multiple functions in the regulation and continued survival of immune cells [Jost & Jurgen \(2006\)](#). Two pathways, that of the canonical and non-canonical or alternative pathway lead eventually to the activation of the NF- $\kappa$ B family of proteins that penetrates into the nucleus and are responsible for the expression of several target genes that are important for immunity, proliferation, and anti-apoptotic mechanisms [Lin & Karin \(2003\)](#). Several experiments done throughout the years have shown the importance of the NF- $\kappa$ B proteins and the proteins of the activation pathways of NF- $\kappa$ B in the functions mentioned. For example, defects in the p50 and p52 subunits led to defects in immunity in mice while constitutive activation of the IKK $\beta$  in mice B lymphocytes led to the proliferation and survival of resting B cells [Sha et al. \(1995\)](#), [Franzoso et al. \(1998\)](#) and [Sasaki et al. \(2006\)](#). While the canonical pathway is activated by the several stimuli such as that of pro-inflammatory cytokines, pathogen-associated molecular patterns (PAMP) and the BCR, and is necessary mainly for innate immunity, the alternative pathway is activated by cell surface receptors playing a role mainly in development of the lymphatic organs and adaptive immunity [Senftleben \(2001\)](#). An example of such a cell surface receptor is that of the BAFF receptor, which, as mentioned, plays an important role in maturation and cell differentiation of B cells. CD30 and CD40 on the other hand, are able to activate both the canonical and alternative pathways. Hence, constitutive activation of

the NF- $\kappa$ B pathways and proteins in both the canonical and non-canonical pathways plays an important role in lymphomagenesis and the transformation of cells. It is, however not as simple as it seems because there are various cross talks which are important in determining the roles of the NF- $\kappa$ B proteins such as the cross talk between both the pathways or even the crosstalk between NF- $\kappa$ B and another pathway that of the PI-3kinase/Akt pathway in PEL formation [Cancro \(2009\)](#) and [Hussain et al. \(2012\)](#) and [Lin & Karin \(2003\)](#). It has been shown that Akt inhibits cell death as well and this in turn enhances the NF- $\kappa$ B pathway [Madrid et al. \(2000\)](#). The BCR activates several pathways downstream such as the PI3K/ Akt kinase pathways and in turn the mTOR and protein kinase C which upregulates transcription factors including that of NF- $\kappa$ B. As such, these pathways are implicated in the survival of certain lymphoma cells [Chavez et al. \(2013\)](#) and [Woyach et al. \(2012\)](#). Apart from the stimuli mentioned, the gammaherpesviruses, namely the Epstein-Barr Virus (EBV) and the Kaposi Sarcoma associated Herpesvirus (KSHV) are associated with classical HL and some NHL. They may activate the NF- $\kappa$ B pathway through the production of their oncogenic viral proteins as well, hence aiding lymphomagenesis.

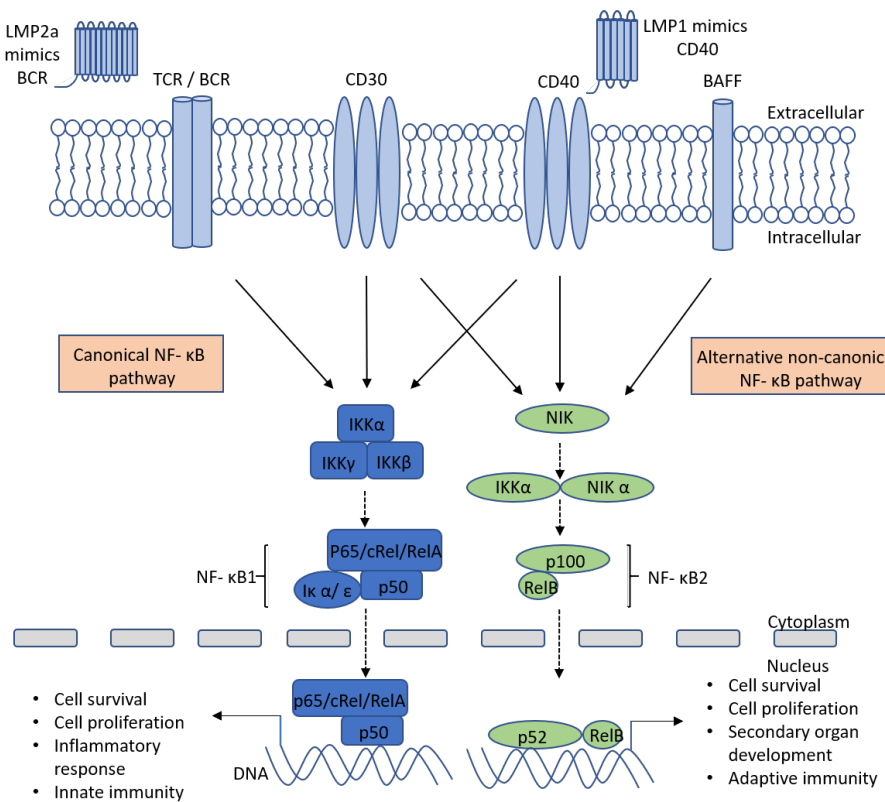


**Figure 1.2: Schematic diagram showing the different cell surface receptors together with the classical canonical and alternative non-canonical NF- $\kappa$ B signalling cascades.** Activation of the canonical and non-canonical pathways through one of several cell surface receptors leads to expression of proteins that in turn contribute to cell survival, proliferation and either responses to promote innate and adaptive immunity respectively. Both the CD30 and CD40 cell surface receptors are able to activate both pathways, whereas the TCR or BCR activate only the canonical pathway. The BAFF, on the other hand, activates only the non-canonical pathway. While LMP2a mimics that of the BCR, the LMP1 transmembrane protein mimics CD40 (Adapted from [Cancro \(2009\)](#) and [Jost & Jurgen \(2006\)](#)).

## 1.4 GAMMAHERPESVIRUSES; EBV AND KSHV

In the *Herpesviridae* family, three subfamilies are found classified based on the architecture of the virion, namely the *Alphaherpesvirinae*, the *Betaherpesvirinae* and the *Gammaherpesvirinae*. The latter in turn consists of the lymphocryptovirus with the human Epstein-Barr Virus (EBV), the Macavirus, the Percavirus and the Rhadinovirus with the Karposi Sarcoma Associated Herpesvirus (KSHV) [Ackermann \(2006\)](#). The gammaherpesviruses are the only viruses in the *Herpesviridae* family that are able to exhibit oncogenic effects and cause tumors. Viruses in this subfamily replicate in lymphoblastoid cells and are usually specific for either B or T lymphocytes. These viruses possess various important characteristics of oncogenic viruses that enable them to persist in the host cell and transform cells forming tumors. KSHV produces latent proteins, such as that of the V-FLIP protein which leads to an aberrant NF- $\kappa$ B signalling that in turn aids the lymphomatogenesis process in PELs and is responsible in the pathogenesis of the Multicentric Castleman's Disease (MCD) and Kaposi Sarcomas. EBV, on the other hand, expresses several other latent proteins responsible for a wide variety of other diseases. In cases of PEL, EBV, which is thought to play a role in promoting proliferation of the PEL cells, has been found to coexist together with KSHV which in this case aids in the maintenance and sustenance of the tumor cells [Mack & Sugden \(2008\)](#). EBV is responsible mainly for various other lymphomas and diseases such as that of the Burkitt's lymphoma, post transplantation lymphoma, Hodgkin's lymphoma and nasopharyngeal carcinoma [Taylor & Blackbourn \(2011\)](#) and [Knipe & Howley \(2013\)](#). It is the type of latency that determines the different proteins expressed and hence the formation of various respective diseases. Classical HL and NHL formation are due to the production of the latency II (default programme) proteins in which LMP1 and LMP2a viral proteins are expressed [Silva & Oliveira \(2011\)](#). This plays a huge role in the pathogenesis.

### 1.4.1 ROLE OF THE VIRAL LMP1 AND LMP2A PROTEINS OF EBV

LMP1 is a membrane protein consisting of six transmembrane domains, with half of the LMP1 within the plasma membrane and its amino and C terminal ends projecting towards the cytoplasm. Playing several roles, LMP1 is an oncoprotein that constitutively mimics the tumor necrosis factor (TNF) receptor CD40. Since CD40 is the main pro-survival TNF receptor [Knipe & Howley \(2013\)](#), it is essential for the conversion of primary B lymphocytes to lymphoblastoid cell lines (LCLs), and thus, the transformation necessary for tumorigenesis. Through the TNF receptor and associated proteins, LMP1 stimulates activation pathways, such as that of the MAPK, PI3K/Akt and that of the NF- $\kappa$ B pathway in cells, stimulating growth and preventing apoptosis [Knipe & Howley \(2013\)](#). By inducing Bcl2 anti-apoptotic protein, LMP1 also protects B lymphocytes from apoptosis leading to their continued survival. LMP1 interferes in several other pathways such as that of the p38 MAPK as mentioned, and the Janus kinase/signal transducers and activators of transcription, all of which may

promote lymphomagenesis and tumor growth Thompson & Kurzrock (2004). Lastly, LMP1 may also play a role in immune evasion as it induces the induction of apoptosis of CTLs and the inhibition of T cell proliferation together with a reduction of natural killer (NK) cell cytotoxicity Knipe & Howley (2013). While LMP1 mimics the CD40 receptor, the LMP2a mimics a constitutively active BCR signal. This BCR signal is an essential factor for normal B cell development. By mimicking the BCR, the LMP2a enables LCL growth even if a functional BCR is lacking, such as the case in classical Hodgkin lymphoma and in the PELs, a type of NHL. LMP2a may also play a similar role as LMP1 in inhibiting apoptosis and B cell survival through the signal transduction cascades that lead to the activation of PI3K, Akt and that of Ras. Moreover, LMP2a helps B cells to colonize peripheral lymphoid organs and hence avoid the normal B cell checkpoints by activation of the Erk/MAPK pathway Knipe & Howley (2013). Similar as that of LMP1, the role of LMP2a in immune evasion is in part due to the induction of apoptosis in CTLs and its suppression of antiviral responses by degradation of the interferon (IFN) receptors found on epithelial cells.

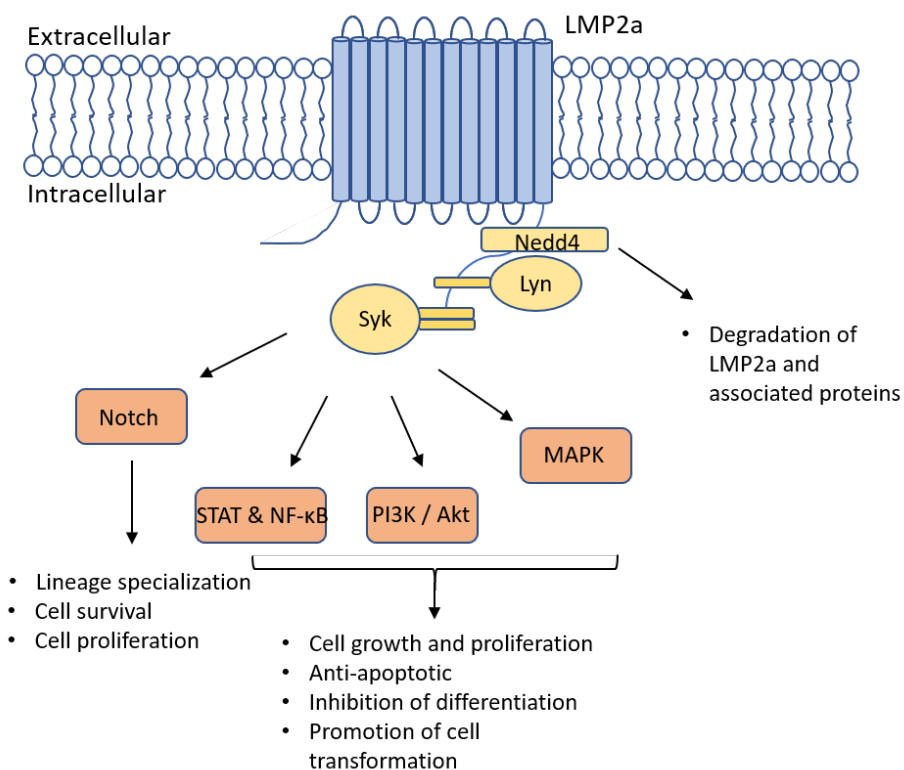


**Figure 1.3: Schematic diagram showing the transmembrane protein LMP2a and the various signalling pathways and cascades that it triggers.** While the Nedd4 pathways lead to self degradation of the LMP2a and associated proteins, that of the STAT, NF- $\kappa$ B, PI3K/Akt and MAPK pathways are responsible for cell growth and proliferation, promotion of cell transformation as well as anti-apoptotic effects on the cells. (Adapted from Knipe & Howley (2013))

## 1.5 MHV68 MODEL AND BAC MUTAGENESIS

MHV68 belongs to the group of gammaherpesviruses and is related based on genomic sequences to the human gammaherpesviruses EBV and KSHV [Simas & Efstathiou \(1998\)](#). Furthermore, in addition to this homology, the complete nucleotide sequence of the MHV68 is already known [Virgin et al. \(1997\)](#). This makes the MHV68 appropriate to be used as a vector to test the effects and interactions of gammaherpesvirus in animal models. While the MHV68 establishes acute phase infection in the lungs of intranasal infected mice by 9 to 12 days post infection, it is able to undergo latency similar to that of the human gammaherpesviruses and persist in the organism [Barton et al. \(2011\)](#). It is thus able to establish chronic infections in mice. The cloning of the MHV68 as an infectious bacterial artificial chromosome (BAC) and site directed mutagenesis of the BAC-DNA has however, enabled even more promising feats to be acknowledged. On one hand, BAC used for cloning instils stability and enables the insertion of large sequences such as that of the MHV68. Site directed mutagenesis, on the other hand, allows for homologous recombination which in turn is used for the insertion of various specific regions of genome into the BAC-MHV68 vector that was generated [Adler et al. \(2001\)](#) and [Adler et al. \(2003\)](#). After site directed mutagenesis and introduction of a segment of interest into the BAC-MHV68, the excision of the BAC vector leads to production of viral progenies consisting of only MHV68 genome together with the cloned segment of interest. Infection with these recombinant MHV68 allows for protein expression of the gene segment of interest in the eukaryotic host. Hence, the effects of the cloned viral genome and its expression in vivo can be investigated. For this project, the LMP2a gene segment together with the PCMV promoter was cloned as the segment of interest. Eventually, viral progenies containing the upstream PCMV promoter, LMP2a viral genome and MHV68 are produced with which eukaryotic hosts are infected. LMP2a protein can then be produced in vivo, and its effects in relation to a deregulated CD30 can be investigated in this project.

## 1.6 CD30 DEREGLULATION IN MICE

In order to achieve a deregulated constitutively activated CD30 signal, the intracellular signalling portion of the CD30 is fused with the transmembrane domain of the EBV LMP1 protein. The transmembrane domain of the LMP1 causes the receptors in the plasma membrane to aggregate leading to the transduction of a ligand independent signalling cascade of CD30. The LMP1/CD30 (LC39) genome segment is flanked by STOP signal and a hCD2 reporter segment. In addition, the STOP signal is flanked by loxP sites. These sequences are inserted into the *rosa26* locus in murine embryonal stem cells, which are used to generate mice. These mice would then consist of cells containing this construct. For the cells to successfully transcribe the LMP1/CD30 (LC39) gene and

subsequently express the transmembrane LMP1 coupled to the intracellular signalling CD30 domain, the STOP sequence upstream needs to be excised by a cre recombinase that is able to recognise the loxP sites and excise the STOP sequence that is between the loxP sites. As mentioned, the majority of B cell lymphomas are a result of mutations during the maturation phase that B cells undergo, which is mainly during the germinal center reaction process Küppers (2005). Hence, for the expression of a cre recombinase,  $C\gamma 1$ -cre mice are used. In these mice, the Cre sequence together with an internal ribosome entry site (IRES) are inserted into a 3' region of the  $C\gamma 1$  locus between the polyA site and membrane coding exons as in the schematic figure shown Casola et al. (2006). The  $C\gamma 1$  gene segment refers to the immunoglobulin constant region gene segment that is transcribed specifically in germinal center B cells. Upon activation, the germinal center reaction generates B cells that are able to produce high affinity class switched antibodies as shown in **Figure 1.1**. Hence, in the presence of immunization such as infection with viruses, germinal center B cells would undergo activation. Through the process of clonal expansion, class-switching and somatic hypermutation, the transcription of the Ig  $\gamma 1$  constant region together with the cre recombinase would occur. Thus, cre/loxP mediated conditional gene targeting is made use in this particular project, which couples germinal center B cell activation to the activation of the LMP1/CD30 construct. This enables mice with activated germinal center B cells to also have a deregulated constitutively activated CD30 signal. In order to obtain mice with both the LMP1/CD30 and the  $C\gamma$  construct (LMP1/CD30 $^{+/-}$ / $\gamma$ cre $^{+/-}$  mice),  $C\gamma$ cre $^{+/-}$  mice are paired with LMP1/CD30 $^{+/-}$  mice and the desired heterozygote offsprings are selected.

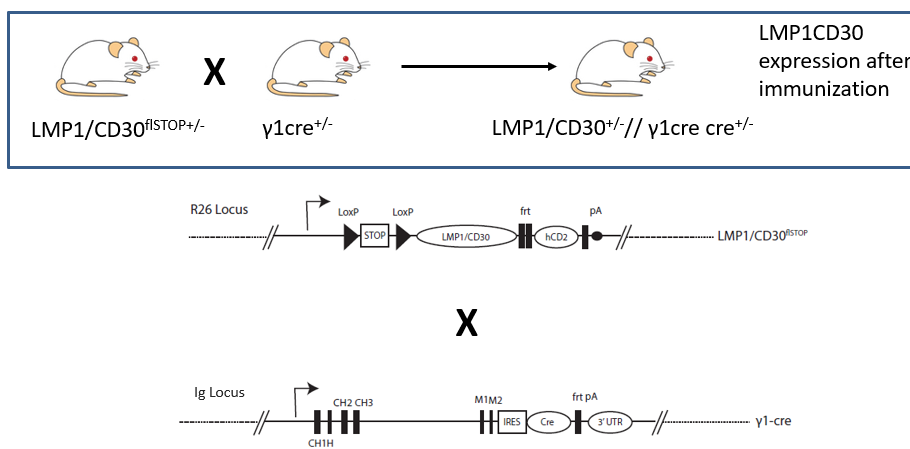


**Figure 1.4: Schematic diagram showing the generation of LMP1/CD30  $\gamma 1$ cre mice.** The LMP1/CD30  $\gamma 1$ cre mice contain the Cre gene on the Ig locus while the LMP1/CD30 gene on the R26 locus. Immunization in the form of viral infection leads to the expression of Ig locus thus transcribing and expressing the Cre recombinase. This would in turn lead to the activation and expression of the genes on the R26 locus and the subsequent expression of the LMP1/CD30 protein leading to the constitutive expression of CD30 (adapted from Casola et al. (2006)).

# 2

## AIM OF THESIS

The two gammaherpesviruses, EBV and KSHV, are classified according to the World Health Organisation (WHO) as tumor viruses. Although it has been shown that both viruses play a part in the tumorigenesis in CD30+ B cell lymphomas, little is known about how these viruses contribute to the initiation or maintenance of these tumors.

The aim of this thesis project was to investigate the interplay between a deregulated, constitutive active CD30 expression and a gammaherpesvirus infection in the pathogenesis of PEL and HL. To this end, a recombinant MHV68 containing the Epstein-Barr viral protein LMP2a was created and used to infect LMP1/CD30 $\gamma$ 1Cre mice (LC30 mice) intraperitoneally. This results in the induction of constitutively active CD30 signaling in all B cells responding to viral infection. Since CD30 expression and EBV infection are known to be involved in PEL and HL pathogenesis, it should be examined whether this induces a PEL-like or HL-like phenotype in these mice.

The thesis consists of two parts: In the first part, a recombinant MHV68-LMP2a was constructed and subsequently tested in wild-type, C57BL/6 mice in comparison to a wild-type MHV68.

In the second and main part, the recombinant MHV68-LMP2a was used to infect LMP1/CD30 $\gamma$ 1cre mice (LC30 mice) and wild type CAR  $\gamma$ 1cre mice (CAR mice). To detect virally infected cells, a recombinant MHV68-NGFR reporter was used as a control virus. The influence of the viral infection

on the expansion of different B cell populations over time was analysed. This mouse model may serve to better understand the contribution of the EBV infection in the process of malignant transformation of CD30+ B cells. Finally, this mouse model may be applied as a preclinical model in the testing of novel therapies.

# 3

## MATERIALS

### 3.1 BACTERIA

<i>E.coli</i> DH10B:	Electrocompetent <i>E.coli</i> with recA mutation
<i>E.coli</i> DH10B-MHV68:	Electrocompetent <i>E.coli</i> with recA mutation, carrying MHV68 cloned as a BAC
MAX Efficiency DH5 $\alpha$ :	Chemical competent bacteria

### 3.2 VIRUSES

MHV68 BAC-derived wildtype:	Wildtype virus derived from BAC-cloned MHV68
-----------------------------	---

### 3.3 EUKARYOTIC CELL LINES

BHK-21 (ATCC CCL-10):	Baby hamster kidney fibroblasts
NIH-3T3 (ATCC CRL-1658):	Mouse embryo fibroblasts
Ref/cre Cells:	Rat embryo-fibroblast expressing Cre recombinase
LCL D2098 Cells:	EBV infected lymphoblastoid cell line

### 3.4 PLASMIDS

pEBNA-G-LMP2A	Plasmid with the LMP2a construct for further cloning and preparation
pCR3	Vector with the PCMV promoter and BGH poly A tail for cloning of LMP2a construct
pST76K-SR+oligonucleotides	Shuttle vector for the BAC Mutagenesis
MHV-68 BAC	Entire MHV68 genome cloned as a BAC

### 3.5 ANTIBIOTICS

Kanamycin	Concentration in the LB plates: 50 $\mu$ g/mL
Ampicillin	Concentration in the LB plates: 100 $\mu$ g/mL
Chloramphenicol	Concentration in the LB plates: 13.6 $\mu$ g/mL
Tetracycline	Concentration in the LB plates: 10 $\mu$ g/mL

## 3.6 MEDIUM

### **MEDIUM FOR THE CELL CULTURES**

BHK-21 Medium

GMEM (Glasgow Modified Essential Medium):

- 5% FCS (Fetal Calf Serum)
- 5% TPB (Tryptose Phosphate Broth)
- 1% Penicillin/ Streptomycin
- 1% L-Glutamin

NIH-3T3 Medium

DMEM (Dulbeccos Modified Eagle Medium):

- 10% FCS (Fetal Calf Serum)
- 1% Penicillin/ Streptomycin
- 1% L-Glutamin

Ref/ Cre Medium

DMEM (Dulbeccos Modified Eagle Medium):

- 10% FCS (Fetal Calf Serum)
- 1% Penicillin/ Streptomycin
- 1% L-Glutamin
- 50 $\mu$ g/ml Geneticindisulphate (G418)

LCL D2098 Medium

RPMI (Roswell Park Memorial Institute):

- 20% FCS (Fetal Calf Serum)
- 1% Penicillin/ Streptomycin
- 1% L-Glutamin
- 1% Pyruvate
- 1% Non-essential amino acids
- 1% 50mM Mercaptoethanol

### **PROKARYOTIC GROWTH MEDIUM**

LB-Medium:

- 1% Casein Extract
- 0.5% Yeast Extract
- 0.5% Sodium Chloride
- 0.1% Glucose (pH 7,0)

LB-Agarose plates

LB Medium

1.5% Agar

### 3.7 MICE STRAINS

C57BL/6:	Infection by the cloned recombinant MHV68-LMP2a is carried out in mice of this strain for characterisation of MHV68-LMP2a.
Balb/C:	Mice of this strain are used to build and generate stable genetic manipulated strains, such as that of the LMP1/CD30 $\gamma$ 1cre mice and the R26-Car $\gamma$ 1cre mice used in this project.
LMP1/CD30 $\gamma$ 1cre (LC30 mice):	Mice of this strain are used as a model for establishing a dysregulated CD30 in vivo after immunization or infection with virus.
R26-Car $\gamma$ 1cre (CAR Mice):	Mice of this strain serve as a control for experiments involving that of the genetic manipulated strain LMP1/CD30 $\gamma$ 1cre mice and expresses the truncated version of the human CAR upon Cre mediated recombination.

### 3.8 OLIGONUCLEOTIDES

The following oligonucleotides listed in the following **Tables 3.1, 3.2 and 3.3** below are used in the different PCR procedures.

Primer	Primer Sequence	Annealing Temperature
M1 forward primer	5' - ATCTCACCTTGCTGGATTCTATTGC - 3'	59
M1 reverse primer	5' - GTTCTGATGGCTTGAAACGATGGC - 3'	59
M2 reverse primer	5' - AACACCCCATGAACCCTGAGATACG 3'	59

**Table 3.1: Primers used for the analysis of the left end of the MHV68 genome**

Primer	Primer Sequence	Annealing Temperature
TV CD30c	5' - CAGTGATCGTGGCTCTGTA - 3'	56
hCD2revr	5' - GGAGACTGCACCTTGGAAAG - 3'	56

**Table 3.2: Primers used for Genotyping**

Primer/ Probes	Primer Sequence	Annealing Temperature
gB forward primer	5` - GGC CCA AAT TCA ATT TGC CT - 3`	59
gB reverse primer	5` - CCC TGG ACA ACT CCT CAA GC - 3`	59
gB probe	5`-6-Fam-ACA AGC TGA CCA GCG TCA ACA AC-Tamra - 3`	-
L8 forward primer	5`- CAT CCC TTT GGA GGT GGT A - 3`	59
L8 reverse primer	5`- CAT CTC TTC CGA TGG TGG A - 3`	59
L8 probe	5`Hex-ACC ACC AGC ACA TTG GCA AAC C- BHQ-1 - 3`	-

**Table 3.3: Primers and probes used for quantitative PCR**

### 3.9 ANTIBODIES

The following antibodies listed in **Tables 3.4 and 3.5** below are used in western blotting and immunohistochemistry respectively.

Antibody	Source	Dilution
$\alpha$ -LMP2A-14B6	Rat	1:5000
$\alpha$ -mouse HRP	Mouse	1:30000
$\alpha$ -rat HRP	Rat	1:10000
$\alpha$ -tubulin	Mouse	1:2500

**Table 3.4: List of antibodies used for western blot** Antibodies were obtained from Christine Bogl

Antibody	Source	Coupling	Dilution	Company
LMP2a	Rat	FITC	1:100	Santa Cruz Biotech
CD4	Rat	BV450	1:100	BD Biosciences
B220	Rat	APC	1:1000	BD Biosciences
Laminin	Rabbit	-	1:100	Sigma
Anti-rabbit 594	Goat	FITC	1:500	Invitrogen

**Table 3.5: List of antibodies used for immunohistochemistry**

### 3.10 INSTRUMENTS, DEVICES, CHEMICALS AND REAGENTS

The list of instruments and devices used, as well as chemicals and reagents used are listed in the **Tables 3.6 and 3.7** respectively.

Company	Product
AB Applied Biosystems	Optical 96 well plates PCR, 7300 PCR system
BD Biosciences	FacsCalibur LSR Fortessa flow cytometry
Beckman Coulter	Avanti j26xp ultracentrifuge
Bender and Hobein	Genie 2 vortexer
Biomed Analytik	Gelelectrophoresis mini cell chamber
Biometra Jena company	T-Professional PCR thermocycler
Biorad	Gene pulser cuvette, Mini-PROTEAN western blot chamber, Transblot system, Gel doc 2000 printer
Biozym	SurPhob tips
Bosch	Freezer (4°C / 20°C)
Braun	Sterican Injection canules
Corning Incorporated	Falcon cell strainer, costar stripette
Corning science	Falcon test-tubes
Diagenode	Bioraptor sonicator
Eppendorf	Centrifuge 5415D, Centrifuge 5417R mastercycler gradient PCR, Thermomixer, Micropipette, Tubes
Equibio	EasyjetcT optima electroporator
GE Healthcare	Ilustra PCR DNA and gel band purification kit
GFL	Water bath incubator, 3031 shaking incubator
Gilson	Transferpette multipipette, Pipette tips
Greiner Bio-one	Tissue culture dish, Cellstar cell culture flasks
Heidolph	MR3001 heating mixer
Henke Sass wolf	Syringe
Hettich	Mikro 200R centrifuge, Rotina 3SR table centrifuge, Rotina 460 centrifuge
Labcon	Roller/ Mixer
Leica Microsystems	M1900uv Cryotom, TCS Sp5II photon microscope
LTF Labortechnik	Gelelectrophoresis X-ray
Macherey Nagel	Nucleo-spin plasmid DNA, RNA, protein purification
Micronic Lelystad	U-bottom FACS tubes,
MP Biomedicals	Fast Prep 24 homogenisation system
NanoEntek	Disposable hemocytometer
Peqlab Biotechnology	Wheel mixer, Electrophoresis power supply, Nanodrop ND1000 spectrophotometer
Qiagen	QIAamp DNA Mini Kit, Plasmid Maxi Kit, Plasmid Midi Kit
Sakura Finetek	Tissue cryomold, O.C.T tissue tek gel
Schubert and Weiss	Neubauer cell counter
Scotsman	AF103 Ice generator
Severin	Microwave
Siemens	Refrigerator (4°C and -20°C Freezer)
Sigma	Centrifuge
Thermoscientific	ART Tips, Heraeus laminar flow, Heraeus Hera-cell 150 incubator, PCR tubes, Superfrost plus microscope slides
TPP	Tissue culture testplate, FACS plate
Unitylab	Heraeus centrifuge, Heraeus freezer -80°C
Winkler	Mettler PC2000, Mettler PE 3000 weighing scale
Zeiss	Telaval 31 light microscope, Axiovert 200M fluorescence microscope

Table 3.6: List of instruments and devices

Company	Product
Amersham Biosciences	Hybond-N nitrocellulose membrane
Amimed	2-mercaptoethanol (50mM)
BD Biosciences	FITC; APC; AF700; BV; PERCP; BIO,
Biomedicals	Hepes
Fermentas	Restriction enzymes
GE Healthcare	Hyperfilm ECL, ECL-Western blotting
Gibco	Trypsin EDTA, DPBS, DMEM, Agarose, L-Glutamine, P/S, PBS
Invitrogen	Goat anti-rabbit FITC, Live/dead fixable green, Pro long glass anti-fade mountant, 1kb DNA ladder, Agar, LB broth base
Merck	Ethanol, Isopropanol, DMSO
Milipore	MACS buffer
New England Biolabs	S.O.C outgrowth medium, T4 ligase and buffer, Restriction enzymes, Antarctic phosphatase, T4 Ligase and buffer
PAN Biotech	BHK21 Glasgow MEM, FCS
Roche	dNTP
Roth	Crystal violet, Milk powder, TEMED, Sucrose, Tris
Santa Cruz Biotech	Car-FITC, CAR-PE, LMP2a FITC
Schleicher and Schüll	Whatmann paper
Serva	Ethidium bromide, Bromphenolblue
Sigma-Aldrich	Tween 20, X-tremeGENE HP DNA Transfection, Trypan blue
Sigma	anti-laminin rabbit antibody, bovine serum albumin (BSA), Ponceaus S
Sigma Life sciences	Tryptose phosphate Broth
Takyon Technology	Master-mix Taqman PCR

**Table 3.7: List of chemicals and reagents**

# 4

## METHODS

### 4.1 MOLECULAR BIOLOGY METHODS

#### 4.1.1 GEL ELECTROPHORESIS

In order to separate the DNA based on size, gel electrophoresis is used. Nucleic acids have different movement speeds along the agarose that is placed in an electric field and move towards the positive pole. They will be separated by their size with smaller fragments travelling faster appearing further on the agarose gel and larger DNA fragments nearer to the negative charged top. In order to visualise the nucleic acid bands, ethidium bromide dye (Serva) is used in the gel and buffer. With the usage of a standardized 1kb plus DNA ladder (Invitrogen) in one of the wells, which acts as a DNA marker, the respective sizes of nucleic acid in the samples can be determined. In order to make the gel (1% or 0.8%), in which the nucleic acid samples are placed, agarose powder is boiled and dissolved with in either TAE or TBE (see **Table 4.1 and 4.2** below). After which, ethidium bromide (0.1- 0.5 $\mu$ g/ml) is added and the gel solution emptied into the brackets and left for an hour to harden before usage. Ethidium bromide intercalates into nucleic acids and emits light when exposed to ultraviolet light to allow for proper visualisation of the bands. Once DNA is added to the hardened gel, a voltage of 120V or 60V is run though the solution for 35 minutes or 14 hours

respectively and the gels containing the separated DNA subsequently visualized under UV light.

Reagents	Concentration
Tris	40mM
Acetic acid	20mM
EDTA	1mM

**Table 4.1: Table showing preparation of 1xTAE**

Reagents	Concentration
Tris	89.1mM
Boric acid	89mM
EDTA	2mM

**Table 4.2: Table showing preparation of 1xTBE**

#### **ISOLATION AND PURIFICATION OF DNA FRAGMENTS FROM AGAROSE GEL**

Isolation and purification of the DNA fragments from the agarose gel is done using the Ilustra PCR DNA gel band purification kit (GE Healthcare). The respective band is cut out from the agarose gel and placed in an eppendorf tube.  $500\mu\text{L}$  of Buffer 1 is added to the eppendorf tube and the gel is allowed to melt and dissolve at  $60^\circ\text{C}$ . After which, the solution is transferred onto a membrane filter and centrifuged at 14000 rpm for a minute at RT. The DNA nucleic acid would then be bound onto the membrane while the eluted supernatant in the eppendorf tube is discarded. Next a wash buffer of 100% ethanol is added to the membrane and after centrifugation, the membrane is transferred to a new eppendorf tube and  $30\mu\text{L}$  elution buffer (gray) is used to elute the DNA, that has been bound onto the membrane. The eluted DNA was then stored at  $-20^\circ\text{C}$ .

#### **4.1.2 PCR**

The polymerase chain reaction allows specific DNA sequences of interest to be amplified and subsequently detected by means of gel electrophoresis and restriction enzyme analysis as mentioned in **4.1.1** and **4.1.5** respectively. It also enables the specific quantification of the amount of DNA in a given sample as in the case of the TaQMan real time PCR. For the amplification process, a DNA template, together with oligonucleotide reverse and forward primers are necessary. In addition, the PCR reaction mix also requires the addition of the reaction buffer, deoxynucleotide mix (dNTPs) and a thermostable DNA polymerase (Taq Polymerase). One complete cycle of the PCR is made up of 3 separate parts; each requiring a specific temperature. The first step is that of denaturation carried out at  $95\text{--}96^\circ\text{C}$ , whereby the double stranded template DNA is separated into two single strands. The next phase is that of annealing which occurs at  $55\text{--}65^\circ\text{C}$  in which the primers are bound to the template DNA, followed by the elongation phase at  $72^\circ\text{C}$  in which the newly synthesized double stranded DNA is generated by the DNA polymerase. Several cycles are carried out

for sufficient amplification of the target sequence.

#### **LEFT GENOME END PCR AMPLIFICATION**

During the process of mutagenesis during cell passage as stated in **4.3.5**, the left genome of the MHV68 end may be spontaneously deleted (Clambey et al., 2002)). Hence, the left genome end PCR amplification is carried out to ensure that the left genome end of the MHV68 is intact. The following PCR procedures and temperatures were carried out for the left genome end PCR amplification as listed in **Table 4.3 and 4.4**:

Reaction step	Temperature( $^{\circ}$ C)	Time(s)	Cycle
Initialization	95	150	30
Denaturation	94	45	30
Annealing	59	45	30
Elongation	72	30	30
Final elongation	72	600	-
Final hold	4		-

**Table 4.3: Table showing left genome end PCR programme**

Reagents	Volume( $\mu$ l)
Q5 reaction buffer (5x)	10.0
Forward primer of M1 and M1-M2	2.5
Reverse primer of M1 and M1-M2	2.5
dNTPs (10 mM)	2.0
DNA template (100ng)	3.0
Q5 Polymerase	0.5
ddH <sub>2</sub> O	29.5
<b>Total</b>	<b>50.0</b>

**Table 4.4: Table showing left genome end PCR reaction procedure**

#### **QUANTITATIVE REAL TIME PCR (TaqMAN)**

100ng of viral DNA isolated is used as the starting material for the quantitative real-time PCR (Taq-Man) using the TaqMan Universal PCR Master Mix and the ABI 7300 Real-time PCR System (Applied Biosystems). This TaqMan method of real time PCR makes use of probe hybridization within the DNA sequence to be amplified. Hence, products can be detected while they accumulate during the PCR amplification process, enabling accurate reproducible quantification of DNA over wide ranges of concentrations. Two genes are amplified, the cellular housekeeping gene L8 and that of the viral glycoprotein gene gB. For each gene, a separate TaqMan reporter probe labelled with a fluorescent reporter dye at the 5 end and a quencher at the 3 end, a forward and reverse primer are introduced into the samples prior to the PCR reaction. Prior to the start of the reaction, fluo-

rescence is suppressed due to the close proximity of both the molecules. During each elongation phase by the Taq polymerase, the Taqman reporter probe, which was formally bound to a specific sequence on the DNA is cleaved and this results in a light signal given out. The fluorescence is then detected by the PCR system. This fluorescence is measured at the end of each elongation phase allowing the increase in amount of DNA to be determined in real-time. The amount of fluorescence and hence amount of amplified DNA gives an indication of the amount of DNA in the samples at the start, before the begin of the PCR reactions. Eight standards containing known dilutions of DNA ranging from 10 to  $10^8$  are amplified together with the unknowns to obtain a standard curve. Through extrapolation with the help of this curve, the amount of DNA in the unknown sample could be quantitatively determined by means of the cycle number. The thermal cycling conditions for the TaqMan assay were listed in **Table 4.5** as follows:

Reaction step	Temperature( $^{\circ}$ C)	Time(s)	Cycle
Initialization	95	600	1
Denaturation	95	15	40
Annealing	60	60	40
Elongation	60	60	1

**Table 4.5: Table showing Taqman PCR programme**

Reagents	Volume( $\mu$ l)
Taqman PCR master mix	13.0
Probes;gB and L8	1.5 each
Forward primers;gB and L8	1.5 each
Reverse primers; gB and L8	1.5 each
DNA template (100ng)	4.0
<b>Total</b>	<b>26.0</b>

**Table 4.6: Table showing Taqman PCR reaction procedure**

For the calculation of the viral genomic load, the obtained gB copy number is normalized to the obtained L8 copy number making use of the following equation:

$$\text{Viral Load} = \text{Copy number gB} \div \text{Copy number L8} \times 1000$$

#### **CD30FLSTOP TAIL GENOTYPING OF TRANSGENIC MICE**

Genomic DNA isolated from the cells of mice tails is used as starting material for the PCR, to de-

termine the genotype of the transgenic mice respectively. In this particular PCR, the murine CD30 sequence in the DNA (and the cytoplasmic portion of the CD30) is amplified making use of corresponding manufactured primers, together with magnesium solution and reagents listed as follows:

Reaction step	Temperature(°C)	Time(s)
Initialization	95	300
Denaturation	95	45
Hybridisation	56	45
Elongation	72	60
Final elongation	72	600

**Table 4.7: Table showing CD30flSTOP PCR programme**

Reagents	Volume(µl)
Taq buffer	2.50
MgCl <sub>2</sub> (25mM)	1.50
dNTP (10mM)	0.50
Primer1: TV CD30c	0.10
Primer2: hCD2rev	0.10
Taq polymerase	0.15
DMSO	0.50
DNA template	1.00
H <sub>2</sub> O	17.65
<b>Total</b>	<b>24.00</b>

**Table 4.8: Table showing CD30flSTOP PCR reaction procedure**

#### 4.1.3 ISOLATION OF DNA

##### **PURIFICATION AND ISOLATION OF PLASMID DNA**

In order to isolate and obtain purified DNA, be it a plasmid vector or other DNA sequences, either the MiniPrep, MidiPrep or MaxiPrep (Qiagen Reaction Kit) is used depending on the copy numbers and amount of the DNA or plasmid that needs to be isolated. The protocol used is as that of the Qiagen Plasmid Mini, Midi and Maxi kits (Qiagen) and the pellet/DNA isolated at the end is resuspended in 50µL TE (+ 1:1000 RNase). For controlling that the bacteria has taken up the correct plasmid and gene of interest, Mini-preps are performed on several cultures at once in a quick manner: Here, from the bacteria culture that was cultivated overnight, 1mL is placed in an eppendorf tube and centrifuged at 14000 rpm for 10 minutes. The pellet is resuspended in 100µL Buffer 1, and subsequently 200µL buffer 2 was added and allowed to react for 5 minutes under room temperature to lyse. After which, 200µL buffer 3 was added to stop the lysis process and the entire solution is placed in ice for 10 minutes, and then centrifuged at 14000 rpm for 10 minutes.

The supernatant was transferred to a clean eppendorf tube with 1mL ethanol added and left on ice for 10 minutes. The solution is next centrifuged again at 14000 rpm for 10 minutes, and the 750 $\mu$ L 70% ethanol is added to the pellet to clean it. It is then centrifuged for 10 minutes at 14000 rpm. After which, the supernatant is discarded and the pellet is left to dry for 10 minutes. Finally, once dried, 50 $\mu$ L TE buffer is added and the DNA is then either stored at -20°C or 10 $\mu$ L used for control restriction enzyme digestion. In the process of restriction enzyme digestion, the DNA is left to run on an agarose gel in order to ascertain which bacteria colony has taken up the correct vector or gene of interest.

#### **PURIFICATION AND ISOLATION OF BAC DNA**

For the isolation of BAC plasmid DNA from *E. coli*, an overnight cultivation of the selected clone in a shake incubator at 37°C is performed. 9mL of the bacteria suspension is transferred to a falcon tube and centrifuged (4000 rpm, 10 minutes, 4°C). For cell lysis, the pellet is resuspended in 200 $\mu$ l solution I (Qiagen DNA Mini Reaction Kit). Solution II is added and the mixture is incubated for 2 minutes at RT. Subsequently, 300 $\mu$ L solution III is added and incubation done on ice for 10 minutes. Samples are centrifuged (14000 rpm, 10 minutes, 4°C) and the supernatant is collected. Separation of DNA and proteins is achieved with chloroform-phenol-isoamyl alcohol. After an incubation period of 10 minutes at RT and mixing by means of constant inversions, centrifugation (14000 rpm, 4°C, 10 minutes) was performed. The upper phase containing DNA is transferred in a fresh microcentrifugation tube. DNA precipitation is carried out by adding ethanol (100%). Samples are centrifuged (14000 rpm, 4°C, 20 minutes) and the obtained pellet containing DNA is washed with 70% ethanol. The pellet is dried and resuspended in 100 $\mu$ l T/E (+RNase) buffer. Samples are stored at 4°C.

Isolation of larger amounts of pure BAC plasmid DNA is performed with Plasmid DNA purification NucleoBond PC 500 Kit (Macherey-Nagel), and the procedure done in accordance to the provided manual. The selected clone is cultivated overnight in 500mL LB medium supplemented with chloramphenicol (13.6  $\mu$ g/ml). Cultivation is carried out in a shake incubator at 37°C. Isolated DNA is eluted with 200 $\mu$ L TE buffer and samples stored at 4°C.

#### **ISOLATION OF TOTAL DNA FROM CELLS**

The QIAamp DNA Mini Kit (Qiagen) is used in order to isolate DNA from the cells (splenocytes, lung cells, lymph node cells, or peritoneal cavity cells). The cell suspension or pellet was resuspended in PBS and made up to a volume of 200 $\mu$ L. 200 $\mu$ L Lysis buffer and 20 $\mu$ L of Proteinase K is added with mixture and subsequently pulse vortexed for 15 seconds and then incubated for 10 minutes at 56°C. After a short centrifugation step to remove condensation from the lid, 200 $\mu$ L ethanol is added, pulse vortexed and the eppendorf tube again shortly centrifuged. The entire mixture is placed onto a spin column over a 2mL collection tube and centrifuged at 8000 rpm for 1 minute.

The collection tube is replaced with a new tube, and the membrane in the spin column washed with wash buffers AW1 and AW2 provided at 8000 rpm for 1 minute and 14000 rpm for 3 minutes respectively. The collection tube is replaced and the membrane is then dried during a subsequent centrifugation step at 14000 rpm for 1 minute. Lastly, 75 $\mu$ L of elution buffer is added to the spin column, incubated at RT for 10 minutes and placed in a new 1.5mL eppendorf tube. Centrifugation at 8000 rpm for a minute elutes the DNA from the membrane and the elute is then stored at -20°C. The concentration of the DNA can then be determined by the use of the Nanodrop ND1000 spectrophotometer (Peqlab Biotechnology) as described in **4.1.4** stated below.

#### **4.1.4 NUCLEIC ACID CONCENTRATION DETERMINATION**

In order to determine the concentration of nucleic acid, the Nanodrop (Peqlab Biotechnology) was used. 2 $\mu$ L H<sub>2</sub>O is placed onto the measuring plate and the nanodrop is then calibrated. Next, the H<sub>2</sub>O is wiped away and the buffer/medium in which the DNA was dissolved/ eluted in is positioned on the measuring plate and a blank measurement is taken. Next, the medium is then cleaned away and the 2 $\mu$ L DNA solution to be measured is placed onto the measuring plate and the measurement is read. The extent of purity is determined by the 260/280 index which is kept between 1.80 and 2.00, and the concentration of DNA is given in ng/ $\mu$ L.

#### **4.1.5 RESTRICTION ENZYME ANALYSIS**

Restriction enzymes are used to both cut particular genes of interest out of a certain plasmid, to linearize vectors/plasmid DNA for cloning, and for controls of plasmid DNA and BAC DNA to identify the desired clones. The enzymes recognize specific palindromic sequences on DNA and catalyse double strand breaks generating either blunt ends or specific "sticky ends". These enzymes require specific and distinct conditions and buffers and hence, depending on the enzyme used, the respective buffer and conditions were imposed. After incubation, the DNA fragment(s) are then run on an agarose gel through electrophoresis and separated depending on their sizes. 1 $\mu$ g DNA was used, with 1 unit of restriction enzyme and 2 units of the respective buffer for every 20 $\mu$ L total solution. A list of the different procedures, enzymes and conditions can be found in the Appendix **A**.

#### **4.1.6 WESTERN BLOT**

Western blot is a method used to detect proteins in solutions. Firstly, cells need to be lysed to release the specific intracellular or membrane proteins whereby proteins in each sample are separated by a special gel electrophoresis making use of SDS-page. The bands of separated proteins are transferred onto a nitrocellulose membrane and further stained with specific antibodies for detection.

### **PREPARING CELLS FOR WESTERN BLOT**

Proteins from two different cell lines, LCL2098 and NIH3T3 cells were used in this western blot. For the preparation of the LCL2098 cells, 5mL LCL2098 cell suspensions each in two 15mL Falcon tube is to be centrifuged (1200 rpm, 4°C, 10 minutes). Supernatant is discarded from both falcons and each cell pellet re-suspended in 1mL PBS are to be transferred to a new 1.5mL eppendorf tube. From one eppendorf tube, cells are counted and protein concentration measured while from the second Eppendorf tube, the cell pellet is resuspended in 200 $\mu$ L Laemmli buffer for use in western blotting.

For the preparation of NIH3T3 cells, firstly, solution from the cell plates containing adherent NIH3T3 cells are discarded and washed with 1mL of PBS per well. The PBS is then discarded and 1mL of trypsin is introduced into each well to detach the adherent NIH3T3 cells. After 5 minutes, the solution is transferred into two 15mL falcons each containing 5mL of NIH medium (with FCS). The solution is then centrifuged, supernatant removed and pellet either resuspended in PBS for cell counting and protein concentration measurements or in 200 $\mu$ L 2x Laemmli buffer for western blot use.

The eppendorf tubes containing the resuspended pellet in Laemmli buffer are to be sonicated using the Bio-Raptur (Diagenode) with the settings set at 30 seconds ON and OFF for 5 minutes. The cold water in the sonicator is mixed with sufficient ice. After sonification, the eppendorf tubes containing the samples are removed from the sonicator, shortly vortexed and incubated for 45 minutes at 50°C. After 45 minutes, further incubation is carried out for 8 minutes at 99°C

Reagents	Concentration
SDS	4%
2-mercaptoethanol	10%
Glycerol	20%
Bromophenol blue	0.004%
Tris-HCL	0.125M

**Table 4.9: Table showing preparation of 2xLaemmli buffer**

### **PREPARATION OF GEL**

A 10% separation gel is to be prepared one day before the running of the western blot. 500 $\mu$ L of bromophenol blue dye is added for the stacking gel so as to allow for better visualisation of the wells. Composition of the 10% separation gel and stacking gel are listed in **Tables 4.11 and 4.10** respectively.

### **SEPARATION OF PROTEIN**

The gel (still enclosed within the 2 glass plates) is placed into the Mini-PROTEAN holder (Biorad) and samples loaded with respective amounts of samples per well . A well is loaded with 8 $\mu$ L marker.

Reagents	Volume
H <sub>2</sub> O	4.2mL
0.5M Tris pH 6.8	1.9mL
10% SDS	75 $\mu$ L
30% Acrylamide	1.3mL
10%	112 $\mu$ L
TEMED	7.5 $\mu$ L

**Table 4.10: Table showing preparation of stacking gel**

Reagents	Volume
SDS	4%
2-mercaptoethanol	10%
Glycerol	20%
Bromphenol blue	0.004%
Tris-HCL	0.125M

**Table 4.11: Table showing preparation of 10% separation gel**

The electrophoresis is allowed to run at 80V for 2 hours and 30 minutes to 3 hours until the dye is completely out of the gel or depending on the size of the proteins that are to be separated (The different bands of the marker are to remain visible on the gel and are ensured not exceed the gel).

Reagents	Concentration
Tris	25mM
Glycine	190mM
SDS	0.1%

**Table 4.12: Table showing preparation of running buffer**

### **BLOTTING**

The blotting buffer is prepared by adding 20% methanol into the ready made blotting buffer. The white sponges, the Hybond-N nitrocellulose membrane (Amersham Biosciences) and a few pieces of whatmann paper (Schleicher and Schüll), that will be later used for the transfer of the protein bands from the gel onto the nitrocellulose membrane are immersed in the blotting buffer.

Reagents	Volume
Tris	25 mM
Glycine	190 mM
Methanol	20%

**Table 4.13: Table showing preparation of blotting buffer**

To first prepare the gel for blotting onto a nitrocellulose membrane, the gel is removed from the

glass plates and placed in the blotting buffer for a short amount of time. Next, the white sponges, 3 pieces of whatmann paper and nitrocellulose membrane are positioned above the gel followed by another 3 pieces of whatmann paper and another white sponge below it. It is important to ensure that in the midst of positioning the whatmann paper, no air bubbles are to be trapped in between the gel and membrane used. This is done by rolling on the whatmann paper with a tube or rod. The entire stack created as mentioned above is then placed in the electrophoresis chamber (Biorad) and electrophoresis allowed to run for about 60 minutes to 135 minutes at 105V.

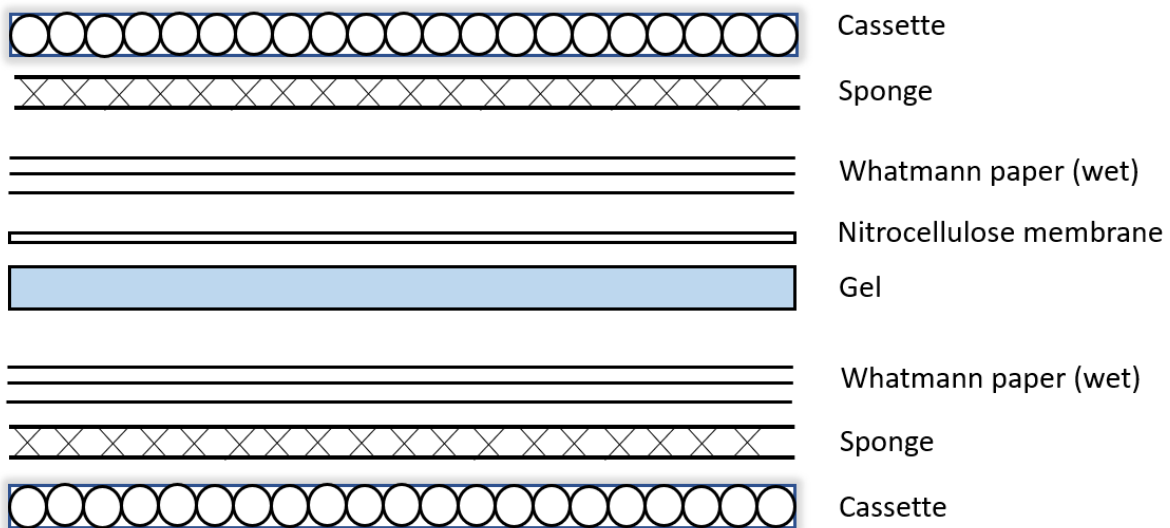


**Figure 4.1: Schematic illustration of the western blot setup for blotting and transfer of proteins from the gel to the membrane.**

### **BLOCKING**

The nitrocellulose membrane with the successfully transferred proteins from the gel is placed in a container and stained with 50mL of Ponceau S solution (Sigma). After three minutes, protein bands are visibly observed. The Ponceau S colouring is washed away with ddH<sub>2</sub>O and the membrane prepared for blocking. 5% milk solution in 200mL 0.1% TBST (0.1% TBST: 1ml Tween 20 (in 1000ml TBS)) in a small glass beaker is prepared as the blocking solution and membrane is blocked by mixing for an hour at RT.

Reagents	Volume
Tris pH 7.5	20 mM
NaCl	150 mM
Tween 20	0.1%
Dry milk powder	5%

**Table 4.14: Table showing preparation of milk blocking solution**

### **PRIMARY ANTIBODY INCUBATION**

For primary antibody incubation of 14B6 purified LMP2a antibody, the antibody is diluted with milk blocking solution in a ratio of 1:5000 in a 50mL falcon. The same is done for the 14B7 impurified LMP2a antibody, however, in a ratio of 1:50 and as for the tubulin antibody which serves as the loading control, in a ratio of 1:2500. The nitrocellulose membranes are immersed with their antibody mixtures overnight at 4°C.

### **SECONDARY ANTIBODY INCUBATION**

Before secondary antibody incubation, the membranes stained previously with primary antibodies are washed thrice in TBST for 10 minutes. Next, the membrane that was stained with the LMP2a antibody is then stained with an anti-rat secondary antibody diluted in a ratio of 1:10000 in 5% milk blocking solution in a 50mL falcon and incubated for 40 minutes at RT. For the membrane that was stained with the tubulin antibody, an anti-mouse secondary antibody was instead used and diluted at 1:30000. After 40 minutes of incubation, the solutions are removed and membranes washed again thrice with TBST for 10 minutes.

Reagents	Volume
Tris pH 7.5	20 mM
NaCl	150 mM
Tween 20	0.1%

**Table 4.15: Table showing preparation of TBST**

### **PREPARATION OF MEMBRANE FOR ECL STAINING AND DEVELOPMENT ON FILM**

The membranes are immersed and washed for a few seconds (5 to 10 seconds) in ddH<sub>2</sub>O before being placed on a thin waterproof film. Next, the membrane is covered with sufficient ECL mixture (GE Healthcare); according to the manufacturers instructions and left to incubate at RT for 5 minutes. The membrane is then exposed to a X-ray film for 1 minute, which was then visualised using the Optimax X-ray Developing System.

### **4.1.7 MOLECULAR CLONING**

#### **CLONING OF VECTOR**

In order to obtain many copies of a gene of interest in a vector, cloning is carried out. The insert fragment is prepared and cut out using 2 different restriction enzymes to generate two different sticky ends for ligation into the vector later on. 1ng of insert DNA is used together with 1 unit of restriction enzyme and 2 units of respective buffer for every 20 $\mu$ L solution. If the restriction enzyme makes use of the same buffer, then both enzymes may be used at once, otherwise, the fragment would have to be cut stepwise starting with the first restriction enzyme with the respective buffer, and the cut fragment then isolated and purified from the solution before being cut with the second

enzyme and respective buffer. Next, the vector is then cut with the same enzymes before ligation can be carried out. In cases whereby blunt end ligation is to be carried out, and a 5' overhang is created from the restriction enzyme digestion of the insert, the overhang is filled in with nucleotide bases with the help of the DNA polymerase I (Klenow enzyme). 1 unit of Klenow is used together with 2mM x 5 $\mu$ L dNTPs and hence each dATP, dGTP, dCTP, dTTP for 15 minutes at 30°C. The Klenow and the dNTPs are to be added after sticky end formation by the first restriction enzyme and hence, no additional buffer is required to be added since Klenow is able to function in different buffers of the restriction enzymes. The restriction enzyme digested insert and vector can be stored at -20°C and concentration measured the following day before ligation is carried out.

### **LIGATION**

The total amount of DNA (vector and insert) used in ligation is between 100ng to 200ng. The vector : insert ratio in terms of number of molecules is in the ratio of 1:5 and the amount of vector and insert, taking into consideration insert and vector size can be calculated using the following equation:

$$\text{Insert mass (ng)} = 5 \times \text{Vector mass (ng)} \times \text{Insert size (bp)} \div \text{Vector size (bp)}$$

For ligation, 1 unit of T4 DNA Ligase is used with 2 units of buffer for every 20 $\mu$ L solution and incubated at 16°C overnight for a minimum of 12 hours. After ligation, the solution is prepared for transformation. For electroporation, dialysis of the solution needs to be done to separate the DNA from the buffer suspension. The entire solution is placed onto a white filter above water, in a beaker and left for 30 minutes. After which, the dialysed solution is then used for electroporation as in **4.3.3**. For chemical transformation as in **4.3.4**, this additional step of dialysis is not necessary.

### **SELECTION OF DESIRED COLONIES**

After transformation and overnight growth of the colonies on the agar medium with the respective antibiotic resistance, inoculation is done in liquid LB medium to prepare the bacteria for mini-preps and restriction enzyme control analysis to identify the colonies that have been transformed with the desired vector and gene of interest insert, and hence finally its DNA isolation and purification. For inoculation, single bacteria colonies are picked using pipette tips, transferred onto a master-plate, and the pipette tip is then placed into a tube consisting of 3mL LB medium mixed with the respective antibiotic for selection. Up to 20 single bacterial colonies are picked and allowed to grow at 37°C (or at 30°C in some cases) overnight. After which, mini-preps are done to isolate the DNA from the bacteria in the liquid culture and after restriction enzyme analysis, the colonies with

the desired vector and gene of interest insert can be selected. Its DNA can be further purified and isolated, and then stored at -20°C.

## 4.2 CELL CULTURE METHODS

For this project, various cell lines with their corresponding mediums are used for different purposes. The baby hamster kidney cell line BHK-21 (ATCC CCL-10) used is cultured in Glasgow Minimum Essential Medium (GMEM) and supplemented with 1% L-glutamine, 1% Penicillin/Streptomycin antibiotics, 5% tryptose phosphate broth (TPB) and 5% heat inactivated fetal calf serum. The mouse embryonic fibroblast cell line NIH3T3 (ATCC CRL-1658) used is cultured in Dulbeccos Modified Eagle Medium (DMEM) and supplemented with 1% Penicillin/Streptomycin antibiotics, 1% L-glutamine and with 5% heat inactivated fetal calf serum. The transfected rat embryo-fibroblast cell line Ref/Cre, that was made to express the Cre recombinase, is obtained from the laboratory of W. Burns (John Hopkins University School of Medicine) and cultured in Dulbeccos Modified Eagle Medium (DMEM) together with 1% Penicillin/ Streptomycin antibiotics, 1% L-glutamine, 10% heat inactivated fetal calf serum and 50 $\mu$ g/mL geneticindisulphate (G418). The lymphoblastoid cell line (LCL) D2098 is obtained from the laboratory of W. Hammerschmidt (AGV, Helmholtz Zentrum) and cultivated in RPMI medium that is supplemented with 1% Penicillin/Streptomycin antibiotics, 1% L-glutamine, 20% heat inactivated fetal calf serum, 1% Pyruvate, 1% non-essential amino acids as well as 1% 50mM Mercaptoethanol.

### 4.2.1 GENERAL CELL CULTURE TECHNIQUES

All cell culture methods are performed under the sterile laminar flow hood making use of sterile pipettes, flasks and solutions while the cells are cultivated in incubators at temperatures of 37°C, 5% CO<sub>2</sub> and 95% humidity. Separate incubators are used for virus infected cells and those that are free from viral infection. After reaching a confluence of 80% to 90%, cells are split. NIH3T3, BHK-21 and Ref/Cre cells are adherent cells and hence for preparation and splitting of these cells, the cells must be made unattached. Cell solution in the T75 flasks are emptied of medium and washed with 5mL PBS (Dulbecco). Subsequently to the washing process, 2mL of trypsin EDTA is added and left for 5 minutes in the incubator. After the cells are unattached, 8mL of medium is added and the contents transferred into a 50mL falcon. The cell density and amount of cells are counted using a Neubauer cell counting chamber (Schubert and Weiss). In order to do this, the cell suspension is mixed with Trypan blue dye (Sigma-Aldrich) in appropriate dilution and applied to the counting chamber. The cells are then used for various experiments.

#### 4.2.2 DISRUPTION OF CELLS BY FREEZING AND THAWING

In order to mechanically disrupt the cells to release intracellular virus, the cells in the flasks or plates are refrigerated in a -80°C freezer for a minimum of two hours. After which, the container containing the frozen cells are taken out of the freezer and left to thaw. This makes up one freeze-thaw cycle. This cycle is repeated for a second time for a total of two cycles to completely disrupt the cells.

### 4.3 BACTERIOLOGICAL METHODS

#### 4.3.1 CULTIVATION OF BACTERIA

To ensure the growth of particular bacteria, antibiotics are added to the LB medium used for the cultivation of bacteria. Due to antibiotic resistance, only bacteria with the respective antibiotic resistance gene may grow in such LB medium. The specific concentrations of antibiotics used are listed on **3.5**. For bacterial cultivation, the LB medium used is inoculated with bacteria and cultivated in a shaking incubator overnight at 37°C.

#### 4.3.2 ESTABLISHMENT OF ELECTROCOMPETENT BACTERIA

The ability of cells to take up DNA from their environment is defined as competence. The process of transformation makes use of competent bacteria so that DNA can be taken up. The *E. coli* strains must first be made competent. In order to do this, a 4mL tube of LB medium is inoculated with the appropriate *E. coli* clone and left for cultivation overnight at 37°C in a shaking incubator. After which, the 1mL of the previously inoculated LB medium is then added to a larger flask of about 200mL LB medium for further cultivation overnight until a adequate cell density with an optical density value of about 0.6 is obtained. Subsequently, the suspension is incubated for a short period of time (10 - 15 minutes) on ice followed by centrifugation at 3500 rpm for 10 minutes at 2°C. With the supernatant discarded, the resulting pellet is washed by resuspension in ddH<sub>2</sub>O. Centrifugation is once again repeated with the resulting pellet now resuspended in 0.2mM Hepes. The steps are then repeated once again with resuspension of the pellet in 15% glycerol and finally in 400 $\mu$ L 10% glycerol. 50 $\mu$ L aliquots of bacteria suspension is pipetted into eppendorf tubes on dry ice and stored at -80°C until required.

#### 4.3.3 ELECTROPORATION

50 $\mu$ L prepared self-competent *E.coli* strain DH10B electrocompetent bacteria are used. Electroporation is done to allow the bacteria to take up the particular vector or gene of interest. For electroporation, 3ng of DNA is mixed with about 50 $\mu$ L of electrocompetent bacteria (either DH10B

or DH10B-MHV68) and placed in a 2mm diameter transformation cuvette. Transformation is then carried out under the following conditions: 15kV/cm, 25 $\mu$ F and 200 $\Omega$ . 500 $\mu$ L LB medium is then transferred to the mixture and the entire solution is left to be incubated in an eppendorf tube for 37°C (30°C for the vector pST76K-SR) on a thermoshaker for an hour. The bacteria suspension is then plated on LB plates mixed with specific antibiotics and left to be cultivated overnight at 37°C (30°C for the vector pST76K-SR). The newly formed bacteria colonies cultivated will then be extracted of its DNA for subsequent analysis.

#### 4.3.4 CHEMICAL COMPETENT BACTERIA

100 $\mu$ L of the *E.coli* strain MAX Efficiency DH5 $\alpha$  chemical competent cells (Invitrogen) is used. Heat shock is done to allow the bacteria to take up the particular vector or gene of interest DNA. For chemical transformation, an eppendorf tube with 100 $\mu$ L aliquot of chemical competent bacteria DH5 $\alpha$  mixed with 10 $\mu$ L ligation solution is placed on ice for 30 minutes. After which, the mixture is placed in a 42°C water bath for 45 seconds and subsequently on ice for 2 minutes. Next, 0.9mL of S.O.C medium is added to the mixture and the entire mixture is shaken for 1 hour at 37°C (30°C for the vector pST76K-SR). 0.5mL of the bacteria suspension is then plated on an LB plate mixed with specific antibiotics and left to be cultivated overnight at 37°C (30°C for the vector pST76K-SR). The newly formed bacteria colonies cultivated will then be extracted of its DNA for subsequent analysis.

#### 4.3.5 BAC SHUTTLE MUTAGENESIS

BAC shuttle mutagenesis is used to generate a MHV68 BAC containing the LMP2a gene. BAC shuttle mutagenesis is performed in the presence of a shuttle plasmid that contains the selection marker in the form of a kanamycin resistance gene, the recA gene for homologous recombination, as well as appropriate homologues to the BAC plasmid that flank the LMP2A gene. The shuttle plasmid pST76K-SR-oligo with the LMP2a gene is transformed into electrocompetent *E. coli* containing the MHV68 BAC plasmid. The shuttle plasmid pST76K-SR-oligo used in this project is provided from the laboratory. Transformation is carried out as described in **4.3.3.** and is followed by subsequent selection steps. Bacteria is cultivated overnight in the presence of chloramphenicol and kanamycin at 30°C. Clones that grew are plated again and cultivated overnight at 43°C on new chloramphenicol and kanamycin plates for removal of the shuttle plasmid. Clones that grew are then plated and cultivated overnight on chloramphenical plates at a temperature of 37°C followed by further cultivation on sucrose/chloramphenicol plates under the same conditions. In the final step, clones are cultivated parallel on separate kanamycin and chloramphenicol plates. This aims to select clones that were sensitive to kanamycin but resistant to chloramphenicol antibiotics. Hence, only such clones are used for further experiments, which include that of plasmid isolation

and restriction enzyme analysis to determine the success of the BAC shuttle mutagenesis that was performed. A simplified schematic illustration of the BAC shuttle mutagenesis process is illustrated in the results **5.1** below.

## 4.4 VIROLOGY METHODS

### 4.4.1 TRANSFECTION OF BAC-MHV68-LMP2A DNA IN BHK-21 EUKARYOTIC CELLS FOR VIRUS RECONSTRUCTION

BHK-21 cells are seeded at different concentrations and the appropriate well with the ideal cell growth is selected for transfection of the BAC-MHV68-LMP2A DNA. Transfection is carried out using 2.2 $\mu$ g of BAC-MHV68-LMP2A DNA that is mixed in 100 $\mu$ L BHK-21 medium and 5 $\mu$ L XtremeGENE HP DNA Transfection Reagent (Sigma Aldrich). The transfection reagent serves to promote the uptake of DNA into the cells. The mixture is vortexed, incubated for 15 minutes at RT followed by a further incubation at 37°C at 5% CO<sub>2</sub> until full cytopathic effect (CPE) is observed. The BAC sequence contains a coding sequence for the green fluorescence protein (GFP). Cells which have been successfully transfected with the BAC-MHV68-LMP2A DNA thus producing many progenies of the virus would appear green under a fluorescence microscope. The plate is frozen and thawed twice as in **4.2.2** to release intracellular virus. The solution is then transferred to a 15mL falcon centrifuged at 2500 rpm at 4°C for 10 minutes to separate the solution with the desired virus as the supernatant and cell debris as the pellet. The supernatant is then transferred to a 1.5mL eppendorf tube and stored at -80°C.

### 4.4.2 BAC SEQUENCE REMOVAL BY INFECTION OF REF/CRE CELLS

Ref/Cre cells express the cre recombinase that would allow the removal of the BAC cassette by recognising the loxP sites which flank it. In doing so, the BAC cassette together with the selection markers of GFP and GPT is removed. Removal of the BAC cassette is necessary because it has been shown that virus progeny containing the BAC displayed reduced growth (Adler et al., 2001). From the BHK-21 cells that are transfected with the BAC-MHV68-LMP2A DNA, 20 $\mu$ L of the supernatant that contained the virus is then added to pre-seeded Ref/Cre cells and medium, and left to incubate at 37°C till 100% CPE is observed. After full CPE is observed, the plate is frozen and thawed twice to release intracellular virus. The solution is then transferred to a 15mL falcon, centrifuged at 2500 rpm at 4°C for 10 minutes to separate the solution with the desired virus as the supernatant and cell debris as the pellet. The supernatant is then transferred to a 1.5mL eppendorf tube and stored at -80°C.

#### 4.4.3 LIMITING DILUTION FOR SELECTION OF VIRUS WITHOUT THE BAC CASSETTE

Limiting dilution is done to select virions which had their BAC cassette successfully removed. Dilution series ( $10^{-1}$  till  $10^{-10}$ ) of the virus are created starting with the  $10^{-1}$  dilution by mixing  $200\mu\text{L}$  of virus from the supernatant, into a testube containing  $1.8\text{mL}$  BHK-21 medium. The solution is then vortexed and  $200\mu\text{L}$  transferred into another test tube containing  $1.8\text{mL}$  for the  $10^{-2}$  dilution. The process was repeated until 10 dilutions were obtained. From each dilution, starting with the  $10^{-3}$  to  $10^{-10}$ ,  $100\mu\text{L}$  per well is then transferred to a row on a pre-seeded 96-well plate, with each well already containing  $100\mu\text{L}$  solution of BHK-21 cells with medium. The plate is then left to incubate until complete CPE is observed. Cells are constantly visualised under a fluorescence microscope and wells, where no green fluorescence is detected despite plaque formation, correspond to those in which the BAC cassette, with its GFP coding gene, has been successfully removed by the cre recombinase of the Ref/Cre cells. These wells are selected and further transferred and grown in larger wells in a pre-seeded 6-well plate containing BHK-21 cells once again. Further screens are carried out for confirmation that the BAC cassette with its GFP gene has been indefinitely removed. After identification of the wells in which the viral genome has had its GFP gene removed, the plate is frozen and thawed twice, and the contents of the desired well centrifuged at  $2500$  rpm,  $4\text{ }^{\circ}\text{C}$  for 10 minutes with the supernatant containing the virions stored at  $-80\text{ }^{\circ}\text{C}$ .

#### 4.4.4 GENERATION OF VIRUS STOCK SOLUTION

For the generation of sufficient virus stock, four T75 culture flasks were pre-seeded a day in advance with BHK-21 cells and  $20\text{mL}$  of medium. The growth medium in each flask is removed and each flask is then infected with  $200\mu\text{L}$  of supernatant diluted in  $6\text{mL}$  of BHK-21 medium and allowed to incubate at  $37\text{ }^{\circ}\text{C}$   $5\%$   $\text{CO}_2$  in an incubator for an hour. This gives the virus time to infect the adherent cells. After an hour, the virus solution is replaced with fresh BHK-21 medium and incubated at  $37\text{ }^{\circ}\text{C}$   $5\%$   $\text{CO}_2$  until full CPE is observed. The flasks are frozen and thawed twice and then transferred to a  $50\text{mL}$  falcon and centrifuged at  $1400$  rpm for 10 minutes at  $4\text{ }^{\circ}\text{C}$ . Pellet containing the cell debris is discarded while the supernatant containing the virus is transferred to another new  $50\text{mL}$  falcon for a second centrifugation step at  $20000$  rpm for an hour at  $4\text{ }^{\circ}\text{C}$  to obtain the virus as pellets. This time, the supernatant is discarded while the pellet is resuspended in  $3\text{mL}$  BHK-21 medium. To ensure proper resuspension and that the viruses are not clumped together, a  $5\text{mL}$  syringe with needle is used to further dissociate the virus in ensuring they are not clumped up.  $500\mu\text{L}$  aliquots are placed in cryotubes and kept at  $-80\text{ }^{\circ}\text{C}$ . The next day, the  $500\mu\text{L}$  aliquot is further aliquoted in  $50\mu\text{L}$  amounts and kept at  $-80\text{ }^{\circ}\text{C}$  until further use for subsequent experiments.

#### 4.4.5 VIRAL GROWTH CURVES FOR VIRUS KINETICS ANALYSIS

In order to determine the growth characteristic of MHV68-LMP2a, specifically its lytic replication kinetics in vitro, a growth curve is done with time points at 0hour, 24hours, 48hours, 72hours, and 96hours using NIH3T3 cells. For each virus analysed (BAC-derived MHV68-WT and MHV-LMP2a), a well on each 6-well plate is preseeded a day before with  $0.2 \times 10^6$  NIH3T3 cells. Four 6-well plates are used (one for each time point: 24hours, 48hours, 72hours, 96hours). The medium in each well is removed and the pre-seeded cells infected with the respective viruses, each with a multiplicity of infection (MOI) of 0.1. After incubating at 37°C for 60 minutes, the virus solution is removed and wells washed with medium before being replaced with fresh medium and left to further incubate at 37°C. The 0 hour time point corresponds to the input control, which represents the amount of prepared virus (MOI of 0.1) used for infection at the start (frozen at -80°C). At various time points after infection (24hours, 48hours, 72hours, 96hours) each 6-well plate is frozen at -80°C. The plates are later frozen and thawed twice with the contents transferred to a 15mL falcon and centrifuged at 2500 rpm for 10 minutes at 4°C. The supernatant contains the virions and is used, together with that of the input control, for plaque assays as in **4.4.6** to determine the viral titer at various times.

#### 4.4.6 PLAQUE ASSAY TO DETERMINE VIRAL TITER

Plaque assays are done to ascertain the number of infectious viruses (measured as plaque forming units; PFU) in samples. Thus, viral titer of MHV68-WT and MHV68-LMP2A can be determined. A series of dilutions from  $10^{-1}$  to  $10^{-8}$  is created starting with the  $10^{-1}$  dilution using 100 $\mu$ L of virus solution mixed with 900 $\mu$ L BHK-21 medium. The solution is vortexed and 100 $\mu$ L transferred to another test tube of 900 $\mu$ L BHK-21 medium to generate the  $10^{-2}$  dilution. The process is repeated until dilutions up to  $10^{-8}$ . Medium, from wells in a 24-well plate pre-seeded a day prior with BHK-21 cells, is removed and 900 $\mu$ L of the different dilutions from  $10^{-1}$  to  $10^{-8}$  are added to each well and left to incubate at 37°C for 90minutes. The virus solution is then removed and replaced with 1.5mL overlay medium (1.5% methylcellulose), and the entire plates are incubated for 5 days in an incubator at 37°C 5% CO<sub>2</sub>. Next, the overlay medium is removed and replaced with 300 $\mu$ L blue dye (0.1% crystal violet solution) for staining of the cells and left to incubate at RT for 15 minutes. The blue dye is then washed away and plates left to dry overnight at RT before counting of the number of plaques and the determination of viral titer with the help of the following formula is done:

$$\text{Viral titer (PFU/ mL)} = \text{Input factor} \times \text{Dilution} \times \text{Number of plaques}$$

$$\text{input factor} = (1 \text{ mL}) \div (0.9 \text{ mL}) = 1.1$$

## 4.5 ANIMAL EXPERIMENTS (IN VIVO)

The animal experiments are conducted in compliance with protocols that are approved by the local "Animal Care and Use Committee" (District Government of Upper Bavaria; permit number 154-13).

### 4.5.1 INFECTION OF MICE

For the first portion of the project, to characterise the newly cloned MHV68-LMP2a virus, female C57BL/6 mice aged between 6 to 8 weeks are used (obtained from Charles River Laboratories (Sulzfeld, Germany)). The mice are intranasally (i.n) infected with a concentration of  $5 \times 10^4$  PFU of virus that is each made into a volume of  $30\mu\text{L}$  in PBS. The mice are intraperitoneally (i.p) anaesthetized with Medetomidine, Midazolam and Fentanyl prior to being i.n infected with virus and placed on warming pads. After some time, the anaesthesia is then antagonized by subcutaneous application of Atipamezole, Flumazenil and Naloxone in order to get the mice conscious again. Throughout this time, the mice were constantly monitored.

For the second part of the project involving tumorigenesis and CD30 desregulation, LMP1/CD30/ $\gamma$ 1 Cre and CAR $\gamma$ cre mice are used. A mixture of female and male mice aged between 3 months to 7 months are intraperitoneally (i.p) infected with a concentration of  $1 \times 10^5$  PFU of virus that is each made into a volume of  $200\mu\text{L}$  in PBS.

### 4.5.2 PREPARATION OF ORGANS; LUNGS, CERVICAL LYMPH NODES, SPLEEN AND PERITONEAL CAVITY

#### LUNGS

The left lungs are harvested from the C57BL/6 mice euthanized on day 6 and stored at  $-80^{\circ}\text{C}$  for later determination of the virus titer and the analysis of its lytic replication. The lungs are homogenized by means of the Fastprep-24 instrument (MP Biomedicals). The lungs are placed in homogenization tubes and filled with  $500\mu\text{L}$  BHK-21 medium prior to homogenization. After homogenization, an additional  $500\mu\text{L}$  of medium is added and the homogenates transferred to a new 1.5mL eppendorf tube.  $100\mu\text{L}$  is then used for the plaque assay as in **4.4.6** whilst the rest stored at  $-80^{\circ}\text{C}$ .

#### SPLEENS

The spleens harvested are placed in separate 15mL falcons filled with 4mL of NIH3T3 medium placed on ice. They are harvested in order to investigate the reactivation from latency of the virus in ex vivo reactivation assays for the determination of viral genomic load, immunohistochemistry

and for FACS analysis. The spleens that are placed in the falcons filled with medium, are weighed with a portion of the spleen cut out for immunohistochemistry staining. They are kept in O.C.T gel in cryomolds, placed on dry ice and subsequently stored at -80°C. The remaining bulk of the spleen is emptied onto a cell strainer of pore diameter 100 $\mu$ m. The spleen is mashed to isolate splenocytes and the suspension carefully transferred into a new 15mL falcon for centrifugation at 1300 rpm for 10 minutes at 4°C. The supernatant is discarded while 4mL of erythrocyte lysis buffer (see **Table 4.16**) is added to the pellet and incubated for 10 minutes at RT. 10mL of NIH3T3 medium is then added and further centrifugation at 1300 rpm for 10 minutes at 4°C is done to isolate splenocytes. The isolated splenocytes as pellets are resuspended and diluted with NIH3T3 medium for cell counting.

Reagents	Concentration
NH <sub>4</sub> Cl	0.15 M
KHCO <sub>3</sub>	10.00 mM
Na <sub>2</sub> EDTA	0.10 mM

**Table 4.16: Table showing preparation of the erythrocyte lysis buffer**

### **CERVICAL LYMPH NODES**

The cervical lymph nodes removed are also placed in separate 15mL falcons filled with NIH3T3 medium. Similarly, the lymph nodes are crushed and sieved with the suspension made up to 10mL and transferred in falcons for centrifugation at 1300 rpm for 10 minutes at 4°C to isolate the cells. With the supernatant being discarded, the pellet obtained is resuspended with NIH3T3 medium for cell counting.

### **PERITONEAL CAVITY**

In order to obtain cells from the peritoneal cavity, 8mL NIH3T3 medium is injected into the cavity and the mice subsequently carefully shaken to mix the cells. After which, the medium is removed using a syringe and placed into new 15mL Falcons. Centrifugation is carried out at 1300 rpm for 10 minutes at 4°C with the pellet obtained being resuspended with NIH3T3 medium for cell counting.

The cell suspensions obtained are diluted and counted using a Neubauer counting chamber and made to a concentration of  $1 \times 10^7$  cells / mL for the FACS analysis. For later use in Taqman Real Time PCR, samples containing a cell count of  $1 \times 10^7$  cells are placed in separate eppendorf tubes, centrifuged at 2500 rpm at 4°C for 10 minutes with supernatants removed and pellets then stored at -20°C for later analysis. From the isolated splenocytes, an additional amount from the samples is used for the ex vivo reactivation assay as explained in **4.5.4**.

### 4.5.3 DETERMINATION OF THE VIRAL GENOMIC LOAD

For the determination of viral genomic load, Taqman Real Time PCR is carried out. The cell pellets from **4.5.2** that were previously stored -20°C are used. DNA is isolated as in **4.1.3**, concentration determined as mentioned in **4.1.4** and real time PCR is later carried out as in **4.1.2** to determine the viral genomic load.

### 4.5.4 VIRAL LATENCY DETERMINATION AND EX VIVO REACTIVATION ASSAY

Only splenocytes are used for the ex vivo reactivation assay. For each virus being examined, splenocytes of mice of each group are pooled together equally to obtain one experimental group each. In each group  $13.5 \times 10^6$  cells are filled to a volume of 9mL with NIH3T3 medium. For example, if there are 3 mice in each experimental group, then  $4.5 \times 10^6$  cells from the spleen of each are harvested and pooled to obtain a total of  $13.5 \times 10^6$  cells. From this 9mL cell suspension, eight threefold dilutions are carried out starting with the initial concentration of  $13.5 \times 10^6$  cells per group as mentioned.  $100\mu\text{L}$  of each of the eight dilutions are added to 24 wells of a pre-seeded 96-well plate of  $0.5 \times 10^4$  NIH3T3 cells per well. The NIH3T3 cells are seeded the day before. By cultivating the latently infected splenocytes together with the NIH3T3 cells, reactivation of the virus will be established. For two weeks at intervals of seven days, microscopic examinations of each individual well is carried out to observe for CPE and thus virus reactivation from latency. The number of wells with CPE is counted and the percentage of wells with CPE to the total number of wells for each dilution is evaluated.

To differentiate between reactivated latent virus and preformed lytic virus particles, the eight three fold dilutions established earlier on are stored at -80°C. After two freeze-thaw cycles as described in **4.2.2**, cells are disrupted and  $100\mu\text{L}$  of each of the eight dilutions, now containing disrupted cells, are added to 24 wells of a pre-seeded 96-well plate of  $0.5 \times 10^4$  NIH3T3 cells per well. The same procedure is carried out as above to determine if CPE is observed. If CPE is now observed, CPE would be attributed to lytically infectious virus. The total number of wells attributed solely to reactivated latent viruses would be the total number of wells with CPE after the freeze-thaw cycles deducted from that of before.

### 4.5.5 FACS ANALYSIS (FLOW CYTOMETRY)

$100\mu\text{L}$  cell suspensions having a concentration of  $1 \times 10^7$  cells/mL are placed per well in a 96-well plate and washed with MACS buffer (PBS; 1%BSA) to reduce any possible unspecific antibody bindings. After centrifugation at 1200 rpm for 5 minutes at 4°C, the supernatants are removed and the cells are stained with a combination of FITC, PE, PERCP, APC, AF700, V450, BIO conjugated monoclonal antibodies that are previously diluted in MACs buffer for a period of 20 minutes in an

enclosed dark container. The cells are then washed with 150 $\mu$ L MACs buffer to remove the excess dyes, and after a centrifugation step at 1200 rpm for 5 minutes at 4°C again, the supernatants are removed, cells resuspended in 90 $\mu$ L 2% PFA in PBS and subsequently transferred onto a FACS plate for further analysis. Cells that are to be stained for Live/Dead with TOPRO-3 are instead resuspended in 90 $\mu$ L MACS, which has been mixed with TOPRO-3. All analysis are carried out with the FACSCalibur<sup>TM</sup> or LSR Fortessa with results tabulated by the Flowjet software. The antibodies, if not otherwise specified are obtained from BD-Biosciences while that of the PNA antibody from Vector Linearis (Wertheim). The TOPRO-3 antibody is obtained from Molecular Probes. Live/Dead-FITC antibody is obtained from Invitrogen. All the steps are carried out on ice.

#### **STORAGE OF ADDITIONAL CELL AND CELL PERMEABILIZATION**

Additional cells are prepared as well for further analysis at other time points. 100 $\mu$ L cell suspensions are pipetted into each well of a 96-well plate and washed with PBS. After centrifugation at 1200 rpm for 5 minutes at 4°C, the supernatants are removed and for wells where Live/ Dead staining are performed, the cells are stained with 50 $\mu$ L Live/Dead-FITC (1:50 dilutions in PBS) for 5 minutes on ice. Excess dyes are removed by washing with PBS and a centrifugation step of 1200 rpm for 5 minutes at 4°C. After centrifugation, the supernatant is discarded and cells fixed by addition of 2% PFA in PBS for 10 minutes at RT. The cell suspension is then centrifuged, supernatant discarded and cell pellet resuspended in ice cold methanol. The cells, once resuspended in ice cold methanol, are now permeabilized and suitable for intracellular staining or can be stored at -20°C for later usage.

#### **PREPARATION OF CELLS FOR INTRACELLULAR STAINING**

For intracellular staining, cells are first permeabilized in ice cold methanol as mentioned above and then prepared for staining. The cells are washed with PBS (Dubeccos) twice with centrifugation steps at 1200 rpm at 4°C. The washed cell pellets may be then stained with 25 $\mu$ L surface or intracellular antibodies in darkness for 60 minutes at RT. After which, excess dyes are washed with MACS buffer and centrifuged at 1200 rpm at 4°C with subsequent supernatants discarded. The stained cell pellets are then resuspended in 2% PFA and transferred into FACS tubes for flow cytometry analysis.

#### **4.5.6 IMMUNOHISTOCHEMISTRY**

##### **SLICING OF SPLEENS**

The harvested spleens that are stored in cryomolds from **4.5.2** are cut into thin slices of diameter 15 $\mu$ m by means of a cryotom (Leica). The slices are placed on microscopic glass slides and stored in slide boxes at -80°C before immunostaining is done.

### **PREPARATION OF SPLEENS FOR IMMUNOHISTOCHEMISTRY STAINING**

The slices that were previously stored at -80°C are left to air dry for a short period of time (10-15 minutes). The sections are then fixed on the slides with 3% PFA solution. After 10 minutes, the sections are rinsed in PBS and then rehydrated with a PBS+ (PBS with 50mM NH<sub>4</sub>Cl) solution for 5 minutes. After rehydration, the sections are blocked with a PBS+ solution containing 1% bovine serum albumin (BSA) and 2% rat serum together with 0.3% Triton X-100 (Abcam) for 30 minutes. The addition of Triton X-100 in this step is to allow for the permeabilization of the intact cell membranes for intracellular staining. Blocking is done for 20 minutes. Subsequently, after rinsing with PBS, the sections are incubated with primary antibodies in 1% BSA at 4°C overnight. The dilutions of the primary antibodies can be found in **Table 3.5**. The following day, the sections are washed in PBS thrice with each wash lasting for 5 minutes. Following that, the sections are incubated with the secondary antibody in 1% BSA for an hour at RT. Secondary antibody used here was an anti-rabbit 594 antibody in a dilution of 1:500. Again, the excess antibodies are washed off with PBS thrice for 5 minutes each and finally embedded in "Pro long glass anti-fade mountant" (Invitrogen). A glass cover slide is placed above the embedded sections ensuring all sections are covered without any air bubbles. Finally, to ensure the embedded sections remain air tight and fixed, nail polish is carefully applied to the edges of the cover slides so as to frame them. The sections mounted onto the slides are then viewed with the aid of the TCS Sp5II photon microscope.

# 5

## RESULTS

### 5.1 GENERATION OF RECOMBINANT VIRUS MHV68-LMP2A

The generation of recombinant MHV68-LMP2a was carried out in 4 steps; (i) Cloning of the LMP2a gene construct with the PCMV (Promoter of the Human Cytomegalovirus), (ii) Cloning of this expression cassette in the shuttle plasmid pST76K-SR, (iii) The shuttle-mutagenesis in bacteria as illustrated in 5.1 and lastly, (iv) Reconstitution of recombinant virus in cell culture. Cloning of the PCMV with the LMP2a allows the gene construct to be expressed in mammalian cells later. The shuttle mutagenesis process enables the insertion of the gene of interest that was cloned into the shuttle vector, to be inserted into the MHV68 genome through a process of homologous recombination. Homologous recombination occurs between the BAC (bacterial artificial chromosome) containing a cloned MHV68 genome, and the shuttle plasmid in bacteria. After selection and identification of positive clones, reconstitution of recombinant virus was then done in cell culture.

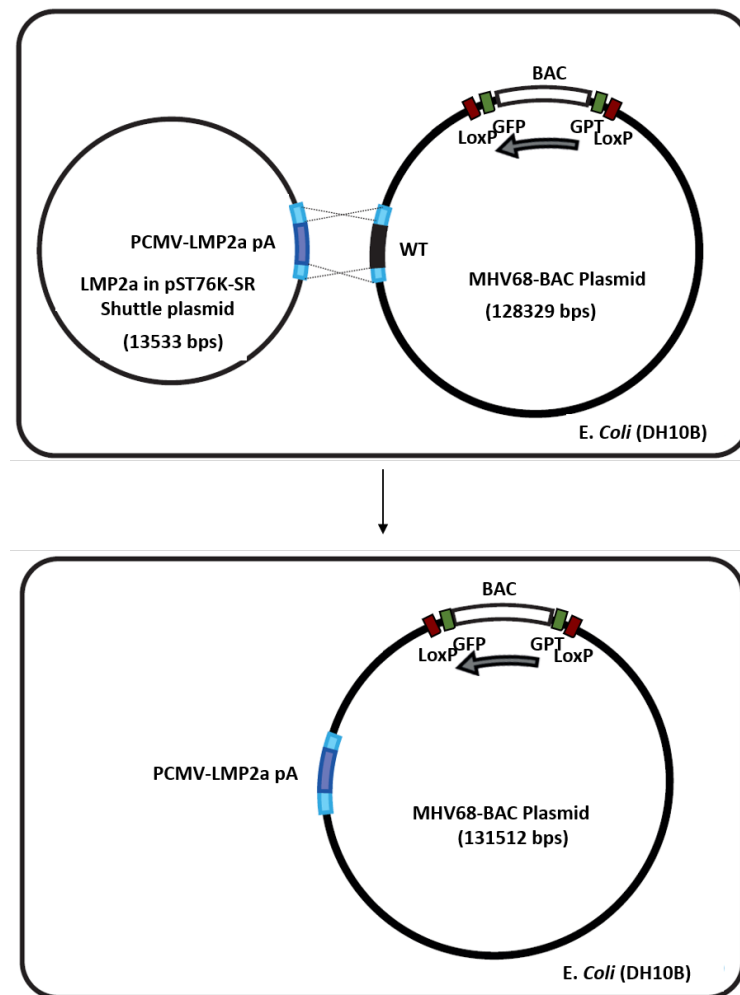


**Figure 5.1: Simplified illustration of the process of BAC Shuttle mutagenesis in *E. coli*.** The shuttle plasmid contains the gene of interest (PCMV-LMP2a) that is to be inserted between the homologous gene segments (light blue rectangles) into the MHV68 genome. The MHV68 genome was cloned as a BAC in *E. coli*. In addition to the BAC sequence, several other sequences are contained in the BAC cassette; GPT (guanosine phosphoribosyl transferase) and GFP (green fluorescent protein) flanked by loxP sequences that serve as sites for excision of the BAC cassette by cre recombinase later on. After shuttle mutagenesis, a recombinant BAC-MHV68 plasmid containing the PCMV-LMP2a gene of interest is created.

### 5.1.1 CLONING OF LMP2A CONSTRUCT WITH THE PCMV PROMOTER IN A SHUTTLE VECTOR

The LMP2a was provided in a construct (pEBNA-G-LMP2a) which included a *tetR* gene that had to be removed and replaced with the PCMV (Promoter of human cytomegalovirus). To reconstruct the 7649bp plasmid pCR<sup>TM</sup>3-LMP2a-*tetR* first, as shown in **Figure 5.3A**, the pEBNA-G-LMP2a plasmid was digested with *Hind*III and *Bgl*II to obtain a 260bp LMP2a fragment that included the *tetR* sequence as illustrated in **Figure 5.2B**. This *tetR*-LMP2a construct was then cloned between the *Bam*HI and *Hind*III (at 682 and 664) sites of the pCR<sup>TM</sup>3 plasmid as shown in **Figure 5.2A**, to obtain the plasmid pCR<sup>TM</sup>3-LMP2a-*tetR*.

The *tetR* sequence was then excised by restriction digestion with *Sac*II (at 711 and 1254) and re-

ligated to give rise to the 7106bp PCMV-LMP2a construct as a new plasmid. These desired plasmids were then selected as illustrated in **Figure 5.3**. This plasmid now contains the PCMV-LMP2a expression cassette without the tetR sequence.

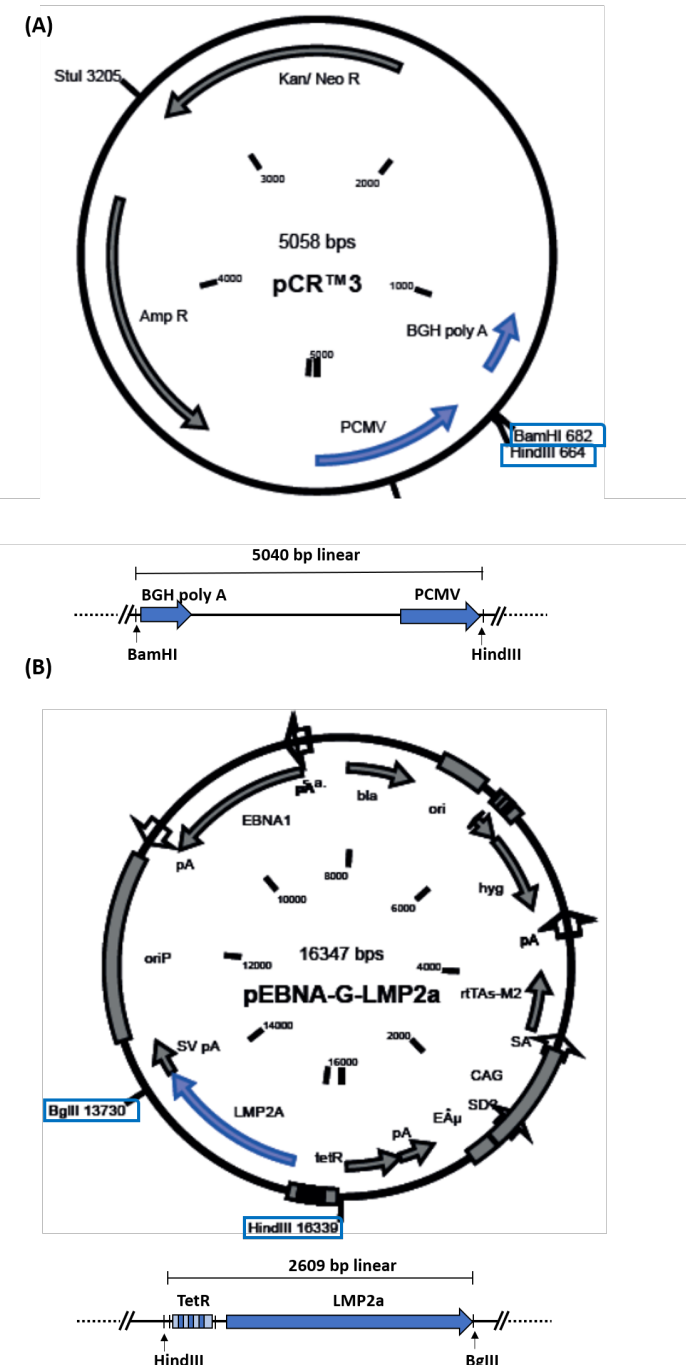


**Figure 5.2: (A) pCR™3 plasmid circular and linearized.** The pCR™3 plasmid is linearized by digestion with BamHI and HindIII. **(B) pEBNA-G-LMP2a plasmid circular and linearized.** The gene of interest LMP2a TetR in the pEBNA-G-LMP2a plasmid is cut out by restriction enzymes HindIII and BglII to give the linear LMP2a-tetR. The circular pCR™3-LMP2a-tetR plasmid encompassing both the PCMV and BGH poly A tail, and the tetR-LMP2a gene of interest is obtained by ligation of both the linearized segments obtained.

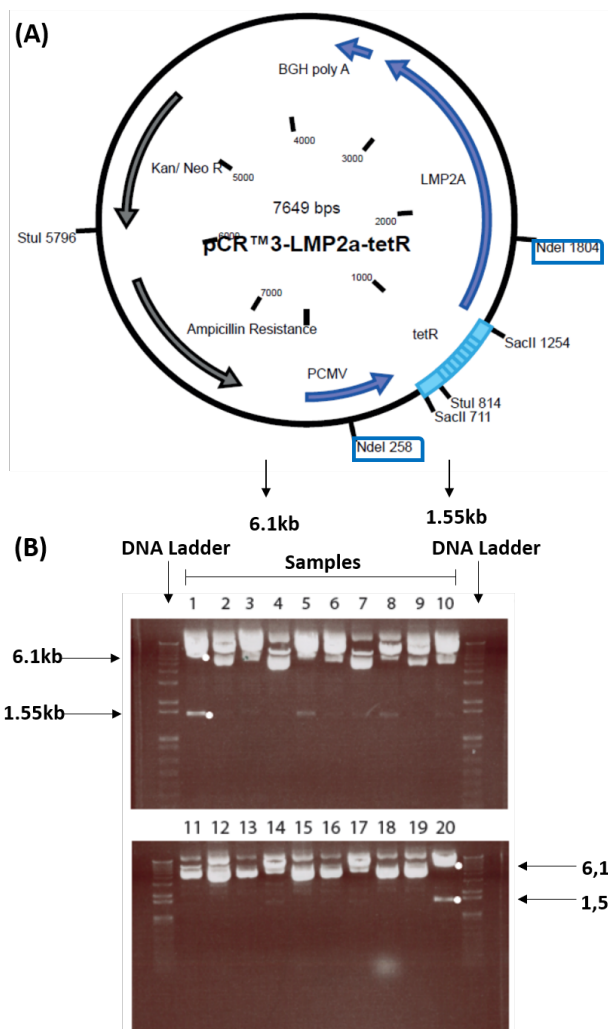


**Figure 5.3:** (A) Plasmid pCR™3-LMP2a-tetR is restriction enzyme digested with NdeI to give rise to two fragments of 6.10kb and 1.55kb in length. (B) Gel electrophoresis showing restriction digestion analysis with NdeI to select for the recombinant pCR™3-LMP2a-tetR plasmid. The desired recombinant plasmid with NdeI is observed in samples 1 and 20.

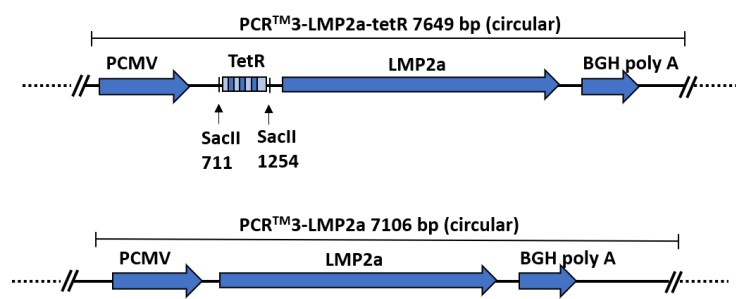


**Figure 5.4:** Removal of the tetR sequence to obtain a plasmid containing the PCMV promoter followed by the LMP2a gene and poly A tail. Removal of the roughly 500bp tetR sequence by restriction digestion with SacII enzyme.

The cloned PCMV-LMP2a expression cassette was then inserted into the shuttle plasmid pST76K-SR. This insertion into the shuttle plasmid pST76K-SR is essential for the process of the BAC shuttle

mutagenesis. To construct this recombination plasmid pST76K-SR with the PCMV-LMP2a expression cassette, the 3179bp PCMV-LMP2a expression cassette was excised from the previously cloned 7106bp plasmid PCMV-LMP2a by restriction digestion using Sspl and AflIII followed by treatment with Klenow, and subsequently cloned blunt end into the SmaI site of the shuttle plasmid pST76K-SR. This gives rise to a 13533bp pST76K-SR with the PCMV-LMP2a expression cassette as illustrated in **Figure 5.5**. Once cloned in the shuttle plasmid, the PCMV-LMP2a expression cassette is flanked on both sides by a homologous sequence of the MHV68 genome, and thus, BAC shuttle mutagenesis previously described in **4.3.5** can now be done, in which the PCMV-LMP2a expression cassette is finally inserted into the MHV68 genome. The MHV68 genome was previously cloned into a BAC, which can be kept as a plasmid in *E. coli* (DH10B) bacteria. The shuttle plasmid pST76K-SR was provided by the Adler laboratory.

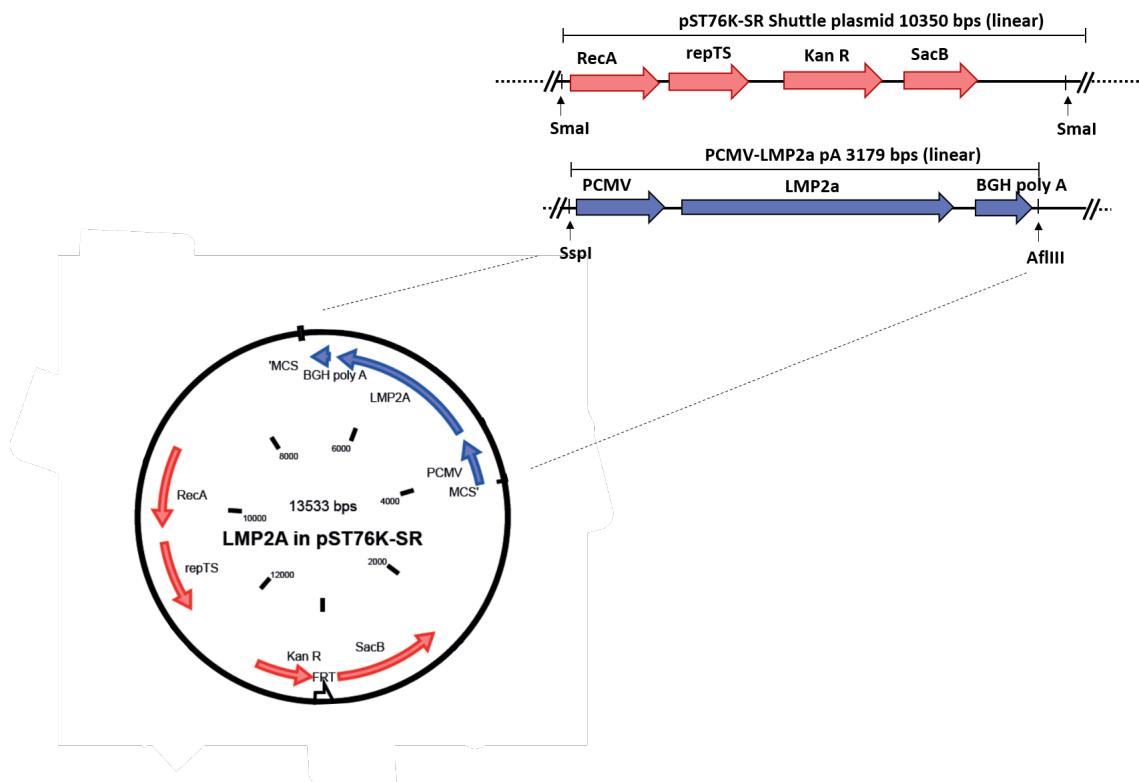


**Figure 5.5: Insertion of the PCMV-LMP2a expression cassette into the shuttle vector pST76K-SR.** Restriction digestion of the shuttle plasmid at the MCS with SmaI and of the PCMV-LMP2a with Sspl and AflIII followed by the DNA polymerase Klenow to generate blunt ends is performed to obtain linear DNA strands. Ligation and subsequent control digestion is performed to identify the correct recombinant plasmid of PCMV-LMP2a in pST76K-SR. The shuttle vector contains a rec A gene that is needed for recombination during the shuttle-mutagenesis while Sac B is a selection marker.

### 5.1.2 GENERATION OF THE MHV68-LMP2A VIRAL CONSTRUCTS

#### RECOMBINATION OF LMP2A FRAGMENT IN BAC-MHV68 DNA

After cloning the PCMV-LMP2a expression cassette into the shuttle plasmid pST76K-SR as seen in

**Figure 5.5**, shuttle mutagenesis was carried out to introduce the PCMV-LMP2a sequence into the MHV68-BAC (Adler et al., 2000). The end product of the mutagenesis is a MHV68-BAC plasmid containing the MHV68-LMP2a sequence. Restriction digestion analysis, which is portrayed in **Figure 5.6**, was done to select the desired clone.

### **VIRUS RECONSTITUTION AND STOCK PRODUCTION**

The MHV68-LMP2a BAC DNA was then transfected into BHK-21 cells for the reconstitution of virus that express LMP2a protein. With the help of the GFP expressed, which is coded by a portion of the sequence in the BAC sequence as seen in **Figure 5.1**, successful reconstitution in the eukaryotic BHK-21 cells could be observed by the appearance of green cells visible with a fluorescence microscope after complete CPE of the eukaryotic cells. Before analysis of the recombinant virus MHV68-LMP2a in vitro and in vivo, the BAC cassette was removed since an interference of the BAC sequence with viral fitness in vivo has been demonstrated (Adler et al., 2001). Excision was carried out with the aid of a recombination reaction of a cre recombinase targeting the LoxP sites that were flanking the BAC sequence as seen in **Figure 5.1** again. This gave rise to MHV68-LMP2a virus particles containing the viral DNA genome without the BAC and GFP sequences. Eventually viral titers were determined by plaque assays as described in **4.4.6**. The process of virus reconstitution is illustrated in **Figure 5.7**.

## **5.2 MHV68-LMP2A VIRUS CHARACTERIZATION AND PHENOTYPIC ANALYSIS**

### **5.2.1 CHARACTERIZATION OF RECOMBINANT MHV68-LMP2A BY LEFT END GENOME PCR**

During in vitro propagation of MHV68, left end genome losses have been observed and thus, the characterization by using left end PCR is to ensure that the genome of MHV68-LMP2a generated is still intact. A control with the MHV68-WT was used which helped to confirm that intact MHV68-LMP2a particles were successfully generated, and not that of truncated unwanted forms. The M1 and M1-M2 genes which are located at the left end of the MHV68-WT genome were tested by PCR to see if the genes were still present in the MHV68-LMP2a genome. The same PCR bands of M1 and M1-M2 MHV68-LMP2a genome were observed as in MHV68-WT indicating that the left end of the MHV68-LMP2a genome was intact. If left end genome deletion had occurred, a shorter band would have been observed in the MHV68-LMP2a group, which was not the case seen in **Figure 5.8**.

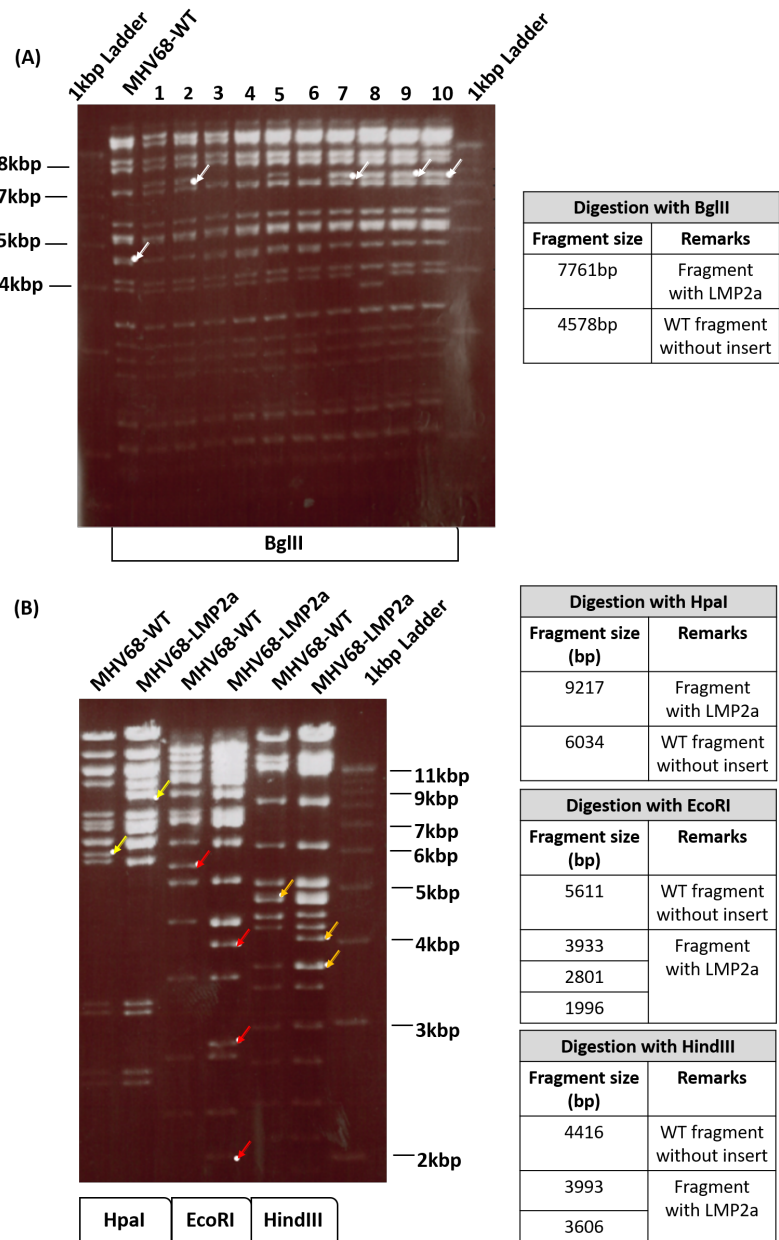


**Figure 5.6: Restriction enzyme analysis of BAC DNA of MHV68-LMP2a in comparison to MHV68-WT to determine and select for the desired recombinant.** (A) The initial ten probes were subjected to restriction digestion with BgIII and results compared to the control containing MHV68-WT. The loss of a 4578bp band with the gain of a 7761bp band, illustrated with white arrows and dots, signifies the correct and successful insertion of the LMP2a gene construct through homologous recombination (Samples 2, 7, 9 and 10). (B) A selected clone (Clone 2) was further restriction digested separately with HpaI, EcoRI and HindIII for further confirmation of the desired recombinant, giving rise to expected band patterns shown. The tables summarize the digestion with the different restriction enzymes used showing fragments without the insert, and fragments with the insert successfully inserted. (Yellow arrows marking out the selected gain or loss of bands when digestion with HpaI was done, red arrows for digestion with EcoRI, orange arrows for digestion with HindIII).

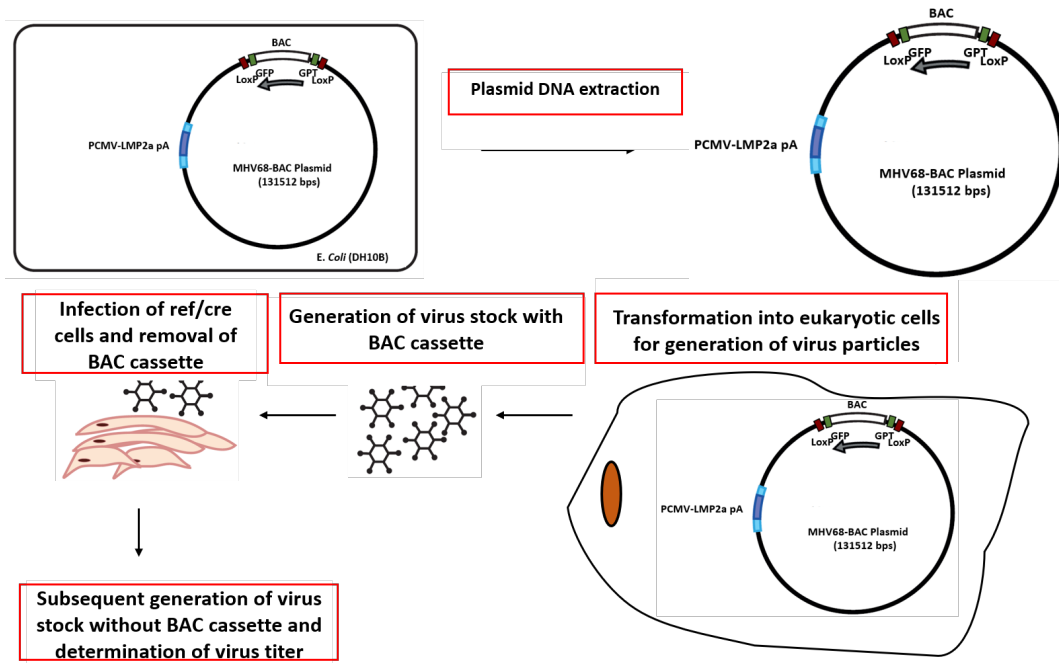


**Figure 5.7: Schematic diagram showing how virus particles are generated from the cloned MHV68-LMP2a viral genome.** BAC cassette is removed and virus without BAC is generated with subsequent determination of virus titer.

### 5.2.2 IN VITRO ANALYSIS OF RECOMBINANT MHV68-LMP2A SHOWED LMP2A EXPRESSION AND UNAFFECTED VIRAL REPLICATION

#### DETECTION OF LMP2A PROTEIN EXPRESSION IN CELLS

After successful reconstitution of the recombinant virus, protein expression of the LMP2a gene, inserted downstream from the PCMV, was determined to ensure that LMP2a was expressed after infection of cells. After infection of cells with MHV68-LMP2a, cell lysates harvested for western blot showed that LMP2a (54kDa) could be detected and was indeed expressed by the recombinant MHV68-LMP2a as seen in **Figure 5.9**. Negative control cell lysates that were not infected or that were infected with MHV68-WT showed no bands as expected. Positive control cell lysates making use of the LCL D2098 (an EBV infected B cell line) showed the equivalent 54kDa LMP2a band.

#### ANALYSIS OF VIRAL REPLICATION KINETICS

To determine the replicative behaviour and viral kinetics in vitro, virus growth curve analysis was done. In addition, the effects of the newly generated MHV68-LMP2a was compared with respect to the MHV68-WT so as to ensure that the recombinant virus was fit and not in any way compromised due to the insertion of the PCMV-LMP2a expression cassette. From **Figure 5.10**, it can be determined that no significant differences with respect to the lytic replication between the MHV68-WT and the recombinant MHV68-LMP2a were observed. This, thus, indicates that the insertion of the expression cassette did not affect the lytic replicative properties of the virus in vitro.

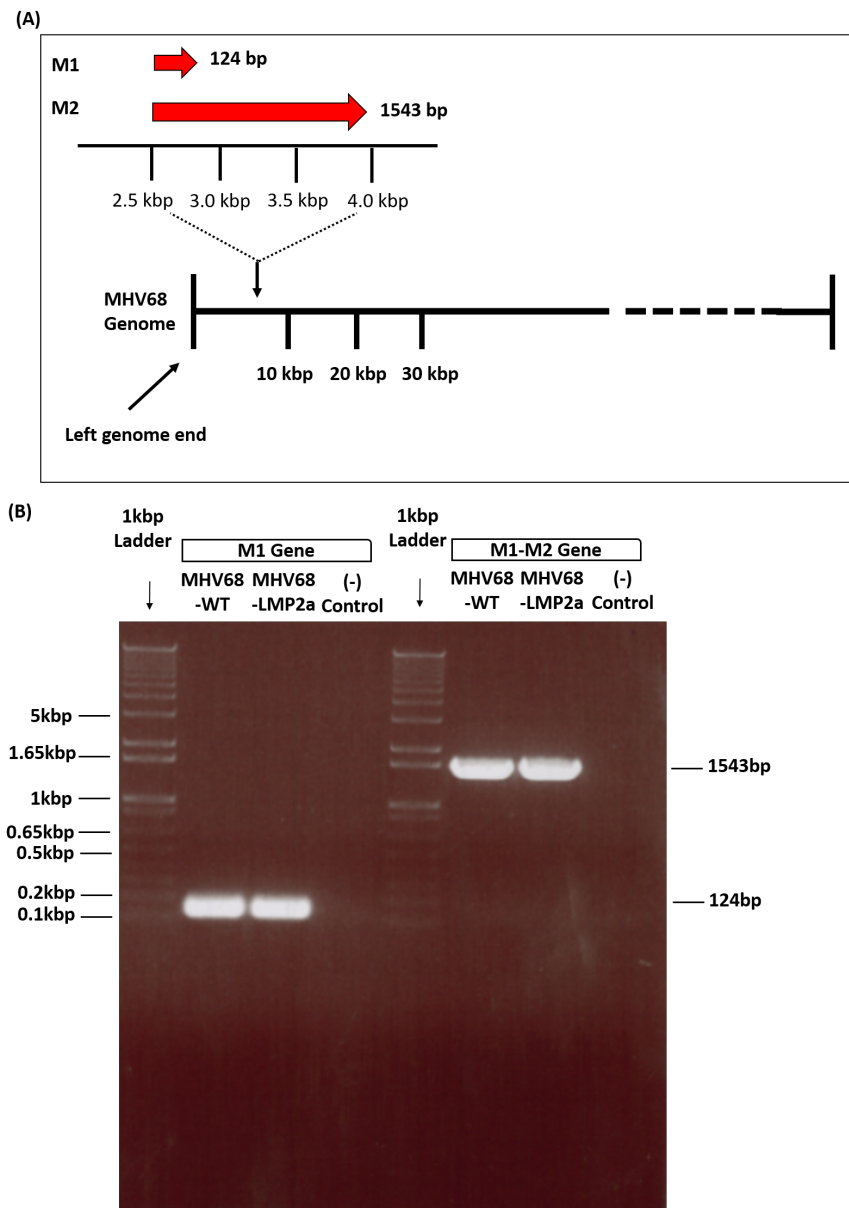


**Figure 5.8: Characterization of the recombinant virus by left end genome PCR.** (A) **Schematic illustration of the left end genome of MHV68-WT.** Primer pairs specific for the left end genome of MHV68-WT were used, producing PCR products of 124bp (M1) and 1543bp (M1-M2) which can be visualised by gel electrophoresis. (B) **Left end genome PCR gel electrophoresis.** The bands observed from MHV68-WT and MHV68-LMP2a show the same band patterns indicating that left end genome deletion had not occurred.

### 5.2.3 IN VIVO ANALYSIS OF RECOMBINANT MHV68-LMP2A AFTER INTRANASAL INFECTION.

In order to fully characterize the recombinant MHV68-LMP2a, infection of C57BL/6 wild type mice was used to analyse the growth characteristics *in vivo*. To determine these characteristics of the recombinant virus, mice were intranasally infected with  $5 \times 10^4$  PFU of the recombinant MHV68-LMP2a and the MHV68-WT. The latter served as a control and as a comparison to the recombinant

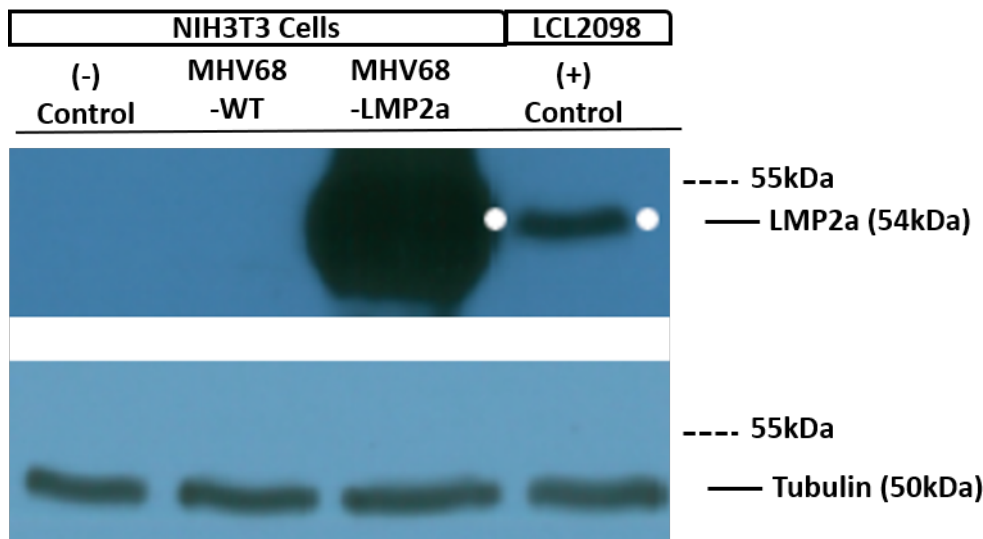


**Figure 5.9: Detection of LMP2a and tubulin protein by western blot analysis.** MHV68-WT or MHV68-LMP2a infected NIH3T3 cells and a lymphoblastic cell line LCL2098 serving as the positive control were harvested and prepared for western blot analysis. LMP2a protein was detected in MHV68-LMP2a infected cells and the LCL2098 controls. Detection of tubulin served as a positive loading control.

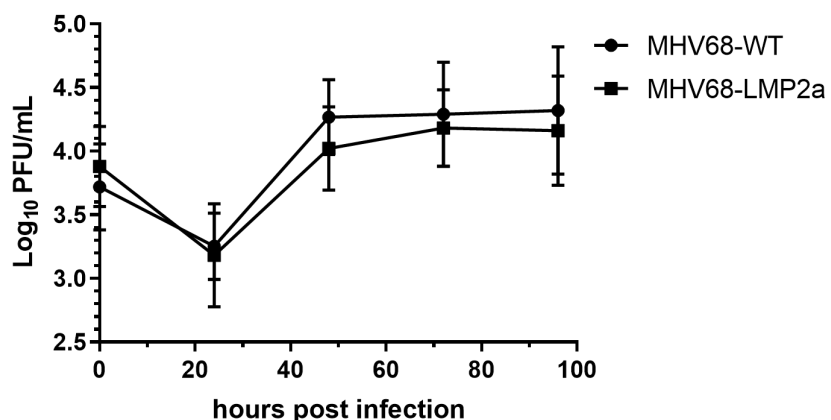


**Figure 5.10: Growth curves showing lytic replication in NIH3T3 cells.** NIH3T3 cells are infected with MHV68-WT or MHV68-LMP2a and harvested after various timepoints with the respective virus titer determined. A multiplicity of infection (MOI) of 0.1 was used. After 96 hours, both the MHV68-WT and the recombinant MHV68-LMP2a reaches comparable titers. Experiment was repeated three times (n=3) with each point representing the mean  $\pm$  SE.

MHV68-LMP2a. The lytic replicative ability of the virus in lungs as well as latency establishment in the spleens were determined.

#### LYTIC REPLICATION OF RECOMBINANT MHV68-LMP2A

In order to determine whether successful intranasal infection had taken place, as well as the lytic replicative ability of the recombinant virus in C57BL/6 mice, the lungs of intranasally infected mice were harvested 6 or 7 days post infection to determine viral titers. As observed from the **Figure 5.11**, viral titers in lungs of MHV68-LMP2a and MHV68-WT infected mice showed that acute infection had

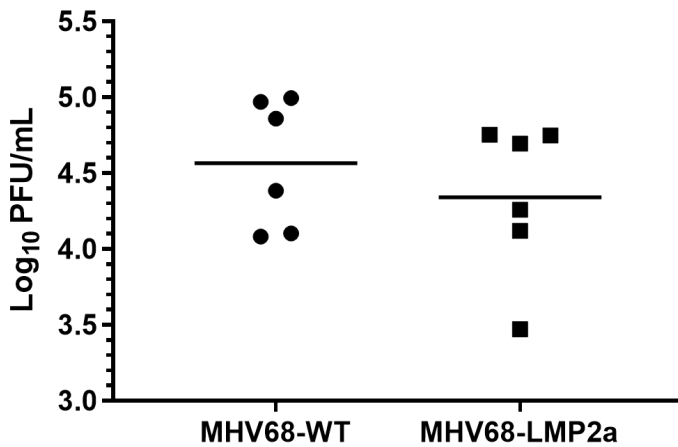


**Figure 5.11: Viral lytic replication.** Viral titers, plotted logarithmically, as a representative of the total viral lytic replication are determined from the homogenized lung tissue of the MHV68-WT and MHV68-LMP2a infected C57BL/6 mice 6 or 7 days post-infection, where the mean (represented by the horizontal line) was determined. C57BL/6 mice were i.n infected with  $5 \times 10^4$  PFU. (n=6) where n= number of mice used and each point on the graph represents virus titer of a mouse. Experiment was repeated twice, each with 6 mice (3 with MHV68-WT and 3 with MHV68-LMPa) for a total of 12 mice.

successfully occurred and no significant differences were observed between the two viruses used, as represented by the viral titers measured.

#### **ESTABLISHMENT OF LATENCY IN SPLEENS OCCURRED BY DAY 10 POST-INFECTION**

As a measure of latency establishment, splenic weights were recorded and frequency of reactivation from latency by means of ex-vivo reactivation assays were analysed.

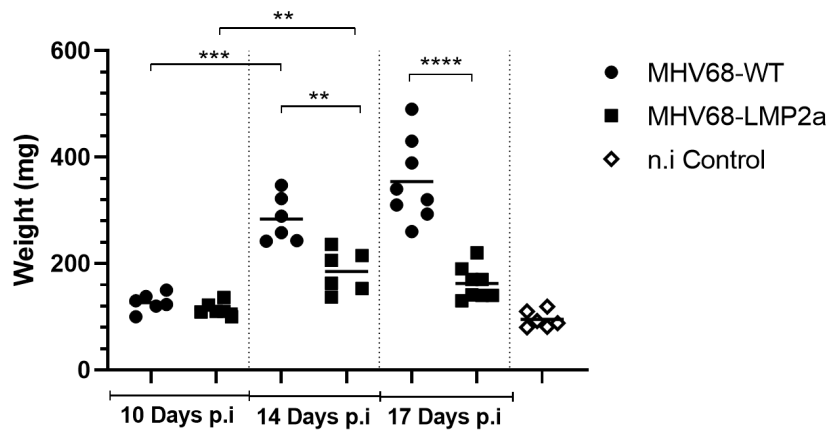


**Figure 5.12: Weight of spleen after intranasal infection.** C57BL/6 mice were i.n infected with  $5 \times 10^4$  PFU. Splenic weights of MHV68-LMP2a and MHV68-WT infected C57BL/6 mice were determined after 10 days (n=12), 14 days (n=12), and 17 days (n=16) of infection, together with the non-infected controls (n=6). n= number of mice used and each point on the graph represents the splenic weight of one mouse with means being tabulated and represented by the horizontal line on the graph.

After 10 days post infection, differences were already observed between the splenic weight of

virus infected mice and non-infected controls but no significant differences were observed when comparing both groups of virus infected mice at that time point seen in **Figure 5.12**. However, from 14 days after infection, MHV68-WT infected mice had significantly enlarged spleens in comparison to MHV68-LMP2a infected mice ( $p=0.0022$ ). Splenic weight of MHV68-WT infected mice showed a steady increase from day 10 to day 17. However, the splenic weight of MHV68-LMP2a infected mice increased less from day 10 to day 17 in comparison to MHV68-WT infected mice and did not further increase by day 17. In conclusion, significant differences were observed in the splenic weight of the respective virus infected mice going from day 10 to 14. Splenic weights of virus infected mice from day 14 post infection were significantly larger when compared to non-infected controls.

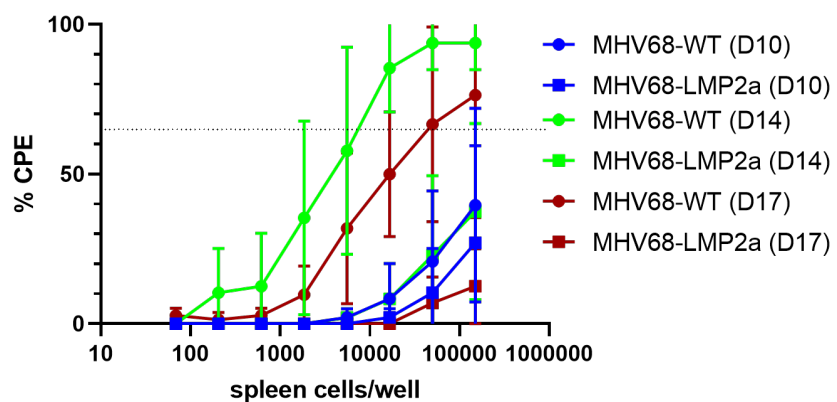


**Figure 5.13: Ex-vivo reactivation of splenocytes after i.n infection of C57BL/6 mice with MHV68-WT and recombinant MHV68-LMP2a at 10, 14 and 17 days post infection.** C57BL/6 mice were i.n infected with  $5 \times 10^4$  PFU of virus. After 10, 14 and 17 days post infection, the incubation of three fold dilutions of the splenocytes with NIH3T3 cells was done to obtain a set of 8 values. Experiment was repeated twice for day 10 and 14 post-infection ( $n=3$  for each virus and experiment) and three times for day 17 post-infection ( $n=3$  for each virus and experiment twice followed by an experiment with  $n=2$ ). Each point on the graph represents the mean  $\pm$  SD.

A second parameter that can be used to determine the latency behaviour of MHV68-WT and MHV68-LMP2a, is by looking at the number of infected splenocytes that are able to enter the lytic phase after establishment of latency. This reactivation occurs ex vivo through the contact of infected splenocytes with fibroblasts in the reactivation assay carried out as described in **4.5.4**. The splenocytes used were those of spleens that were previously weighed. At all time points, the MHV68-LMP2a infected splenocytes showed a lower reactivation from latency when compared with MHV68-WT infected splenocytes 10, 14 and 17 days post-infection as observed from **Figure 5.13**.

#### MHV68-LMP2A INFECTED MICE HAD LOWER VIRAL GENOMIC LOADS THAN MHV68-WT INFECTED MICE

As illustrated in **Figure 5.14**, viral genomic loads measured in spleens were higher for MHV68-WT infected mice in comparison to that of MHV68-LMP2a infected mice during the three time points.

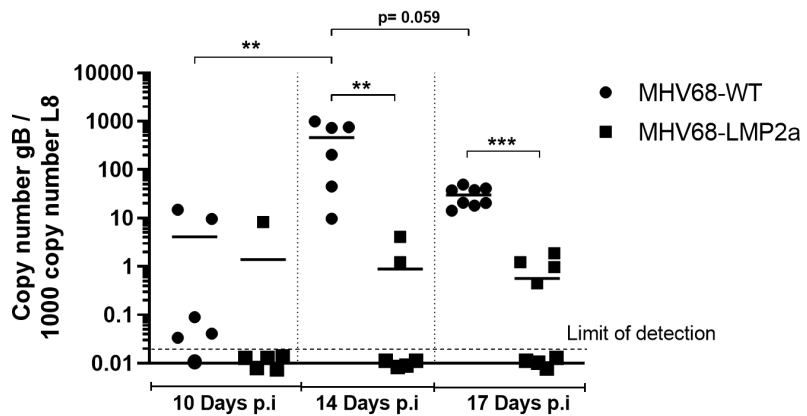


**Figure 5.14: Viral genomic load in spleen.** The quotient of copy number of the gB gene to the copy number of the L8 gene multiplied by 1000 was used as a suitable index for viral genomic load determination, so that quantities could be effectively compared between the experimental groups. Graph shows viral genomic load in spleens, that were previously weighed. Experiment was repeated twice for day 10 and 14 post-infection ( $n=3$  for each virus and experiment) and three times for day 17 post-infection ( $n=3$  for each virus and experiment twice followed by an experiment with  $n=2$ ) where  $n$  = number of mice used. Each point on the graph represents viral genomic load of a mouse with means being tabulated and represented by the short horizontal line on the graph. A dashed horizontal line near the bottom of the graph represents the detection limit of the PCR, with points below it representing viral genomic loads that remain undetected.

Thus, recombinant MHV68-LMP2a, though detected in spleens, was present in much lower levels compared to the MHV68-WT indicating that the recombinant virus might be eliminated from the mice at higher rates. The relative values of the viral genomic loads measured were in line with the values obtained from the reactivation assays, that also showed a lower rate of reactivation for the recombinant MHV68-LMP2a.

#### 5.2.4 FACS ANALYSIS OF MHV68-LMP2A IN INFECTED WILD TYPE C57BL/6 MICE

FACS was carried out by harvesting the spleen cells and staining with various antibody mixes as described in 4.5.5. Various different experiments were conducted with the data summarized in the illustrations and graphs. Each point on the graph is a representation of data from 1 mouse investigated.

#### COMPARABLE B CELL EXPANSION AFTER INFECTION OF MICE WITH MHV68-WT AND MHV68-LMP2A

Infection with gammaherpesviruses has been observed in B cell lymphomas (Cesarman, 2014). Hence, B cell numbers and activation were measured to determine expansion and proliferation with respect to virus infection. To compare the effect of the newly generated MHV68-LMP2a with the MHV68-WT on B cell profiles, comparisons of the different lymphocyte populations at days 10, 14, and 17 post infection were done. The total B cell numbers in the spleens of MHV68-LMP2a infected mice were at comparable levels with those of the non-infected controls. At day 14 post infection, B cells numbers were slightly higher in MHV68-WT infected mice than in MHV68-LMP2a as

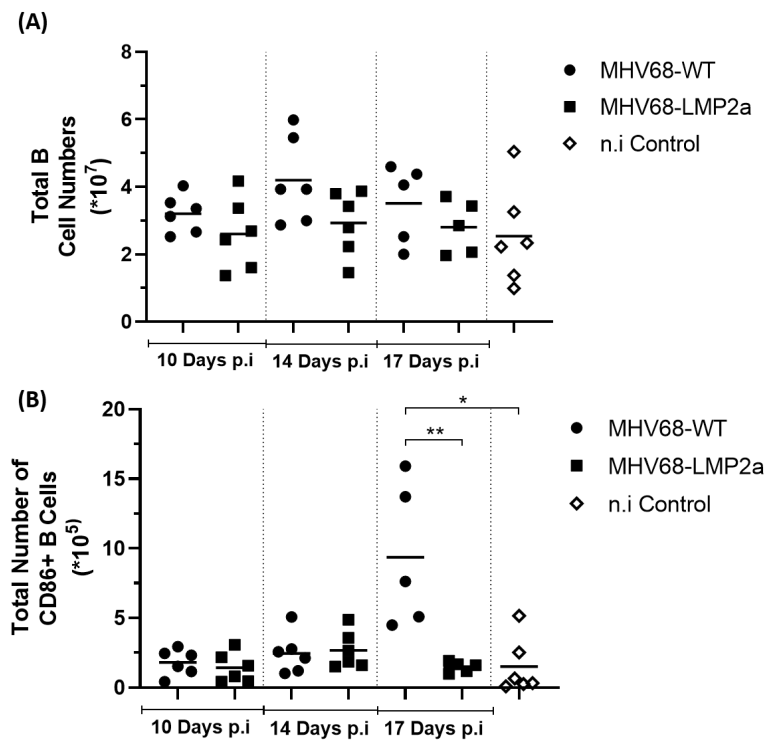


**Figure 5.15: Total B cell numbers were slightly higher in MHV68-WT infected mice with higher B cell activation at day 17 post infection in comparison to MHV68-LMP2a. (A) Total B cell numbers.** Living lymphocytes were gated and cells that were  $CD19^+Thy1.2^-$  were gated as B cells. Total B cell numbers were calculated with respect to total splenocytes tallied. **(B) Total number of CD86<sup>+</sup> B cells.** Lymphocytes were gated followed by gating of  $B220^+$  cells. Next,  $CD86^+$  cells were gated and total numbers were calculated with respect to total splenocytes tallied.

shown in **Figure 5.15A**. When looking at B cell activation with the help of the activation marker CD86 as depicted in **Figure 5.15B**, more activated B cells could be detected at 17 days post infection in spleens of MHV68-WT infected mice compared to that of MHV68-LMP2a infected mice.

#### **COMPARABLE T CELL NUMBERS IN MHV68-WT AND MHV68-LMP2A INFECTED MICE**

After infection with MHV68-WT and MHV68-LMP2a, a slight increase in T cell numbers could be observed in MHV68-WT infected mice compared to MHV68-LMP2a infected mice. The highest total T cell numbers was observed at 14 days post infection as observed in **Figure 5.16**.

By looking at  $CD69^+$  stained cells,  $CD4^+$  and  $CD8^+$  T cells activation were determined. With respect to the  $CD4$  T cell activation illustrated in **Figure 5.17A**, T cell activation increases upon infection at day 14 and 17 with slightly more activation observed in MHV68-WT infected mice.

As seen in **Figure 5.17B**, when looking at  $CD8^+$  T cell activation, as early as 10 days post infection as well as on the following days of 14 and 17 post infection, MHV68-WT infected mice had higher total cell numbers of  $CD8^+$  activated T cells in comparison to MHV68-LMP2a infected mice.

In conclusion, slightly higher lymphocyte numbers but lower activations of B and T lymphocytes were observed in MHV68-LMP2a infected mice as compared to MHV68-WT infected mice.

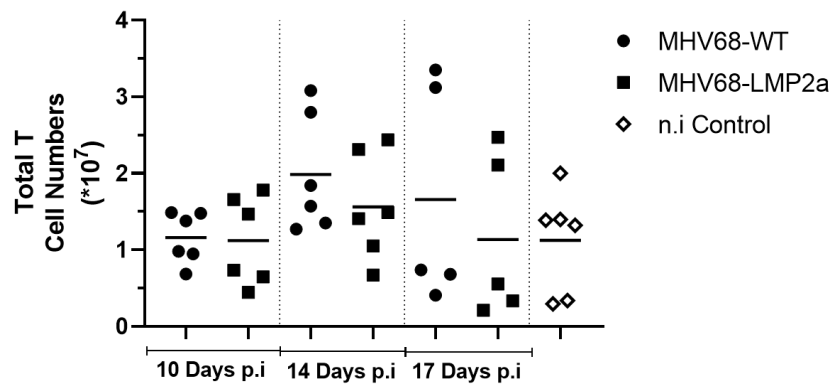


**Figure 5.16: Total T cell numbers of MHV68-WT infected mice were higher compared to MHV68-LMP2a infected mice.** Living lymphocytes were gated and cells that were  $CD19^- Thy1.2^+$  were gated as T cells. Total T cell numbers were calculated in relation to total splenocytes tallied.

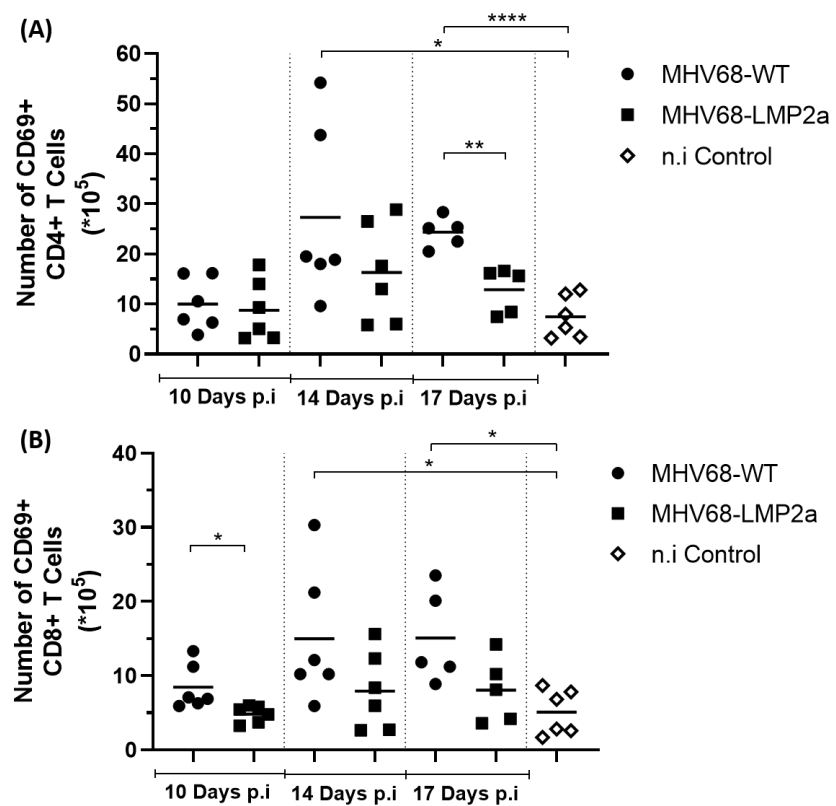


**Figure 5.17: Higher CD4<sup>+</sup> and CD8<sup>+</sup> T cell activation (CD69<sup>+</sup>) in MHV68-WT infected mice than MHV68-LMP2a infected mice.** (A) **CD69 expression on CD4<sup>+</sup> T cells.** Lymphocytes were gated and CD69<sup>+</sup> was gated after CD4<sup>+</sup> T cells (CD4<sup>+</sup> CD8<sup>-</sup>) and total numbers of CD69<sup>+</sup> CD4<sup>+</sup> T cells were calculated with respect to total splenocytes. (B) **CD69 expression on CD8<sup>+</sup> T cells.** Lymphocytes were gated and CD69<sup>+</sup> was gated after CD8<sup>+</sup> T cells (CD4<sup>-</sup> CD8<sup>+</sup>) and total numbers of CD69<sup>+</sup> CD8<sup>+</sup> T cells were calculated with respect to total splenocytes. A significant difference was observed between MHV68-WT and MHV68-LMP2a infected mice groups at day 10 post infection ( $p=0.033$ ).

## INFECTION WITH BOTH VIRUSES LEAD TO A GRADUAL INCREASE IN GCB CELLS IN SPLEENS AND LYMPH NODES

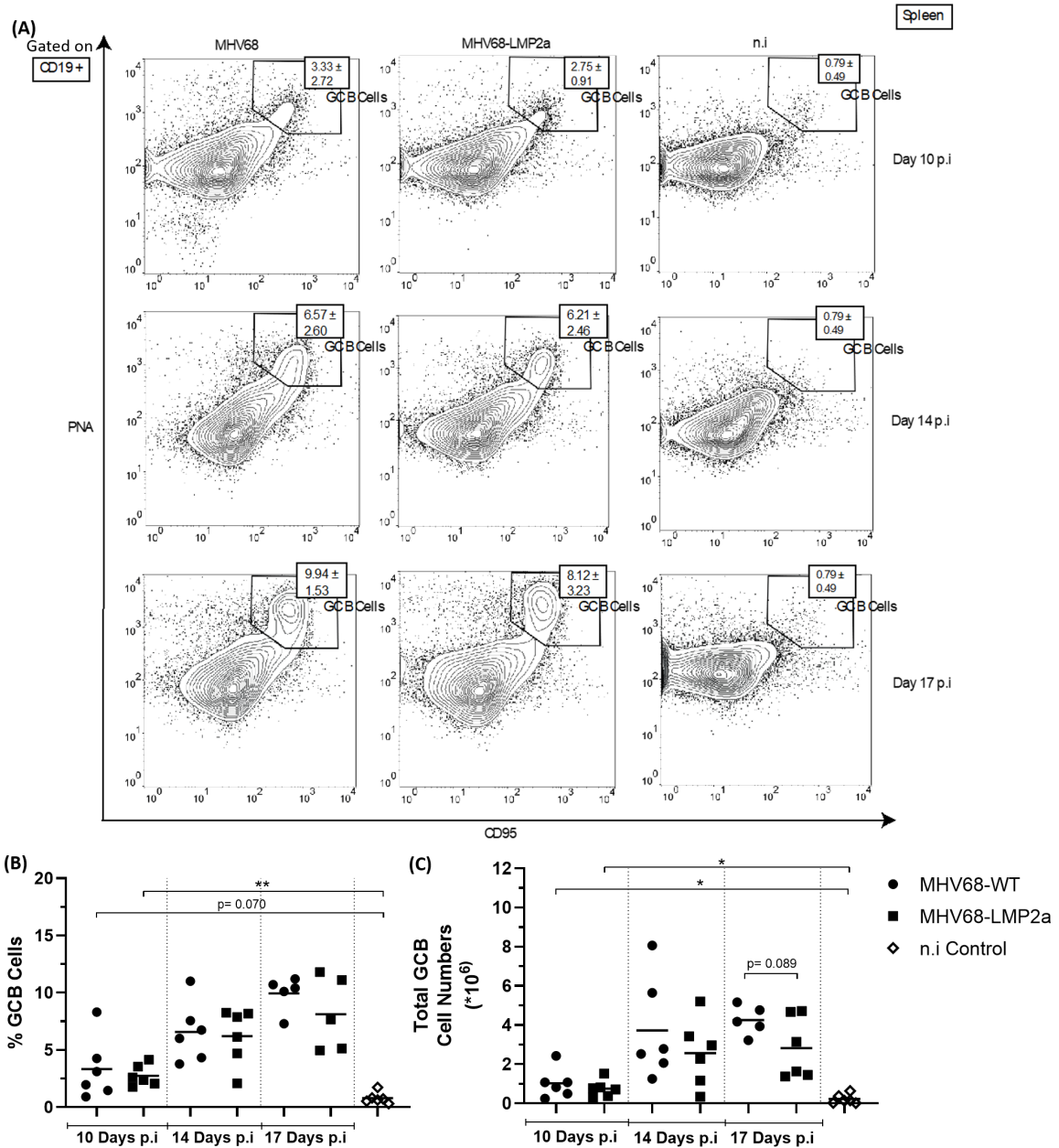


**Figure 5.18: Comparable GCB cell formation after infection with MHV68-LMP2a and MHV68-WT.** (A) FACS diagram showing the percentages of GCB cells ( $\text{CD}95^+ \text{ CD}19^+$ ) in spleens. (B) Percentage of GCB cells in spleens. The plots are gated on lymphocytes and B cells ( $\text{CD}19^+$ ). (C) Total GCB cell numbers in spleens. Total GCB cell numbers were calculated with respect to total splenocytes tallied.

After gammaherpesviral infection, primary B cells become activated and form germinal centers in the spleen and lymph nodes, where they undergo SHM and CSR. These germinal center B cell reactions and post-germinal center reactions are common sites where mutations can occur, leading to lymphoma development Küppers (2009). Hence, germinal center B cells were investigated.

The percentage of GCB cells as well as total GCB cell numbers in the spleen showed a gradual increase from day 10 to day 17 post infection with no significant differences observed between MHV68-WT and MHV68-LMP2a infected mice as seen in **Figures 5.18A+B+C**.

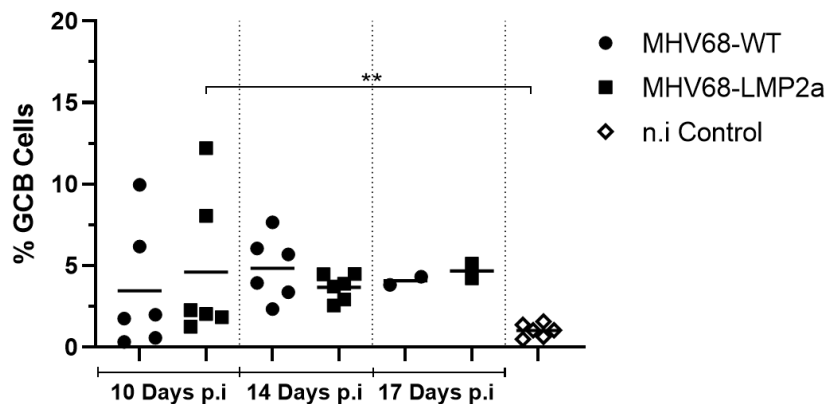


**Figure 5.19: Percentage of GCB cells in the cervical lymph nodes showed no difference between the viruses used.** GCB cells ( $CD95^+ CD19^+$ ) were gated in a similar manner as that of GCB cells in spleens.

When looking at the percentage of GCB cells in cervical lymph nodes in **Figure 5.19**, a gradual increase was similarly observed from day 10 to day 17 post infection with no significant differences being observed between the two virus infected mice groups at all time points measured.

Thus, virus infection, regardless of whether it was the MHV68-WT or the recombinant MHV68-LMP2a, led to a germinal center reaction in spleens and cervical lymph nodes with no difference observed between both viruses used.

#### SIMILAR PLASMA CELL NUMBERS AFTER MHV68-WT AND MHV68-LMP2A INFECTION

Plasma cells, being one of the fates of the post germinal center B cell reaction, were thus investigated as well. The highest percentages of plasma cells as seen in **5.20A+B** as well as total plasma cell numbers in **Figure 5.20C** were observed at 14 days post infection for both virus infected mice groups. At all three time points, there were no significant differences observed between the two different virus infected mice groups.

In conclusion, experiments done in wild type C57BL/6 mice to characterize the recombinant MHV68-LMP2a in comparison to MHV68-WT showed that both the wild type and recombinant virus led to generation of GCB cells as well as plasma cells to a similar extent. B and T cells expansion too did not differ from each other when comparing between the two virus infected mice groups. More activation of lymphocytes was observed in MHV68-WT infected mice in comparison to MHV68-LMP2a infected mice with similarities in the numbers of GCB cells and plasma cells generated. Hence, the newly generated recombinant virus MHV68-LMP2a behaves in a similar way as the MHV68-WT in wild type mice.

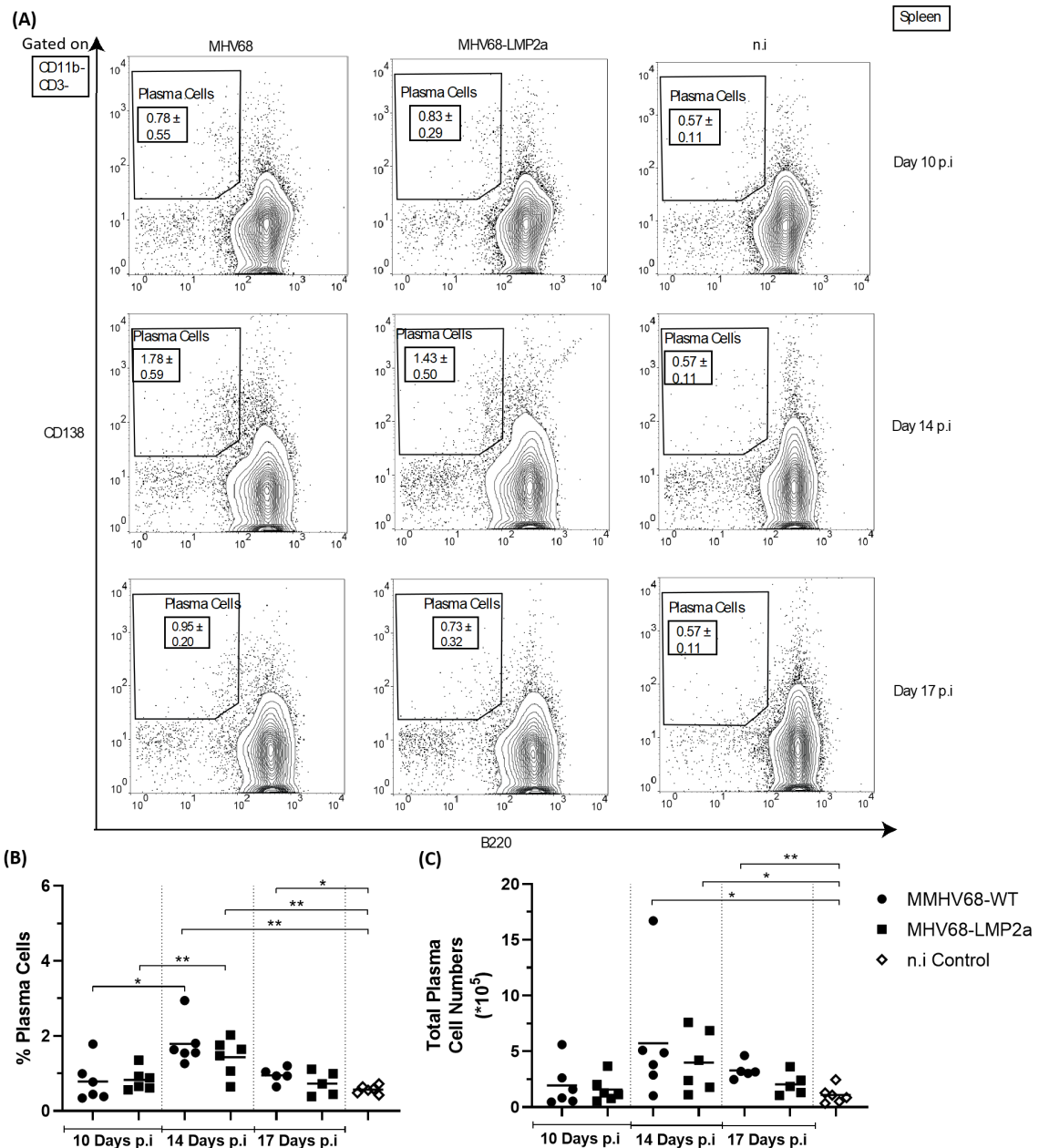


**Figure 5.20: No differences between percentages of plasma cells as well as total plasma cell numbers between both viruses used. (A) FACS diagram showing the percentages of plasma cells ( $CD138^+ B220^-$ ). (B) Percentage of plasma cells. The plots were gated on lymphocytes followed by  $CD3^-$  and  $CD11b^-$ . (C) Total plasma cell numbers. Total plasma cell numbers were calculated with respect to total splenocytes tallied.**

### 5.3 EFFECT OF RECOMBINANT MHV68-LMP2A IN LMP1/CD30 $\gamma$ 1CRE MICE

The gammaherpesvirus EBV has long been associated with various different lymphomas Grywalska & Rolinski (2015). EBV expresses many different viral proteins that, in combination, lead to the formation of such lymphomas Price & Luftig (2015). One such viral protein of EBV is the LMP2a protein that mimics a constitutively active BCR signal. This enables B cells without a proper BCR to survive and avoid apoptosis. Apart from viral proteins such as that of the LMP2a protein, many lymphomas have been associated with CD30, which belongs to the tumor necrosis factor receptor superfamily Sotomayor et al. (2014). Thus, this gives rise to another classification of lymphomas, the CD30+ lymphomas, such as the primary effusion lymphoma (PEL) and the classical hodgkin lymphoma. These lymphomas, as well as many other lymphomas, derive from GCB cells Küppers (2005). Thus, the final aim of this project is to investigate whether the combined effects of the viral protein LMP2a and a dysregulated CD30 would lead to accelerated lymphomagenesis. Cloning of the LMP2a in the MHV68 allowed the introduction and investigation of the viral protein LMP2a in the context of a herpesviral infection in mice. To induce a dysregulated CD30 signalling in GCB cells, LMP1/CD30 mice were paired with  $\gamma$ 1cre mice to generate LMP1/CD30  $\gamma$ 1cre mice. These mice express the cre recombinase genome under the control of the  $\gamma$ 1 immunoglobulin locus resulting in the deletion of the stop-cassette in activated and GCB cells. In the presence of infection, such as the MHV68-LMP2a infection, cre recombinase would be expressed, which would later excise the STOP cassette upstream of the LMP1/CD30 protein as depicted in **Figure 1.4**. This leads to the expression of the LMP1/CD30 protein that causes a constitutive dysregulated CD30 signalling in the cells. The transmembrane domain of the LMP1 causes the independent and constitutive signalling cascade of the CD30 with signalling not dependent on CD30 ligand binding Sperling et al. (2019). In order to tag cells that have this constitutive CD30 signalling, a reporter, the hCD2 protein, whose coding sequence is downstream of the LMP1/CD30 genome, is used. Thus, reporter positive cells are cells which have the LMP1/CD30 expressed. As control mice, the R26-Car  $\gamma$ 1cre mice were used in which the truncated version of the human CAR was expressed upon infection and cre recombination.

From the results obtained in wild type mice, MHV68-LMP2a and MHV68-WT showed similarities in viral kinetics as well as the different cell populations measured. Thus, having found out that the recombinant MHV68-LMP2a, in comparison to MHV68-WT, was not severely compromised, the recombinant virus was now tested in relation to a dysregulated CD30 in LMP1/CD30  $\gamma$ 1cre (LC30) mice and control R26-Car  $\gamma$ 1cre (CAR) mice. LC30 and CAR mice were intraperitoneally (i.p) in-

fected with a concentration of  $1 \times 10^5$  PFU of virus and organs (lungs, lymph nodes and spleens) harvested after 14 days and 2 months of infection for analysis. Furthermore, instead of the MHV68-WT being used here, a second recombinant virus, the MHV68-NGFR was used as a control for the experiments. The MHV68-NGFR is a recombinant virus that was reconstituted in a similar way as that of the recombinant MHV68-LMP2a. The human NGFR (Nerve growth factor receptor) gene that is cloned into the MHV68 genome is a truncated and mutated form. This ensures that it expresses only the surface marker without the ability to trigger any signalling cascades. Hence, after MHV68-NGFR infection, NGFR receptors expressed on the cell surface can be utilized to detect cells that have been successfully infected by the recombinant MHV68-NGFR. These cells can be stained with antibodies and further analysed. In addition, the use of the recombinant virus MHV68-NGFR serves as a good control since it is a recombinant virus that was reconstituted in a similar way as that of the recombinant MHV68-LMP2a. The recombinant MHV68-NGFR was cloned, tested and characterized by the research group and was not severely compromised, based on experiments conducted (unpublished data from research group).

### 5.3.1 SPLENIC WEIGHT AND FREQUENCY OF REACTIVATION

#### SLIGHTLY INCREASED SPLENIC WEIGHT IN LC30 MICE IN COMPARISON TO CAR MICE 2 MONTHS POST INFECTION

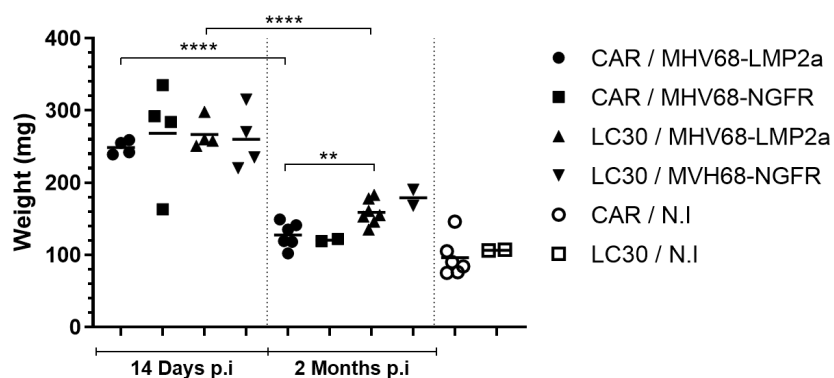


**Figure 5.21: Splenic weight.** LC30 and CAR mice were intraperitoneally (i.p) infected with a concentration of  $1 \times 10^5$  PFU of virus. Splenic weight of MHV68-NGFR and MHV68-LMP2a infected LC30 and CAR mice were determined after 14 days and 2 months of infection, together with non-infected controls. Decreased splenomegaly observed 2 months post infection than 14 days post infection in virus infected mice.

Since gammaherpesviruses undergo latency in the spleen, the splenic weights of virus infected mice were recorded as an index to determine a potential lymphocyte expansion. With reference to **Figure 5.21**, after 14 days, no differences were observed regardless of the virus or mice used but virus infected mice showed significant splenomegaly in comparison to non-infected controls. Even 2 months post infection, splenomegaly was still observed for both MHV68-LMP2a and MHV68-NGFR infected CAR or LC30 mice in comparison to non-infected controls. However, when compared

to the spleens 14 days post infection, the splenic weight of infected mice 2 months post infection showed significant decrements.

When comparing among the spleens of the 2 months mice, mice dependent differences were observed, with MHV68-NGFR and MHV68-LMP2a infected LC30 mice having larger splenic weights in comparison to their virus infected CAR mice counterparts. Thus, splenomegaly was observed both 14 days and 2 months after infection, with LC30 expression inducing a slightly stronger splenomegaly 2 months post infection for both viruses used.

#### **VIRAL REACTIVATION WAS SIMILAR IN BOTH VIRUS INFECTED CAR AND LC30 MICE.**

Next, to test how many latently infected cells were present, ex vivo reactivation of splenocytes

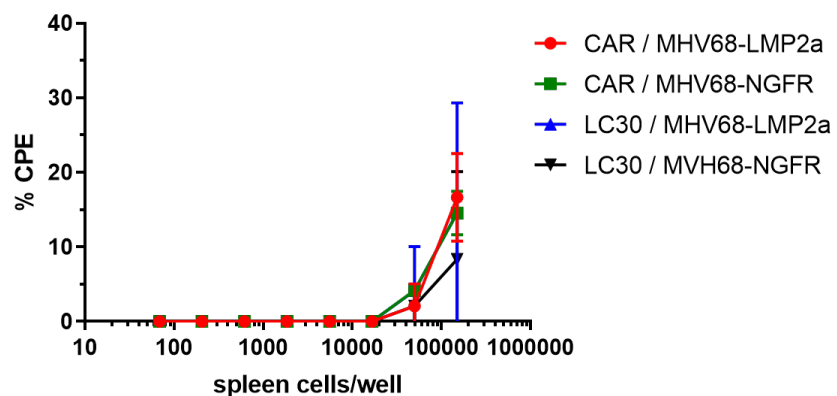


**Figure 5.22: Virus reactivation from latency in spleens at 14 days post infection.** LC30 and CAR mice were intraperitoneally (i.p) infected with a concentration of  $1 \times 10^5$  PFU of virus. After 14 days and 2 months post infection, the incubation of three fold dilutions of the splenocytes with NIH3T3 cells was done to obtain a set of 8 values. Virus reactivation from latency was similar across the four different experimental groups with no differences observed between the two recombinant viruses used.

was analysed. Virus reactivation from splenocytes at 14 days post infection showed no significant differences between the four experimental groups as observed in **Figure 5.22**. At 2 months post infection, virus reactivation from splenocytes was undetectable in the ex vivo reactivation assay (data not shown).

From the results obtained, no differences were observed between the two viruses infected CAR and LC30 mice.

#### **5.3.2 NO DIFFERENCES IN THE VIRAL GENOMIC LOAD IN MICE INFECTED WITH THE TWO RECOMBINANT VIRUSES**

In addition to the virus reactivation, viral genomic load was assessed in order to determine the amount of viral genomes found in cells of the infected mice.

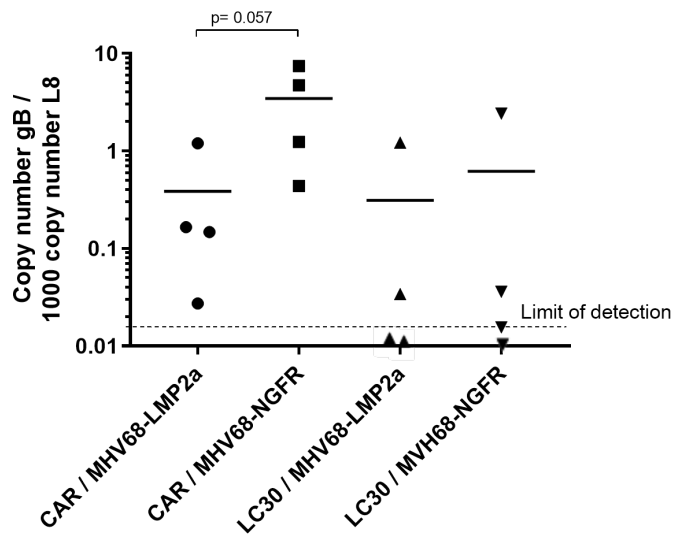


**Figure 5.23: Viral genomic load in spleen at 14 days post infection.** The quotient of copy number of the gB gene to the copy number of the L8 gene multiplied by 1000 was used as a suitable index for viral genomic load determination, so that quantities could be effectively compared between the experimental groups. Graph shows viral genomic load in spleens, that were previously weighed. Virus infected LC30 mice have lower viral genomic loads than their virus infected CAR mice counterparts. Each point on the graph represents viral genomic load of a mouse with means being tabulated and represented by the short horizontal line on the graph. A dashed horizontal line near the bottom of the graph represents the detection limit of the PCR, with points below it representing viral genomic loads that remain undetected.

With reference to **Figure 5.23**, making use of the quotient of copy number of the gB gene to the copy number of the L8 gene multiplied by 1000 as a suitable index for comparing viral genomic load, no significant differences were observed at 14 days post infection in terms of the viral genomic load in spleens harvested between the LMP2a and NGFR infected CAR or LC30 mice.

The viral genomic load in spleens of LC30 infected mice was slightly lower compared to their CAR counterparts, although these differences were not statistically significant. MHV68-NGFR infected mice had spleens with higher genomic viral load compared to that of the MHV68-LMP2a infected mice, though these differences were also not statistically significant.

At 2 months post infection (data not shown), viral genomic loads in spleens harvested from all four experimental mice groups were undetectable by the TAQMAN realtime PCR method used, indicating that during chronic infection, the presence of virus in spleens is greatly reduced regardless of the virus or mice type used.

Thus, there was no difference in the viral load and the virus reactivation from latency between CAR and LC30 mice infected with either MHV68-NGFR or MHV68-LMP2a.

### 5.3.3 FACS ANALYSIS OF MHV68-NGFR AND MHV68-LMP2A IN CAR AND LC30 MICE

In order to investigate whether LMP2a expression or a dysregulated CD30 expression leads to accelerated lymphomagenesis, various lymphocyte populations as well as specific B cell population profiles were measured using FACS. FACS was carried out by harvesting the spleen, cervical lymph nodes and peritoneal cavity cells and subsequently staining them with various antibody mixes in order to ascertain and determine different cell populations, as described in **4.5.5**.

#### B CELLS; SPLEENS OF LC30 MICE HAD MORE REPORTER POSITIVE B CELLS DESPITE COMPARABLE B CELL NUMBERS

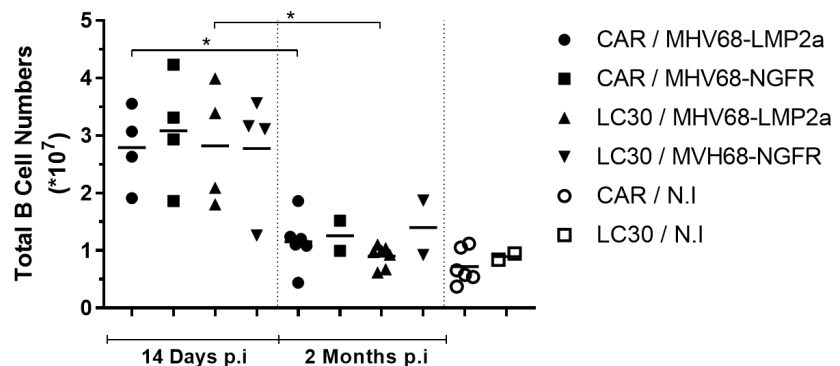


**Figure 5.24: Total B cell numbers were higher 14 days post infection compared to 2 months post infection with no differences observed between the viruses used.** Living lymphocytes were first gated followed by the B cells ( $CD19^+ Thy1.2^-$ ).

In terms of percentages of B cells in spleens, no differences were observed between the experimental groups (not shown in figures). As expected, total B cells in spleens after 14 days of infection as seen in **Figure 5.24** showed increased levels in comparison to spleens from mice after 2 months of infection, as well as to the non-infected controls. No differences were observed between the virus infected CAR and LC30 mice, as well as between the viruses used.

To determine the percentage of reporter positive cells within B cells in LC30 and CAR mice, we stained for the reporters hCD2 and CAR, respectively (reporter positive cells). These reporter positive cells are cells that, upon cre recombination triggered by viral infection, have the STOP cassette removed thus leading to the subsequent expression of LMP1/CD30 and hCD2 reporter proteins or CAR proteins in LC30 and CAR mice, respectively. This is illustrated in **Figure 1.4**. From **Figure 5.25A**, within the 14 days post infection and 2 months post infection time points, virus infected LC30 mice showed higher percentages of reporter positive B cells in comparison to that of virus infected CAR mice. When comparing between the two time points, the percentage of reporter positive B cells

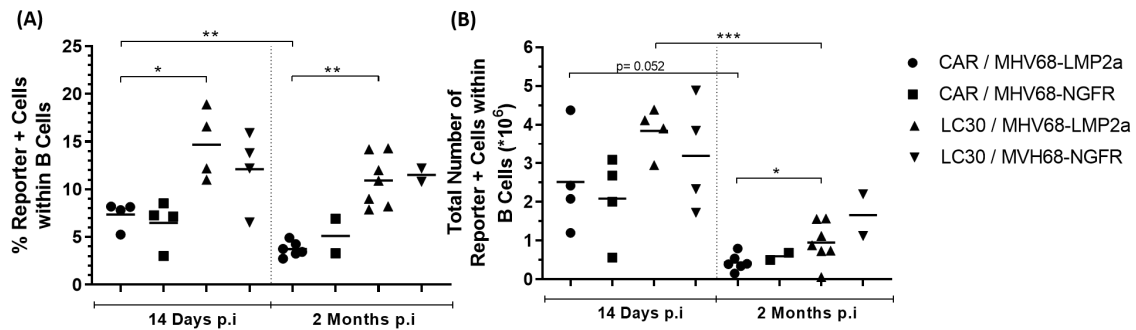


**Figure 5.25: Virus infected LC30 mice show larger expansion of reporter positive cells within B cells at 14 days and 2 months post infection. (A) Percentage reporter positive cells within B cells in spleens.** Lymphocytes were gated followed by B cells ( $B220^+CD19^+$ ) and finally reporter positive cells ( $hCD2^+$  or  $CAR^+$ ) were gated to obtain the percentages of reporter positive cells within B cells. **(B) Total reporter positive B cells in spleens.** After reporter positive cells within the B cells were gated, total number of reporter positive cells were calculated with respect to the total splenocytes tallied.

in CAR mice and LC30 mice were higher at 14 days post infection in comparison to those at 2 months post infection.

The total number of reporter positive cells within B cells showed a similar pattern as seen in **Figure 5.25B**, with LC30 mice having more reporter positive B cells in comparison to CAR mice.

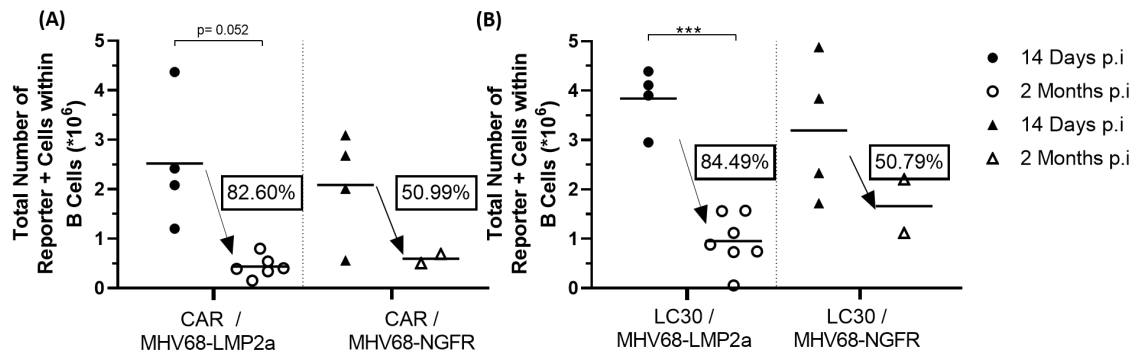


**Figure 5.26: Virus dependent differences were observed with MHV68-LMP2a infected mice showing a greater percentage of decrease in terms of total number of reporter positive cells within B cells measured moving from 14 days to 2 months post infection when comparing with MHV68-NGFR infected mice. (A) Percentage change among virus infected CAR mice. (B) Percentage change among virus infected LC30 mice.**

When looking at the percentage change closely in **Figure 5.26A+B**, there was a greater decrease in the total reporter positive B cells from day 14 to 2 months post infection in MHV68-LMP2a infected CAR and LC30 mice in comparison to MHV68-NGFR infected CAR and LC30 mice, respectively (Virus dependent change regardless of mice type).

#### T CELLS; T CELLS POPULATIONS ARE SIMILARLY EXPANDED IN THE FOUR EXPERIMENTAL GROUPS

Higher cell numbers were tallied in all four experimental groups at day 14 post infection when compared to those at 2 months post infection, as well as when compared to their non-infected controls as seen in **Figure 5.27**. No differences were observed between the viruses used and between mice

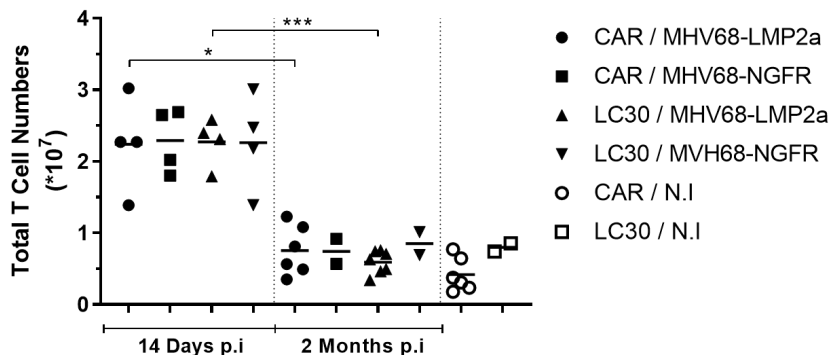


**Figure 5.27: Total T cell numbers were higher 14 days post infection compared to 2 months post infection with no differences observed between the mice type or virus strains used.** Living lymphocytes were gated and cells that were  $CD19^- Thy1.2^+$  were gated as T cells. Total T cell numbers were calculated in relation to total splenocytes tallied.

type.

After looking at the B and T cell populations which did not show any differences between the mice and viruses used, we compared populations of GCB cells in spleens and cervical lymph nodes in the different groups. Since CD30+ lymphomas as well as many other lymphomas are derived from GCB cells, by looking at the GCB cell populations in spleens and cervical lymph nodes, information about the effects of LMP2a protein and CD30 expression in relation to GCB cell expansion can be made. By making use of reporter studies, information about the origins of these cells can be made. In LC30 mice as mentioned in **1.6**, the cre recombinase is expressed under the control of the  $\gamma 1$  immunoglobulin constant region that is transcribed mainly in GCB cells. Hence, after virus infection, the cre recombinase protein is expressed in GC B cells, resulting in the deletion of the stop cassette upstream of the LMP1/CD30 transgene. Subsequently LMP1/CD30 and the reporter gene hCD2 are expressed, while in CAR mice, which are used as controls, the reporter gene CAR is expressed. Since deletions of the STOP cassette occur mainly in GCB cells, it can be said that reporter positive cells are mainly cells that originate from the GC [Casola et al. \(2006\)](#).

#### **GCB CELLS IN SPLEENS; MHV68-LMP2A INFECTION LED TO THE LARGEST GCB CELL EXPANSION**

GCB cells were gated as in **Figure 5.28A**. First, we compared percentages and total cell numbers of GCB cells in spleens of mice from the different groups 14 days and 2 months post infection. As expected, the percentages of GCB cells in spleens of mice 14 days post infection was higher in comparison to that 2 months post infection as well as to non-infected controls as seen in **Figure 5.28B**. By 2 months post infection, the percentages of GCB cell levels were comparable to those in the non-infected controls. In addition, at 2 months post infection, the percentage of GCB cells in virus infected LC30 mice was lower in comparison to their virus infected CAR mice counterparts, while MHV68-LMP2A slightly enhances the GC reaction in comparison to the control MHV68-NGFR.

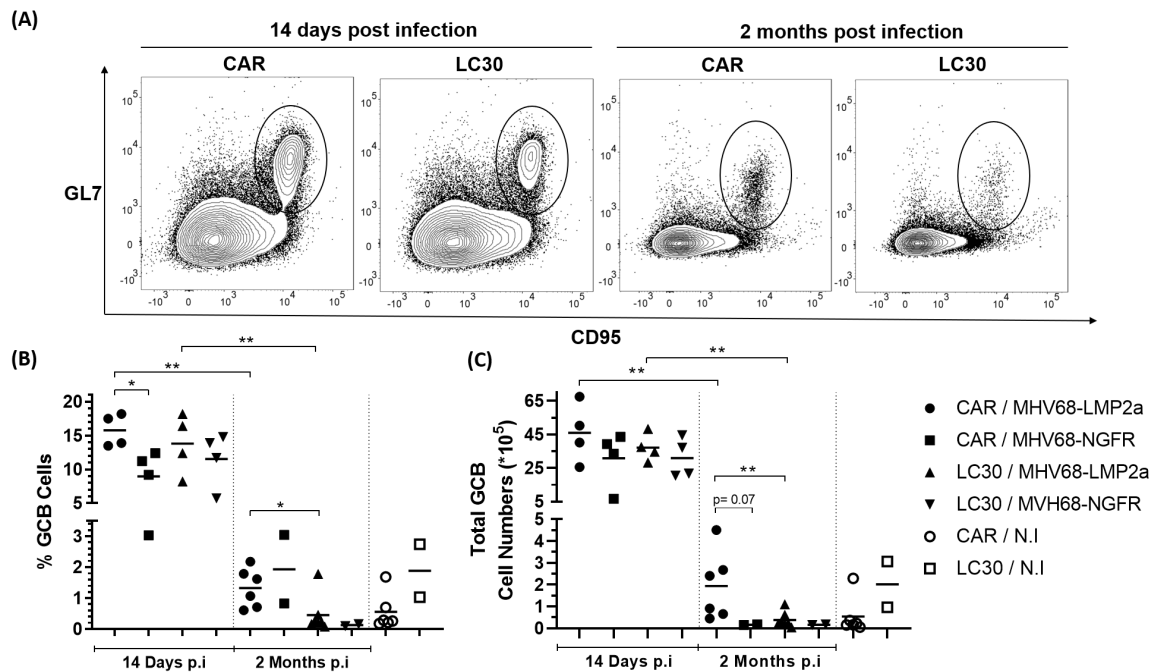


**Figure 5.28: LMP2a enhances the generation of GC reactions.** (A) FACS diagram showing gatings of GCB cells (GL7<sup>+</sup> CD95<sup>+</sup> B220<sup>+</sup>) from spleens of virus infected LC30 mice and CAR mice. The FACS diagram depicts how GCB gatings were done and observed in virus infected LC30 or CAR mice and does not differentiate between which recombinant virus was used. (B) Percentage of GCB cells in spleens. Plots were gated on lymphocytes followed by B cells (B220<sup>+</sup>) and GCB cells (GL7<sup>+</sup> CD95<sup>+</sup>). (C) Total GCB cells in spleen. Total GCB cell numbers were calculated with respect to total splenocytes tallied.

In terms of total GCB cell numbers, a similar pattern was observed like the percentages of GC cells as depicted in **Figure 5.28C**.

In summary, MHV68-LMP2A seems to enhance the GC formation in comparison to its control MHV68-NGFR, while LMP1/CD30-expression decreases the percentages and numbers of GCB cells.

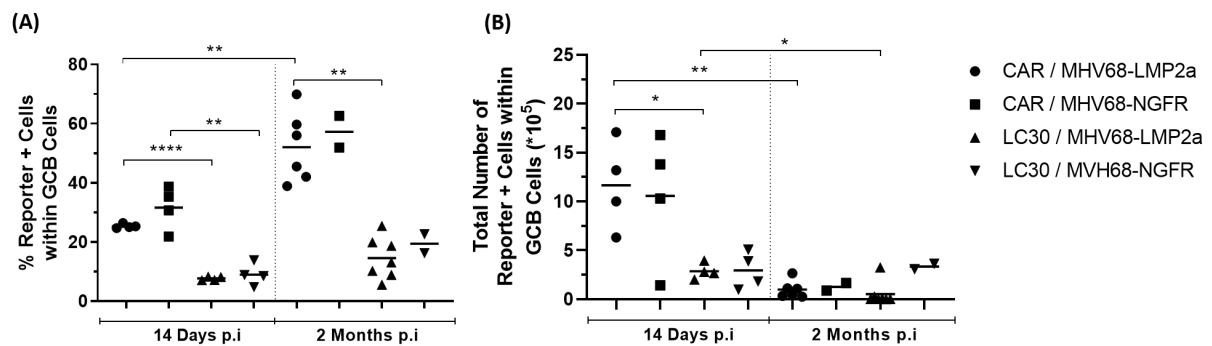


**Figure 5.29: LC30 mice had lower percentages and total numbers of reporter positive cells within GCB cells in comparison to CAR mice.** (A) Percentage reporter positive cells within GCB cells in spleens. Reporter positive cells (hCD2<sup>+</sup> or CAR<sup>+</sup>) were gated from GCB cells (GL7<sup>+</sup> CD95<sup>+</sup> B220<sup>+</sup>). (B) Total number of reporter positive cells within GCB cells in spleens. Total number of reporter positive cells were calculated with respect to the total splenocytes tallied.

**GCB CELLS IN SPLEENS; THE PERCENTAGE OF REPORTER POSITIVE CELLS WITHIN GCB CELLS WAS LOW ESPECIALLY IN LC30 MICE**

Next, we determined the percentages of GCB cells that expressed the reporter thus signifying the removal of the STOP cassette. With the cre recombinase being expressed only in GCB cells, one would expect that during GCB cell proliferation, the percentage of reporter positive cells within GCB cells be high since deletions occur mainly in GCB cells. Lower percentages of reporter positive cells within GCB cells were observed in virus infected LC30 mice in comparison to virus infected CAR mice at 14 days and 2 months post infection. Furthermore, in both mouse genotypes, the percentage of reporter positive GCB cells increases from 14 days to 2 months post infection.

However, when looking at total number of reporter positive cells within GCB cells, numbers of reporter positive GCB cells decreased from 14 days to 2 months post infection as seen in **Figure 5.29B**. Infected CAR mice at 14 days post infection, regardless of virus, had higher numbers of GCB cells when compared with infected LC30 mice at the same time point.

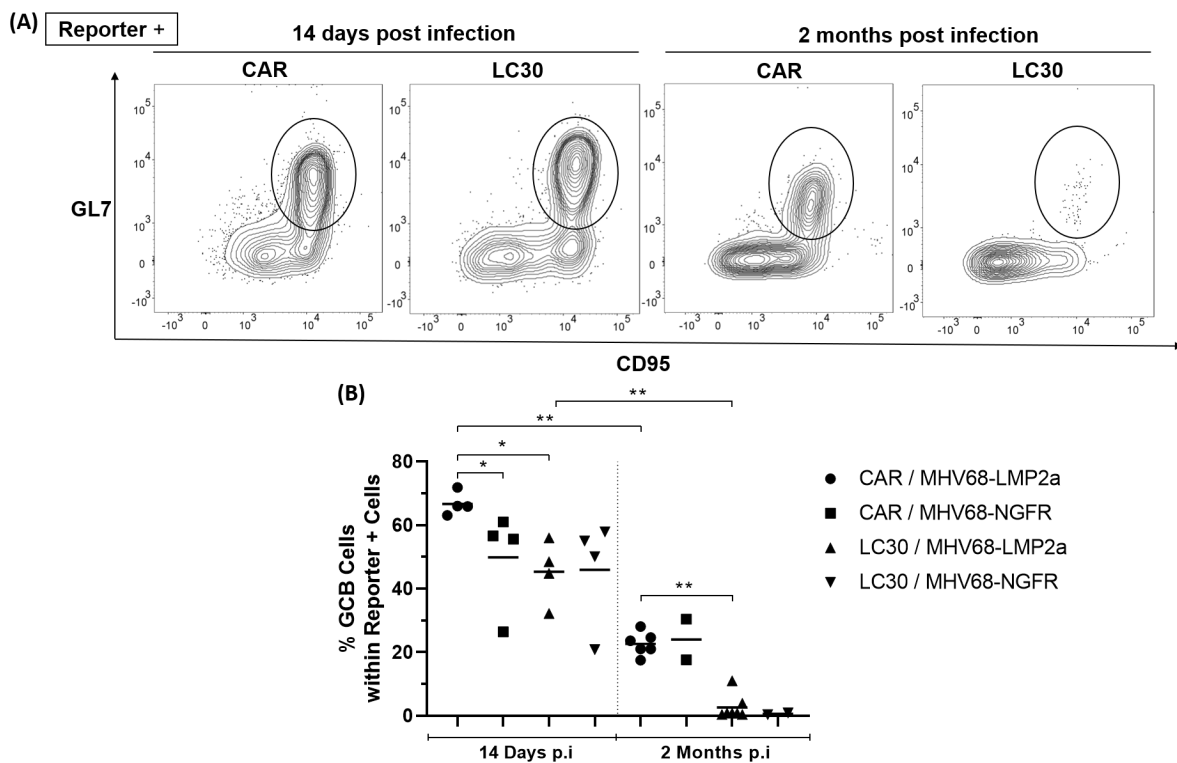


**Figure 5.30: LC30 mice had lower percentages of GCB cells within reporter positive cells in comparison to CAR mice at both time points, with MHV68-LMP2a infected CAR mice showing the largest percentages at 14 days post infection. (A) FACS diagram showing gatings of GCB cells within the fraction of reporter positive cells from spleens of virus infected LC30 mice and CAR mice. The FACS diagram depicts how GCB gatings were done and observed in virus infected LC30 or CAR mice and does not differentiate between which recombinant virus was used. (B) Percentage of GCB cells within reporter positive cells. GCB cells (GL7<sup>+</sup> CD95<sup>+</sup>) were gated from reporter positive B cells (hCD2<sup>+</sup> B220<sup>+</sup> or CAR<sup>+</sup>) B220<sup>+</sup>.**

**GCB CELLS IN SPLEENS; PERCENTAGE OF GCB CELLS WITHIN REPORTER POSITIVE CELLS WAS LOW MOSTLY IN LC30 MICE WITH GCB CELLS DIFFERENTIATING TO OTHER CELL TYPES BY CHRONIC INFECTION.**

Next, GCB cells within reporter positive cells were gated as depicted in **Figure 5.30A**. The percentages of reporter positive GCB cells decreased in all groups from day 14 to 2 months post infection as depicted in **Figure 5.30B**. This indicates that the GCB cells differentiated to other cell types by 2 months post infection. In accord with the previous results, virus infected CAR mice for both the 14 days and 2 month time points still had higher percentages of GCB cells within the reporter positive cells than virus infected LC30 mice. In addition, virus dependent differences were observed at 14 days post infection. Here, higher percentages of GCB cells within the reporter positive cells were observed in MHV68-LMP2a than MHV68-NGFR infected CAR mice.

In conclusion, some virus dependent as well as mice type dependent differences were observed from data from GCB cells in spleens. MHV68-LMP2a infection led to higher percentages and cell numbers of GCB cells in acute infections at 14 days than infection with control MHV68-NGFR. Having the LC30 genotype led to decreased percentages and cell numbers of GCB cells mainly at 2 months post infection. Additionally, a large majority of reporter positive cells seem to display a non-GC phenotype especially in that of LC30 mice. These data suggest that constitutive CD30 signalling enhances the differentiation from GC into non-GC cells, while LMP2a in the context of MHV68 seems to enhance the generation of GCs at least during early time points of infection.

**GCB CELLS IN LYMPH NODES; SIMILAR OBSERVATIONS TO THOSE FROM SPLEENS WERE RECORDED**

Not only were GCB cells in spleens investigated but since GCB cells are also found in the lymph nodes, GCB cell populations in the lymph nodes were also investigated between the experimental groups.

From **Figure 5.31A+B**, it can be seen that in the lymph nodes, the percentages of GCB cells were higher 14 days post infection than at 2 months post infection, as well as than in the non-infected controls. No significant differences were observed between the mice and viruses.

In conclusion from results obtained from GCB cells in cervical lymph nodes, observations were similar to that of GCB cells in spleens with differences mainly due to the mice type. Moreover the infection with MHV68-LMP2a appeared to slightly enhance the formation of GC in comparison to infections with the control virus in CAR mice at early time points. The data indicated that GCB cells, especially in LC30 mice, differentiated to other non-GC cell types since percentages decreased much more in these mice than in CAR mice moving from acute to chronic infection.

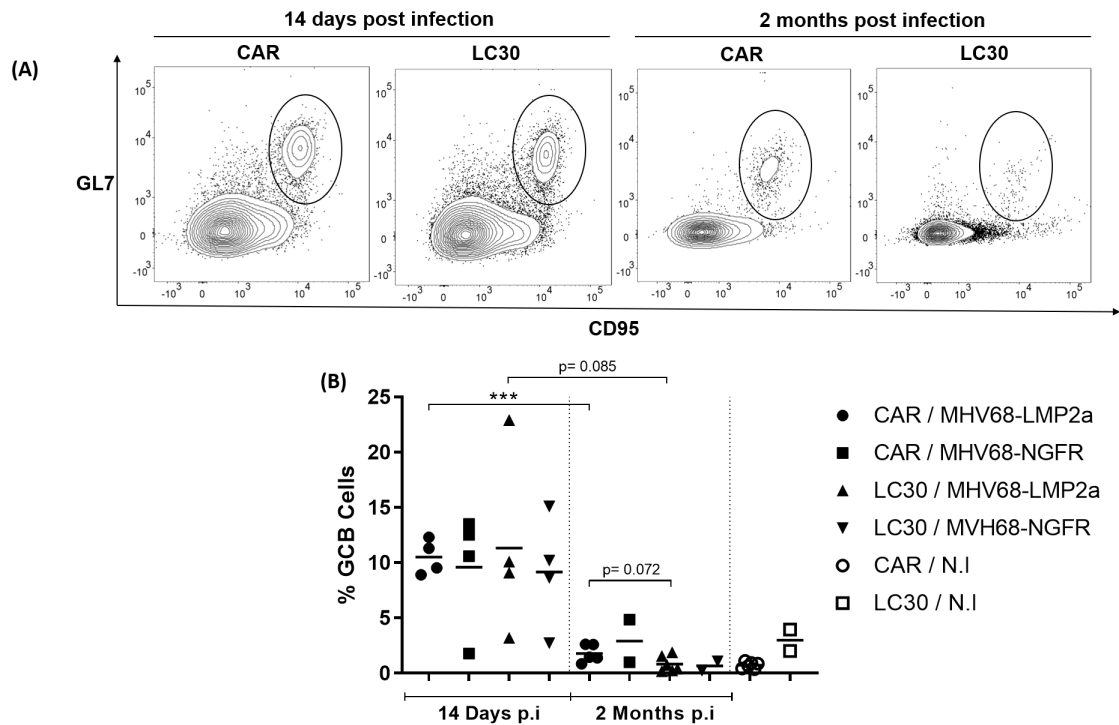


**Figure 5.31: No clear virus dependent differences were observed between the recombinant viruses used.** (A) FACS diagram showing gatings of GCB cells from cervical lymph nodes of virus infected LC30 mice and CAR mice. The FACS diagram depicts how GCB gatings were done and observed in virus infected LC30 or CAR mice and does not differentiate between which recombinant virus was used. (B) Percentage of GCB cells in cervical lymph nodes. GCB cells (GL7<sup>+</sup> CD95<sup>+</sup> B220<sup>+</sup>) were gated in a similar manner as that of spleens.

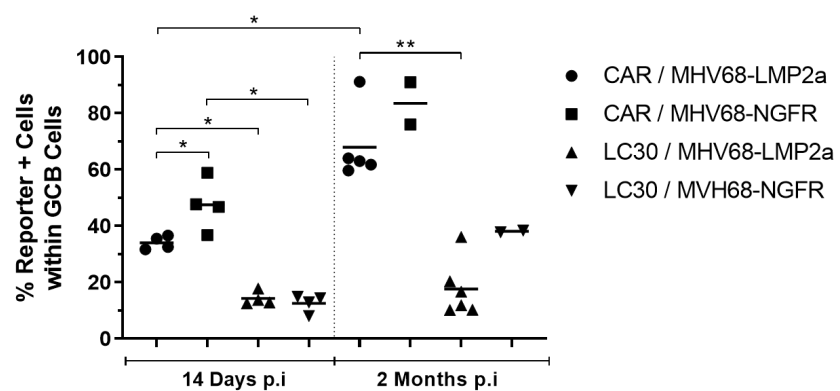


**Figure 5.32: Mice dependent differences were observed with virus infected LC30 mice having lower percentages of reporter positive cells within GCB in the cervical lymph nodes and higher percentages being observed in comparison to CAR mice at 2 months than 14 days post infection.** Percentage of reporter positive cells within GCB cells were gated in a similar manner as that of spleens.

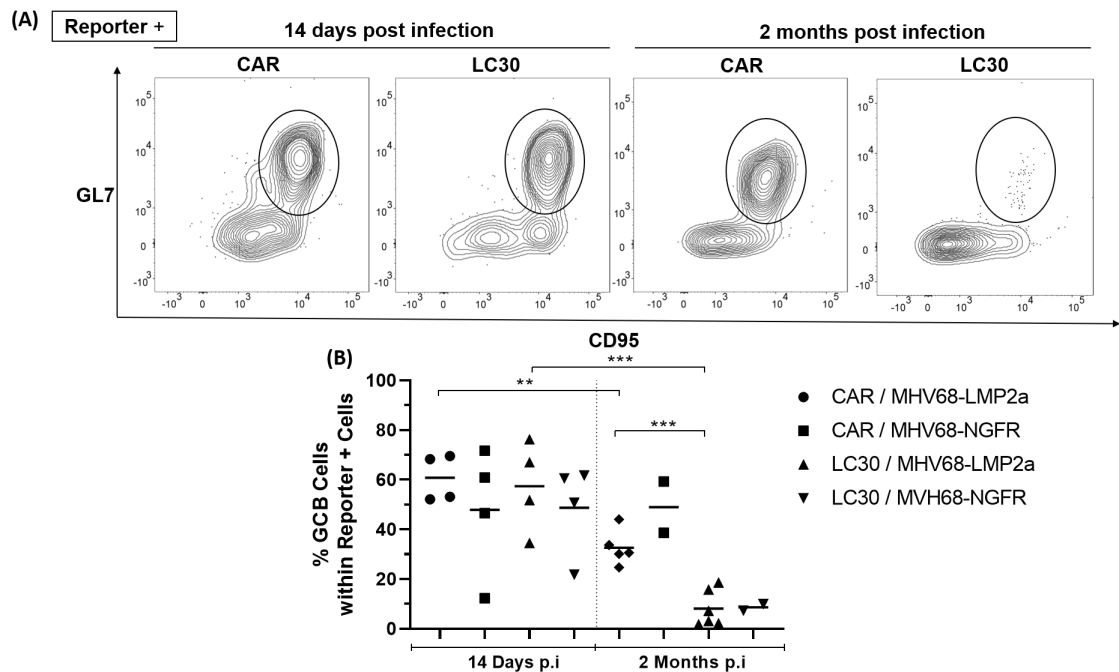


**Figure 5.33:** Mice dependent differences were observed with MHV68-NGFR and MHV68-LMP2a infected CAR mice having higher percentages of GCB cells within reporter positive cells when compared to virus infected LC30 mice at 2 months post infection. **(A)** FACS diagram showing gatings GCB cells within reporter positive cells from cervical lymph nodes between virus infected LC30 mice and CAR mice. The FACS diagram depicts how GCB cell gatings were done and observed in virus infected LC30 or CAR mice and does not differentiate between which recombinant virus was used. **(B)** Percentage of GCB cells within the reporter positive cells in cervical lymph nodes. Percentage of GCB cells within the reporter positive cells in the cervical lymph nodes were gated in a similar manner as that of spleens.

#### B1A, B1B AND B2 CELLS IN SPLEEN; CONSTITUTIVE CD30 SIGNALLING LED TO INCREASED PROLIFERATION OF B1 CELLS WITHIN THE FRACTION OF REPORTER POSITIVE CELLS

As mentioned, deletions occur mainly in GCB cells. However, to a small extent, deletions of the STOP cassette in B1 cells have also been observed Casola et al. (2006). Hence, B1 cell populations were also investigated to determine the effects of the constitutive CD30 signalling and the viruses used. B1 cells are immune cells found mainly in the peritoneal cavity but also in spleens and play a part in innate immunity Scanlon (2019).

Lymphocytes were first gated with subsequent gatings of B1a, B1b and B2 cells as depicted in **Figure 5.34A** to obtain the respective percentages of the different cell populations. With reference to the percentages of the B1a, B1b and B2 cell compartments in the spleen, no observable differences were seen between the four virus infected mice groups as well as the non-infected controls (not shown in figures). However, when looking in terms of the reporter positive cells as well as the percentage of B1a, B1b or B2 cells within the reporter positive cells, a higher percentage of B1 cells could be detected in LC30 mice in comparison to control CAR mice. This preferential expansion of B1 cells can be clearly seen from **Figure 5.34B**, when reporter positive cells were gated.

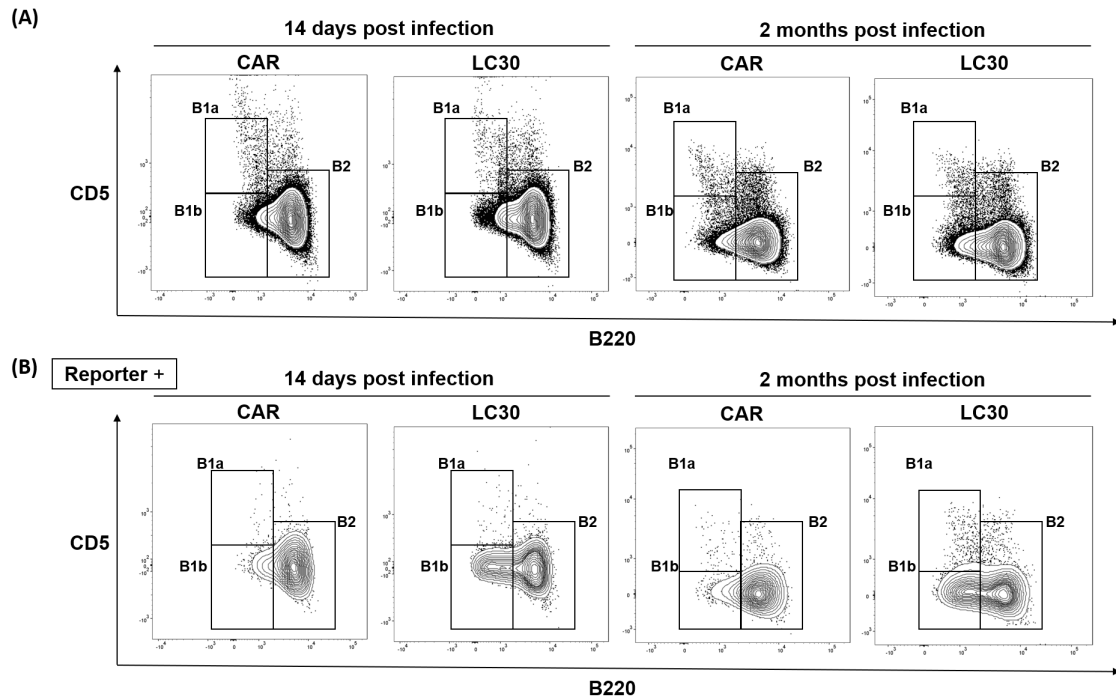


**Figure 5.34: (A) FACS diagram showing gatings of B1a, B1b and B2 cells in spleens between virus infected LC30 mice and CAR mice.** The FACS diagram depicts how the B cell gatings were done and observed in virus infected LC30 or CAR mice and does not differentiate between which recombinant virus was used. Lymphocytes were CD19<sup>+</sup> B220<sup>+</sup> gated and the subsequent B1a cell (CD5<sup>+</sup> B220<sup>low</sup> CD19<sup>+</sup>), B1b cell (CD5<sup>low</sup> B220<sup>low</sup> CD19<sup>+</sup>) and B2 cell (B220<sup>high</sup> CD19<sup>+</sup>) populations gated. **(B) FACS diagram showing gatings of B1a, B1b and B2 cells within reporter positive cells in spleens of virus infected LC30 mice and CAR mice.** The FACS diagram depicts how the B cell gatings were done and observed in virus infected LC30 or CAR mice and does not differentiate between which recombinant virus was used. Reporter positive B220<sup>+</sup> CD19<sup>+</sup> B cells were gated from lymphocytes and subsequently B1a cell (CD5<sup>+</sup> B220<sup>low</sup> CD19<sup>+</sup>), B1b cell (CD5<sup>low</sup> B220<sup>low</sup> CD19<sup>+</sup>) and B2 cell (B220<sup>high</sup> CD19<sup>+</sup>) populations gated.

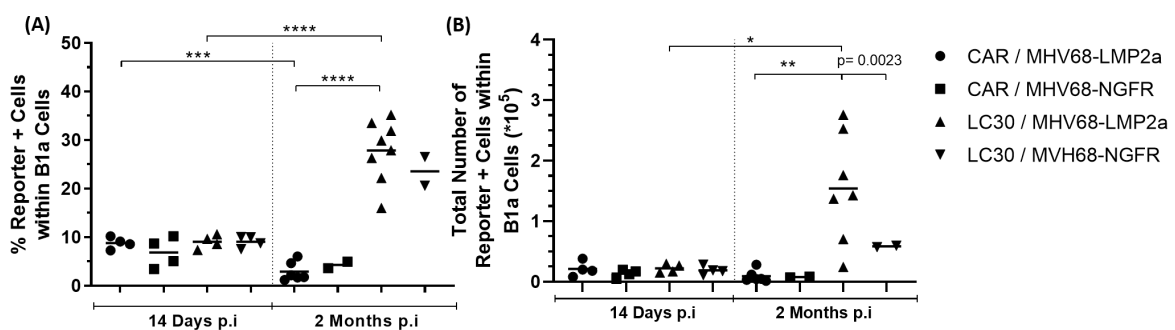


**Figure 5.35: Mice dependent differences were observed at 2 months post infection with virus infected LC30 mice having higher percentages of reporter positive cells within B1a cells as well as total number of reporter positive cells within B1a cells than virus infected CAR mice.** (A) Percentage reporter positive cells within B1a cells in spleens. Reporter positive cells (hCD2<sup>+</sup> or CAR<sup>+</sup>) were gated from B1a cells (CD5<sup>+</sup> B220<sup>low</sup> CD19<sup>+</sup>). (B) Total number of reporter positive cells within B1a cells in spleens. Total number of reporter positive cells within B1a cells were calculated with respect to the total splenocytes tallied.

From **Figure 5.35A**, between the four experimental groups, no comparable differences were observed at 14 days post infection in terms of the percentage of reporter positive cells within B1a

cells. However, at 2 months post infection, much higher levels were observed in virus infected LC30 mice in comparison to that of virus infected CAR mice. No differences were observed between the two different viruses used.

This was also reflected in the total numbers of reporter positive cells within B1a cells in **Figure 5.35B**, which were higher in virus infected LC30 mice in comparison to virus infected CAR mice after 2 months of infection. The MHV68-LMP2a infected LC30 mice seemed to have an even higher total number of reporter positive cells within B1a cells than the MHV68-NGFR infected LC30 mice. Furthermore, the levels observed in virus infected LC30 mice 2 months post infection were higher as well than those after 14 days of infection.

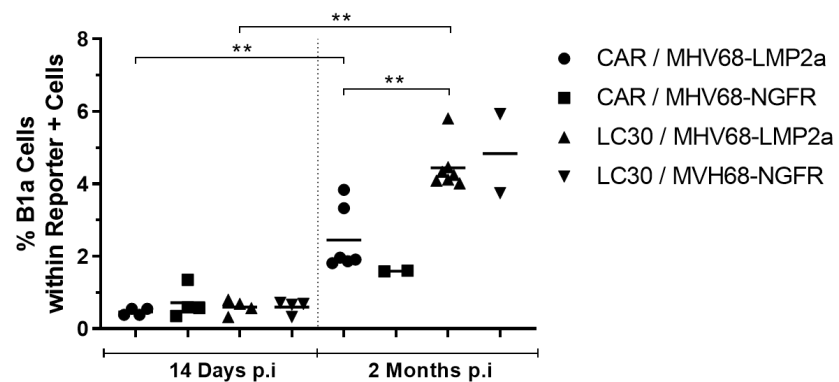


**Figure 5.36: Percentage of B1a cells within reporter positive cells.** Reporter positive B220<sup>+</sup> CD19<sup>+</sup> B cells were gated from lymphocytes and subsequently B1a cell population (CD5<sup>+</sup> B220<sup>low</sup> CD19<sup>+</sup>) gated from the reporter positive cells. Mice dependent differences were observed with virus infected LC30 mice having higher percentages than virus infected CAR mice. Higher percentages were observed at 2 months post infection than at 14 days post infection.

From **Figure 5.36**, a similar pattern was observed when looking at the percentage of B1a cells within reporter positive cells with LC30 mice having higher percentages than CAR mice at 2 months post infection. Higher percentages were also observed at 2 months than at 14 days post infection.

With reference to **Figure 5.37**, when looking at total reporter positive B1b cells, cell numbers observed in LC30 mice were also higher than levels in CAR mice at both 14 days and 2 months post infection. 2 months after infection, B1b cell numbers seemed to be higher in MHV68-NGFR infected LC30 mice than MHV68-LMP2a infected LC30 mice.

Similar observations were made with respect to the percentage of B1b cells in reporter positive cells in spleens as observed in **Figure 5.38**, with virus infected LC30 mice having higher percentages when compared to virus infected CAR mice at 14 days and 2 months post infection. No differences were observed between the two viruses used.

There were more reporter positive cells within B2 cells, both in terms of the percentage as well as total cell numbers of reporter positive cells in LC30 mice than in CAR mice at 14 days and 2

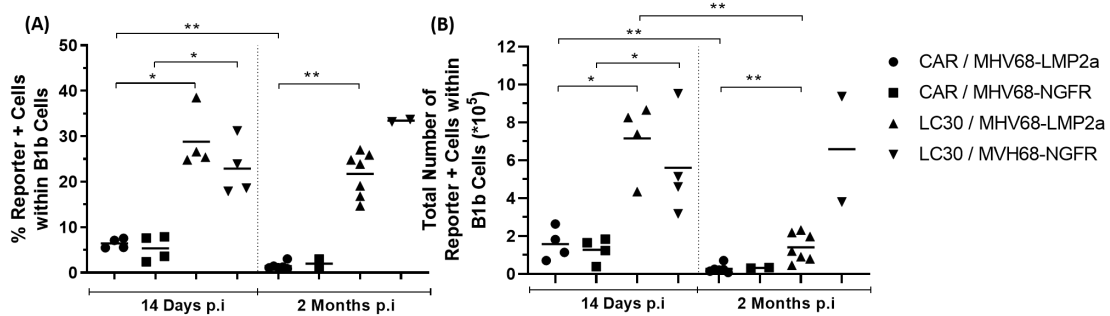


**Figure 5.37: Mice dependent differences were observed with virus infected LC30 mice having higher percentages and total numbers of reporter positive cells within B1b cells in comparison to virus infected CAR mice at 14 days and 2 months post infection. (A) Percentage reporter positive cells within B1b cells in spleens. B1b cells ( $CD5^{low}$   $B220^{low}$   $CD19^+$ ) were gated from reporter positive cells ( $hCD2^+$  or  $CAR^+$ ). (B) Total reporter positive cells within B1b cells in spleens. Total number of reporter positive cells within B1b cells were calculated with respect to the total splenocytes tallied.**

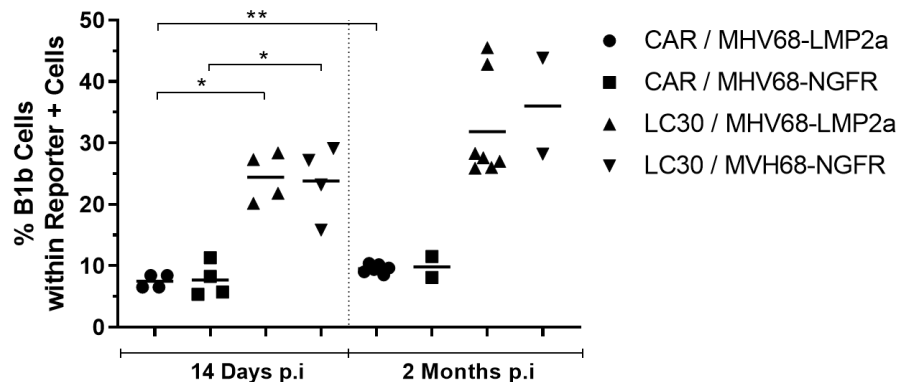


**Figure 5.38: Percentage of B1b cells within reporter positive cells in spleens.** B1b cells ( $CD5^{low}$   $B220^{low}$   $CD19^+$ ) were gated from reporter positive cells ( $hCD2^+$  or  $CAR^+$ ). Mice dependent differences were observed with virus infected LC30 mice having higher percentages than virus infected CAR mice. Higher percentages were observed at 2 months post infection than at 14 days post infection.

months post infection as observed in **Figure 5.39A**. Levels decreased from 14 days to 2 months post infection in all experimental groups.

From **Figure 5.39B**, the total reporter positive B2 cells in spleens showed this similar trend with levels at 2 months post infection being lower when compared to those 14 days post infection.

However, as in **Figure 5.40**, when looking at the percentage of B2 cells within the reporter positive cells, a reversed pattern was observed with virus infected LC30 mice having lower percentages in comparison to CAR mice for both 14 days post infection and 2 months post infection time points. The percentage of B2 cells within the reporter positive cells were lower 2 months post infection when compared to their respective groups 14 days post infection.

In conclusion, despite percentages of B1a, B1b and B2 cells in spleens having comparable levels, when looking in terms of percentage reporter cells within the total B1a, B1b and B2 cells,

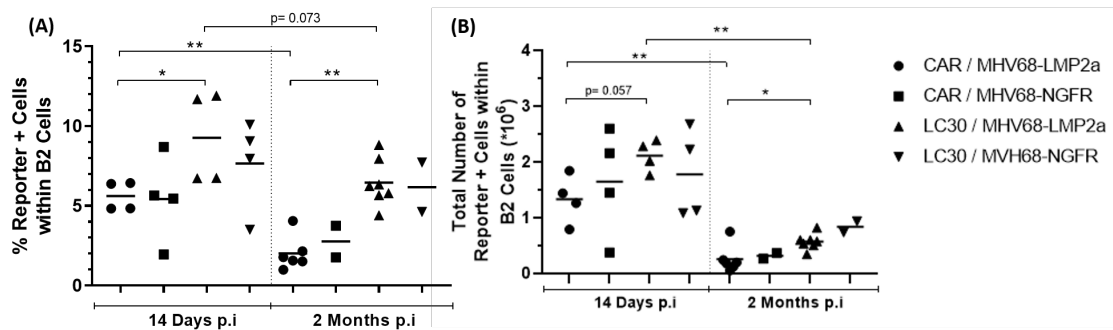


**Figure 5.39:** Mice dependent differences were observed with virus infected LC30 mice having higher percentages and total numbers of reporter positive cells within B2 cells in comparison to virus infected CAR mice. Percentages decreased at 14 days to 2 months post infection. **(A) Percentage reporter positive cells within B2 cells in spleens.** Reporter positive cells ( $hCD2^+$  or  $CAR^+$ ) were gated from B2 cells ( $B220^{high} CD19^+$ ). **(B) Total number of reporter positive cells within B2 cells in spleens.** Total number of reporter positive cells within B2 cells were calculated with respect to the total splenocytes tallied.

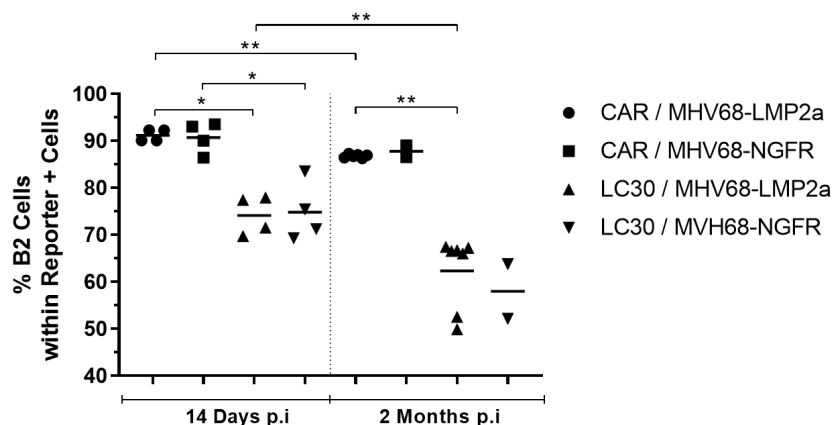


**Figure 5.40: Percentage of B2 cells within reporter positive cells in spleens.** B2 cells ( $B220^{high} CD19^+$ ) were gated from reporter positive cells ( $hCD2^+$  or  $CAR^+$ ). Mice dependent differences were observed with virus infected LC30 mice having lower percentages than virus infected CAR mice. Lower percentages were observed at 2 months post infection than at 14 days post infection.

respectively, differences that were due mainly to mice type (CAR or LC30 mice) were observed. Specifically, B1a, B1b and B2 cells from spleens of LC30 mice had higher percentages that were reporter positive when compared to CAR mice. This, thus, indicates that in LC30 mice, these B cell groups, mainly that of B1a and B1b cells, underwent more expansion than in CAR mice. Similarly, when dwelling into the percentages of B1a, B1b and B2 cells within the reporter cells, mice dependent difference were again observed. Going from acute infections of 14 days to 2 months, having the LC30 mice genotype led mainly to expansions of the B1a and B1b cells within the reporter positive cells when compared to that of CAR mice. Additionally, it has been shown that deletions of the STOP cassette do occur in B1 cells although in very small percentages of less than 1% (Casola et al., 2006). This is further substantiated from our results which show that the percentages of B1 cells within the reporter positive cells were low but increased further after 2 months, especially

in LC30 mice. This suggests that the few B1 cells with STOP cassette deletions and thus LC30 expression, proliferated and expanded to a great extent in LC30 mice. Virus dependent differences were, however, not observed.

**B1A AND B1B CELLS IN PERITONEAL CAVITY; CONSTITUTIVE CD30 SIGNALLING LED TO GREATER EXPANSION IN B1 CELLS WITHIN THE FRACTION OF REPORTER POSITIVE CELLS IN PERITONEAL CAVITY THAN IN SPLEENS**

A large majority of B1 cells are located in the peritoneal cavity and in the case of lymphomas, such as that of the primary effusion lymphoma (PEL), B1 phenotyped cells were present [Sanchez-Martin et al. \(2017\)](#). As such, B1 cells in the peritoneal cavity were also investigated. The percentages of B1 cells in the peritoneal cavity did not differ among the four different virus infected mice groups as well as the non-infected controls across both time points (not shown in figures).

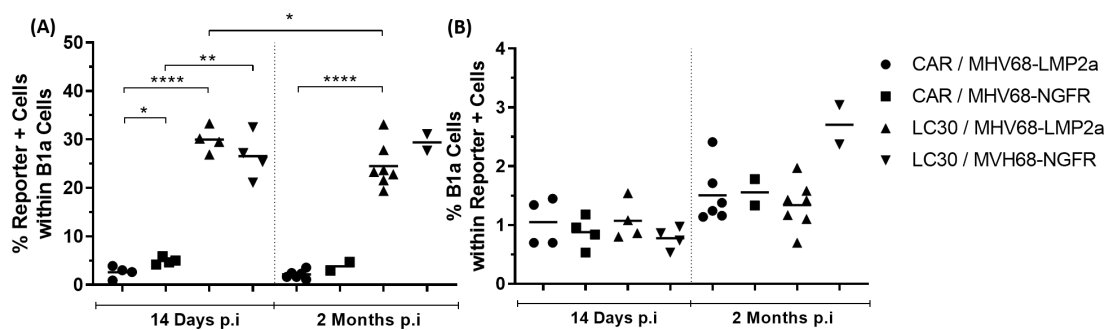


**Figure 5.41: (A) Percentage reporter positive cells within B1a cells in the peritoneal cavity.** Reporter positive cells (hCD2<sup>+</sup> or CAR<sup>+</sup>) were gated from B1a cells (CD5<sup>high</sup> B220<sup>low</sup> CD19<sup>+</sup>) similar to that of spleens. Mice dependent differences were observed with virus infected LC30 mice having higher percentages than virus infected CAR mice. Only MHV68-LMP2a infected LC30 mice had lower percentages at 2 months than at 14 days post infection. **(B) Percentage of B1a cells in reporter positive cells in the peritoneal cavity.** B1a cells (CD5<sup>high</sup> B220<sup>high</sup> CD19<sup>+</sup>) were gated from reporter positive cells (hCD2<sup>+</sup> or CAR<sup>+</sup>) in a similar manner as that of spleens. Highest percentages observed in MHV68-NGFR infected LC30 mice at 2 months post infection.

However, when dwelling into the percentage of reporter positive cells within B1a cells, a mice dependent behavior was observed with significantly higher percentages in virus infected LC30 mice in comparison to virus infected CAR mice at both 14 days and 2 months post infection as seen in **Figure 5.41A**.

The percentage of B1a cells within the fraction of reporter positive cells as depicted in **Figure 5.41B** showed the highest levels in MHV68-NGFR infected CD30 mice at 2 months post infection with comparative levels in the other groups.

With reference to **Figure 5.42A** and the percentage of reporter positive cells within B1b cells, percentages were higher in virus infected LC30 mice than CAR mice at both 14 days and 2 months post infection.

Lastly, as illustrated in **Figure 5.42B**, when looking at the percentage of B1b cells within reporter positive cells, a similar pattern was observed with virus infected LC30 mice having higher percentages

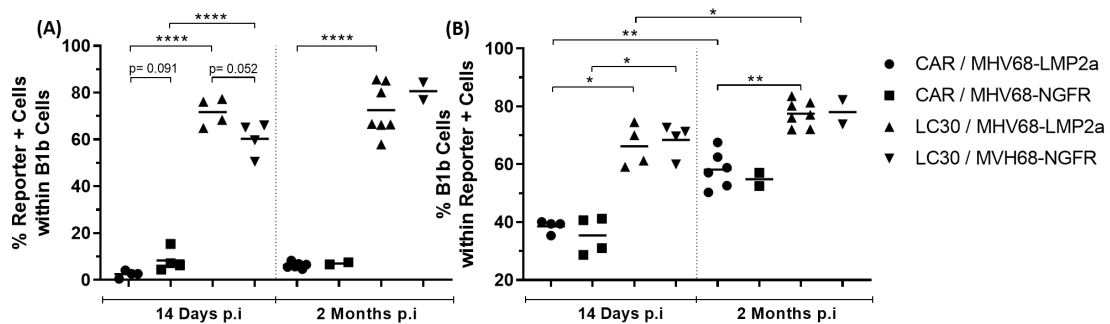


**Figure 5.42: (A) Percentage reporter positive cells within B1b cells in the peritoneal cavity.** Reporter positive cells ( $hCD2^+$  or  $CAR^+$ ) were gated from B1b cells ( $CD5^{low}$   $B220^{low}$   $CD19^+$ ) similar to that of spleens. Mice dependent differences were observed with virus infected LC30 mice having higher percentages than virus infected CAR mice. MHV68-LMP2a infected CAR mice had higher percentages at 2 months post infection than at 14 days post infection. **(B) Percentage of B1b cells within reporter positive cells in the peritoneal cavity.** B1b cells ( $CD5^{low}$   $B220^{high}$   $CD19^+$ ) were gated from reporter positive cells ( $hCD2^+$  or  $CAR^+$ ) in a similar manner as that of spleens. Virus infected LC30 mice had higher percentages than virus infected CAR mice at both time points. Higher percentages were observed 2 months post infection than at 14 days post infection.

when compared to virus infected CAR mice within both time points.

Thus, LC30 expression leads to the expansion of B1a cells and B1b cells both in the spleen and the peritoneal cavity, with no differences between the viral strains used.

#### **PLASMA CELLS IN SPLEENS; MORE REPORTER POSITIVE CELLS WITHIN PLASMA CELLS IN LC30 MICE**

B cells leave the GC as plasma cells or memory B cells. To determine the extent of effects of LMP2a protein as well as CD30 expression on the generation and expansion of these populations, we investigated the fraction of reporter positive cells within plasma cells and memory B cells.

In terms of the percentages of plasma cells in the spleen, no differences were observed in percentages across all four experimental groups at the two time points being investigated as depicted in **Figure 5.43A+B**.

However, when looking at the percentages of reporter positive cells within plasma cells in spleens, higher percentages were observed at 14 days and 2 months post infection in virus infected LC30 mice compared to CAR mice as seen in **Figure 5.44A**, whereas no differences were observed between the two viral strains used. This indicates that a larger portion of the plasma cells are generated in LC30 mice as compared to CAR mice, with viral strain used not playing a role. From 14 days to 2 months post infection, the percentage of reporter positive cells within plasma cells decreased slightly in all four experimental mice groups, but they were still higher in LC30 mice than CAR mice.

With reference to **Figure 5.44B**, a similar pattern was observed when looking at the total number of reporter positive cells within plasma cells in spleens. The total number of reporter positive cells

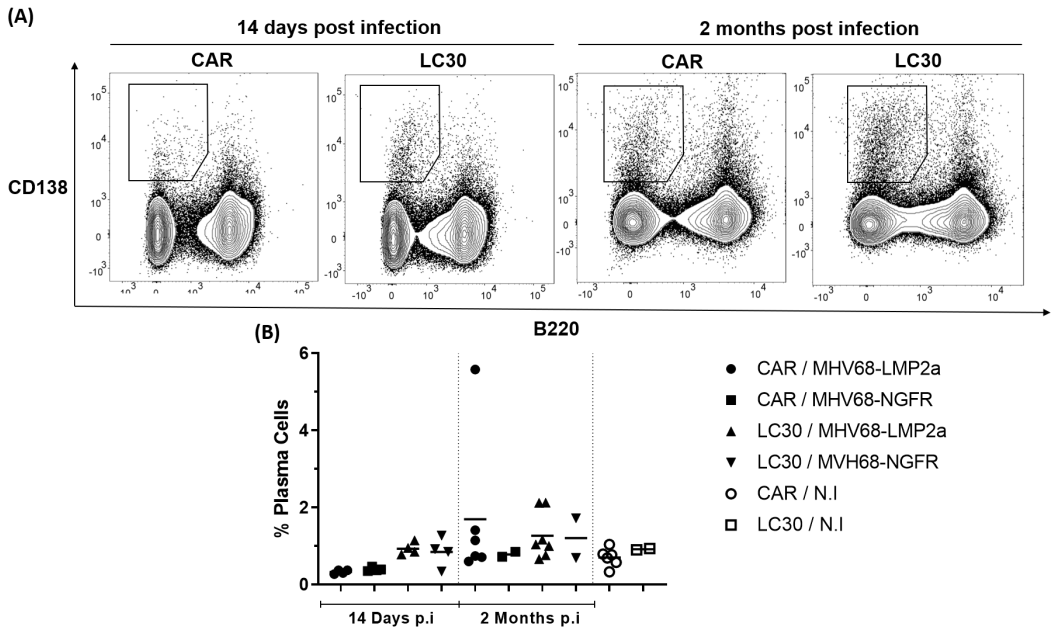


**Figure 5.43: (A) FACS diagram showing gatings of plasma cells from spleens of virus infected LC30 mice and CAR mice at 14 days and 2 months post infection.** The FACS diagram depicts how plasma cell gatings were done and observed in virus infected LC30 or CAR mice and does not differentiate between which recombinant virus was used. Plots were gated on lymphocytes and subsequently plasma cells (CD138<sup>+</sup> B220<sup>low</sup>). **(B) Percentage of plasma cells in spleens.** No significant differences were observed between the different experimental groups in terms of percentage of plasma cells generated in the spleen, at 14 days or 2 months post infection.

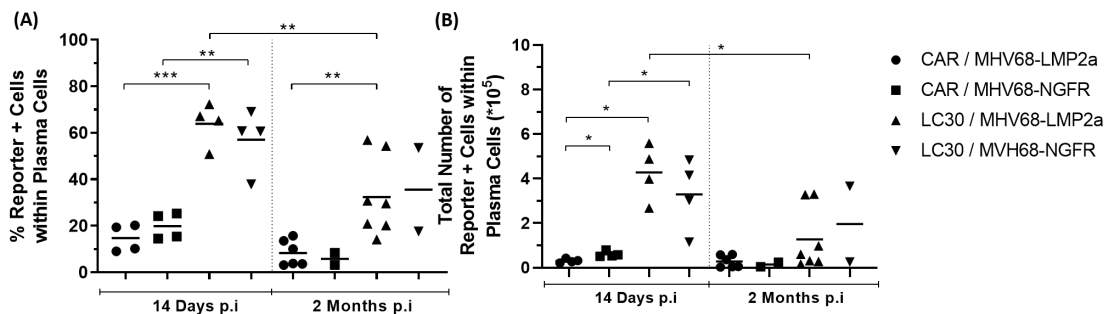


**Figure 5.44: Mice dependent differences were observed with virus infected LC30 mice having higher percentages and total number of reporter positive cells within plasma cells in spleens. Percentages at 2 months post infection were lower than those at 14 days post infection.** (A) Percentage reporter positive cells within plasma cells in spleens. Reporter positive cells (hCD2<sup>+</sup> or CAR<sup>+</sup>) were gated from plasma cells (CD138<sup>+</sup> B220<sup>low</sup>). (B) Total number of reporter positive cells within plasma cells in spleens. Total number of reporter positive cells within plasma cells were calculated with respect to total splenocytes tallied.

within plasma cells was higher in virus infected LC30 mice compared to CAR mice at 14 days post infection and 2 months post infection. From 14 days to 2 months post infection, total number of reporter positive cells within plasma cells decreased slightly in the four groups. No clear differences were observed between the viruses used. The decrease of plasma cells between 14 days and 2 months post infection is most likely due to the generation of short lived plasma cells at early time points after infection.

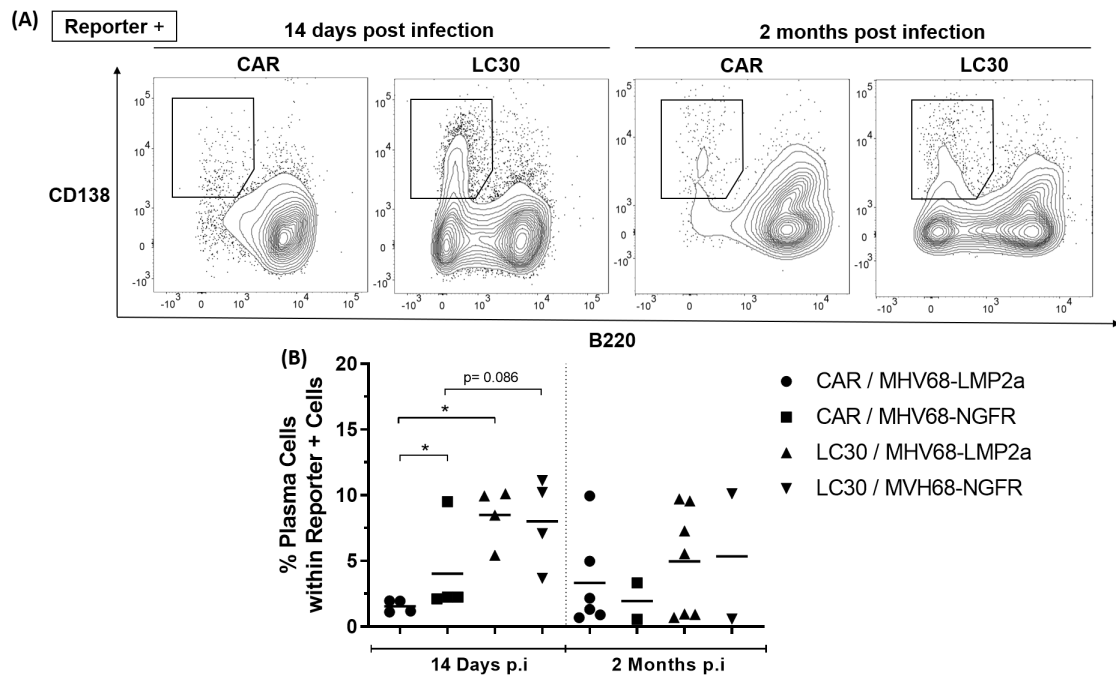


**Figure 5.45: Mice dependent differences were observed with lower percentages of plasma cells within reporter positive cells being observed in virus infected CAR mice compared to virus infected LC30 mice. (A) FACS diagram showing gatings of plasma cells within the reporter positive cells from spleens between virus infected LC30 mice and CAR mice.** The FACS diagram depicts how plasma cell gatings were done and observed in virus infected LC30 or CAR mice, and does not differentiate between which recombinant virus was used. Reporter positive cells (hCD2<sup>+</sup> or CAR<sup>+</sup>) were first gated, followed by the subsequent gatings of plasma cells (C138<sup>+</sup> B220<sup>low</sup>) from these reporter positive cells (hCD2<sup>+</sup> or CAR<sup>+</sup>). **(B) Percentage of plasma cells within reporter positive cells.** Lower percentages of plasma cells within the fraction of reporter positive cells were observed in virus infected CAR mice when compared to virus infected LC30 mice at both time points. At 14 days post infection, virus dependent differences were observed with MHV68-NGFR infected CAR mice having higher percentages than MHV68-LMP2a infected CAR mice.

Vice versa, we gated on reporter positive cells and then analysed the percentage of plasma cells. When looking at the percentage of plasma cells within the fraction of reporter positive cells, lower percentages were observed in virus infected CAR mice as compared to LC30 mice at 14 days and 2 months post infection as depicted in **Figure 5.45A+B**, indicating that LC30 expression leads to GCB cells differentiating more to plasma cells. However, the percentages were highly variable at 2 months post infection and no clear differences were observed between the viruses used.

#### MEMORY CELLS; CONSTITUTIVE CD30 SIGNALLING DID NOT LEAD TO INCREASED PRODUCTION OF REPORTER POSITIVE CELLS WITHIN IgG1 CELLS

Apart from plasma cells, another fate of the GCB cells are that of memory B cells. After virus infection, during phases of affinity maturation, CSR and SHM occur in GCB cells in order to generate high affinity class switched Ig memory B cells. Most memory B cells are IgG1 positive, therefore, IgG1 positive memory B cells were investigated here. With reference to **Figure 5.46A**, the percentage of reporter positive cells within IgG1 memory cells was the lowest in MHV68-LMP2a infected

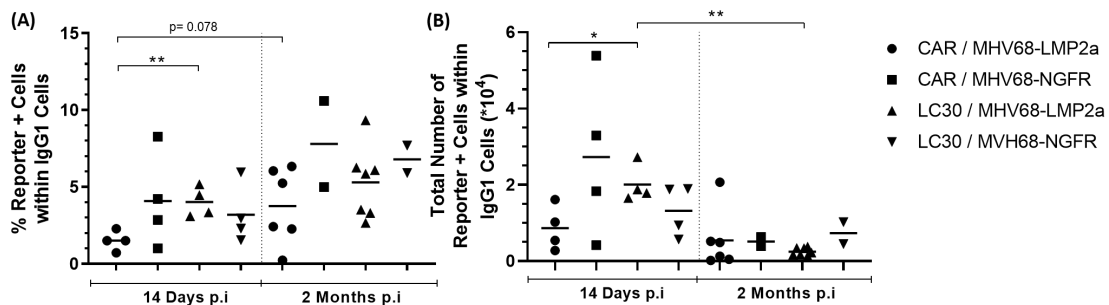


**Figure 5.46: Lowest percentages and total number of reporter positive cells within IgG1 memory cells were observed in MHV68-LMP2a infected CAR mice at 14 days post infection. Percentages at 2 months post infection were lower than those at 14 days post infection. (A) Percentage reporter positive cells within IgG1 memory cells in spleens.** IgG1 memory cells plots ( $\text{IgM}^{\text{low}} \text{ IgG}^+$ ) were gated from lymphocytes and B cells (B220 $+$ ). Subsequently, reporter positive cells (hCD2 $^+$  or CAR $^+$ ) were gated from IgG1 memory cells. **(B) Total reporter positive cells within IgG1 memory cells in spleens.** Total number of reporter positive cells within IgG1 memory cells were calculated with respect to total splenocytes tallied.

CAR mice in comparison to the other three experimental groups, in both 14 days and 2 months infected spleens.

In terms of the total number of reporter positive cells within IgG1 memory cells in spleens as seen in **Figure 5.46B**, when the total number of reporter positive cells were tallied, numbers were much higher 14 days post infection in all 4 experimental groups than at 2 month post infection. The reason may be that most of the memory B cells have left the spleen 2 months after infection and were now distributed in the blood to the different secondary organs, and in the bone marrow.

As seen from **Figure 5.47A**, IgG1 cells were now gated from the reporter positive cells. Here, at 14 days post infection, a mice dependent result was observed, in that the percentage of IgG1 cells within reporter positive cells in LC30 mice was significantly lower when compared to those of virus infected CAR mice as depicted in **Figure 5.47B**. This behaviour was opposite to what was observed in plasma cells earlier where percentages of plasma cells within reporter positive cells were higher in LC30 mice compared to CAR mice. Thus, LC30 expression seems to develop plasma cells preferentially over IgG1 memory B cells. After 2 months of infection, percentages of IgG1 cells in reporter positive cells decreased across all experimental groups.

### **SUMMARY**

In conclusion, from experiments done to decipher the effects of the recombinant MHV68-LMP2a and the control virus MHV68-NGFR in LMP1/CD30  $\gamma$ 1cre and R26-Car  $\gamma$ 1cre mice, various different effects were observed. These effects were mainly attributed to mice type and the constitutive CD30 signalling, though the MHV68-LMP2a virus did show some distinct effects in comparison to the control MHV68-NGFR virus used.

Firstly, splenomegaly was observed by 14 days post infection in all experimental groups, and this decreased during chronic infection at 2 months. No virus dependent differences were observed

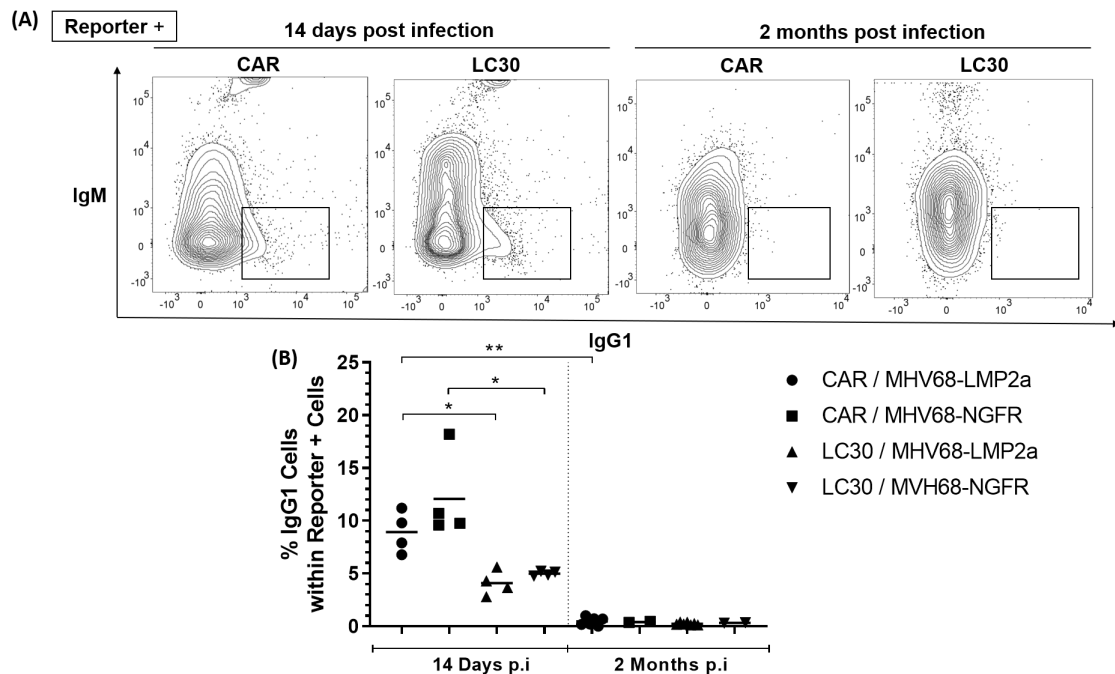


**Figure 5.47: Mice dependent differences were observed at day 14 with lower percentages of IgG1 cells within reporter positive cells being observed in virus infected LC30 mice compared to virus infected CAR mice. Higher percentages were observed 14 days post infection compared to 2 months post infection. (A) FACS diagram showing gatings of IgG1 memory cell within the reporter positive cells from spleens between virus infected LC30 mice and CAR mice. FACS diagram depicts how IgG1 memory cell gatings were done and observed in virus infected LC30 or CAR mice, and does not differentiate between which recombinant virus was used. (B) Percentage of IgG1 memory cells within reporter positive cells. Plots were gated to lymphocytes and B cells ( $B220^+$ ). Subsequently, reporter positive cells ( $hCD2^+$  or  $CAR^+$ ) were gated followed by IgG1 memory cells ( $IgM^{low} IgG^+$ ). Significant differences were observed between the virus infected LC30 mice and CAR mice at 14 days post infection ( $p= 0.0286$ ).**

but LC30 mice did show a greater splenomegaly compared to CAR mice at 2 months post infection, indicating that having the LC30 genotype did play a role in delaying the rate of decrease of splenomegaly in mice during chronic infection.

In terms of cell populations observed, T cells, B cells, B1 and B2 cells, as well as GCB cells, plasma cells and IgG1 memory cells were investigated. Expansion of B and T cells occurred at 14 days post infection with decreased proliferation during chronic infection at 2 months. As for GCB cells, virus dependent differences were observed with MHV68-LMP2a infected mice having the highest percentage of GCB cells in the spleens as well as in cervical lymph nodes at 14 days. When looking at plasma cells and IgG1 memory B cells, percentages were similar across all experimental groups with no differences regardless of the virus used or the mice type (LC30 or CAR mice).

When looking in terms of reporter positive cells, more differences were observed. As mentioned, since  $\gamma 1cre$  mice were used, reporter positive cells are cells that are either GCB cells or cells, which have left the GC reaction, such as plasma cells and memory B cells. Earlier studies have shown that reporter positive cells could also be B1 cells that underwent deletion of the STOP cassette

though in minute percentages of less than 1% Casola et al. (2006). By dwelling into reporter cells, we observed that LC30 expression led to increased percentages of reporter positive B1 cells both in spleens and peritoneal cavity, suggesting that constitutive CD30 signalling led to expansions of B1 cells in spleens and even more in the peritoneal cavity. We could not differentiate whether these expanded B1 cells originated from a minor fraction of deleted B1 cells, which massively proliferated after switching on LMP1/CD30 expression, or from deleted GCB cells that adopted a B1-like phenotype due to the LMP1/CD30-expression.

Next, percentages of GCB cells within the fraction of reporter positive cells were lower in LC30 mice, and these percentages dropped further moving from acute to chronic infection at 2 months. This suggests that constitutive CD30 signalling drives the differentiation of GCB cells to other non-GC cells. Reporter positive cells within GCB cells were also remarkably lower in LC30 mice suggesting that LMP1/CD30 expressing B cells quickly leave the GC and differentiate into other cell types. Percentages of plasma cells within the fraction of reporter positive cells were much higher in LC30 mice, while percentages of IgG1 memory cells were lower in comparison to CAR control mice. In addition, higher percentages of reporter positive cells within plasma cells were observed in LC30 mice compared to CAR mice both at acute and chronic time points, indicating that from all the plasma cells in spleens, more had origins from GCB cells. This suggests that constitutive CD30 signalling causes a larger differentiation of GCB cells to plasma cells rather than IgG1 memory B cells.

In summary, although the recombinant MHV68-LMP2a did show certain prominent effects in the proliferation of GCB cells, majority of the differences observed in the experiments were due to the constitutive signalling of the CD30 in LMP1/CD30  $\gamma$ 1cre when infected with virus.

# 6

## DISCUSSION

### 6.1 INFLUENCE OF MHV68 INFECTION IN MICE

MHV68 is a murine gHV that is related to the EBV and KSHV based on genomic sequences, as well as pathological properties, that show similarities, and is thus used in experiments in this project to decipher gHV pathogenesis *in vivo*, in a mouse model [Simas & Efstathiou \(1998\)](#). Studies regarding the human herpesviruses EBV and KSHV on the role of virus-host interactions *in vivo* are limited because these viruses only infect humans, but several new models have recently arisen, that have enabled the testing of EBV in mice [Wirtz et al. \(2016\)](#) and [Münz \(2017\)](#). Such models involve cloning and expressing proteins of the human herpesviruses such as that of the LMP1 in mice, to mimic responses that could help to generate new therapies for gammaherpesvirus driven diseases. As such, the MHV68, being a virus that has been widely characterized and investigated on, has been established as a model to study the pathogenesis of gHVs [Barton et al. \(2011\)](#). Furthermore, the cloning of the MHV68 in a bacterial artificial chromosome has enabled many genes to be cloned into the MHV68 genome and tested *in vivo* in mice [Adler et al. \(2000\)](#). In characterization studies of the recombinant MHV68-LMP2a, MHV68-WT is used as a control to ascertain if any differences between the recombinant virus were present *in vitro* and *in vivo*. If significant differences were present, though not the case here, it could have been due to the recombination process that

rendered the virus unfit. From experiments carried out, acute infection was established in the lungs as early as 7 days post infection as observed from viral titers measured from lungs harvested, for both the recombinant and MHV68-WT used. This has been shown in various studies and this acute infection is usually cleared by 12 days post infection as stated [Cardin et al. \(1996\)](#) and [Sunil-Chandra et al. \(1992\)](#). Splenomegaly was observed as early as 10 days post infection with largest spleens observed in MHV68-WT infected mice by day 17 post infection. Thus, the virus had migrated from the lungs and its way to the spleen. Here, establishment of latency occurs in the GCB as observed by the expansion of GCB cells also by 10 days post infection all the way through to 17 days post infection. Even at 2 months post infection, splenomegaly was still observed in the mice infected by the recombinant viruses (MHV-LMP2a and MHV68-NGFR), though reduced. MHV68 is known to establish chronic infection in immune competent mice, that can control the latent infection, whereas in immune-compromised mice, occurrence of lymphomas has been observed in long term studies from 6 months post infection [Sunil-Chandra et al. \(1994\)](#).

Thus, MHV68-WT, together with the recombinant virus MHV68-LMP2a were able to establish acute infections in the lungs as well as latency successfully in the spleen, though answers relating to lymphomagenesis would need to be addressed with longer term infection studies, in healthy or immune compromised mice.

## 6.2 GENERATION AND CHARACTERIZATION OF RECOMBINANT MHV68-LMP2A

### 6.2.1 IN VITRO ANALYSIS OF RECOMBINANT MHV68-LMP2A

#### **IN VITRO INFECTION LED TO OVEREXPRESSION OF LMP2A DESPITE NORMAL VIRAL GROWTH KINETICS**

Before the effects of LMP2a expression can be tested in vitro or in vivo, the LMP2a gene would need to be cloned into a suitable vector that would facilitate its transcription and expression of the protein. In order to achieve this, the LMP2a gene was inserted downstream a CMV promoter before being introduced into MHV68. The resulting recombinant MHV68 enabled the introduction of LMP2a into mice. As observed from the growth curve analysis carried out to determine viral kinetics the recombinant virus did not differ from that of MHV68-WT. However, when dwelling into the LMP2a protein expression, the presence of the CMV promoter led to overexpression of the LMP2a protein as seen in western blot, in comparison to the LCL D2098 cells used as control, an EBV infected lymphoblastoid cell line. The PCMV is a strong promoter that allows for expression of membrane proteins in mammalian cells and overexpression of the protein has been reported as well, for the case of GFP tagged expression of MHV68 proteins [Suárez & van Dyk \(2008\)](#). However, this overexpression did not alter or affect the viral kinetics of the recombinant virus in vitro.

## 6.2.2 IN VIVO ANALYSIS OF RECOMBINANT MHV68-LMP2A AFTER INTRANASAL INFECTION OF C57BL6 WILD TYPE MICE

### LOWER LEVELS OF RECOMBINANT MHV68-LMP2A MAY BE DUE TO INCREASED VIRAL ELIMINATION AND IMMUNOGENICITY OF LMP2A PROTEINS EXPRESSED

During characterization of the recombinant MHV68-LMP2a by comparisons with MHV68-WT, lower detection of MHV68-LMP2a was observed as measured by viral genomic loads detected and the reactivation from latency in splenocytes in acute infections. This corresponded to the splenic weights observed with MHV68-LMP2a infected mice showing reduced splenomegaly compared with the MHV68-WT. This reduced splenomegaly and lower detections of virus genomic loads could be due to the immunogenicity of LMP2a in vivo, which was demonstrated by Chen et. al., in which CTL responses were shown to be elicited to LMP2a [Chen et al. \(2009\)](#).

Various studies have shown a higher immune response, specifically in terms of CD8+ and CD4+ T cells responses as well as cytokines secretion against the LMP2a protein in comparison to controls (controls using antigens; phytohemagglutinin or unloaded dendritic cells) [Chen et al. \(2009\)](#) and [Sohn et al. \(2015\)](#). However, the levels of CD4+ and CD8+ T cell activation we observed did not reciprocate this and were not higher in the MHV68-LMP2a group. Instead, MHV68-WT showed higher CD8+ activation by day 10 as well as higher CD4+ T cell activation by day 14. Viral genomic loads in lungs measured by real time PCR were similar between the two different viruses used and even at day 10 post infection, viral genomic loads in spleens were also at similar levels. However, the viral genomic loads by day 14 showed that MHV68-WT had undergone exponential replication with levels much higher than that of MHV68-LMP2a, that remained at similar levels as that at 10 days post infection. This implies that there were mechanisms that prevented MHV68-LMP2a from eliciting the same replicative responses as that of MHV68-WT. In this case, another cell that could play a larger role in the response to latent EBV infection may be that of the natural killer cells which has been shown to elicit an effective, if not better immune response against EBV viral proteins [Hatton et al. \(2016\)](#) and [Fish & Longnecker \(2017\)](#). Furthermore, Minamitani et. al. have shown that co-depletion of both the NK cells as well as T cells led to development of lymphoma in all C57BL/6 mice used tested by day 12 [Minamitani et al. \(2017\)](#). Thus, the T cell response could have occurred earlier than the time points measured as CD8+ T cells that were specific to MHV68 and this has been observed in infected C57BL/6 mice as early as 1 week after infection [Stevenson et al. \(1999\)](#) and [Gredmark-Russ et al. \(2008\)](#).

### LATENCY ESTABLISHMENT IN GCB CELLS AND PLASMA CELLS AFTER ACUTE INFECTION

After infection, latency of all gHVs is established in various cells such as that of dendritic, epithelial, endothelial cells and many B cell subsets [Flaño et al. \(2002\)](#), [Suárez & van Dyk \(2008\)](#) and [Feldman et al. \(2016\)](#). Whether by intranasal or peritoneal infection, the virus eventually transits to the spleen

in a B cell dependent manner establishing latency, thus leading to splenomegaly observed from the spleens harvested [Usherwood et al. \(1996\)](#). In the spleen, the GCB cells become the target of gHVs infection where latent infection has been found to be detected at the highest of frequencies [Sunil-Chandra et al. \(1994\)](#). Thus, from experiments that have been conducted during the characterization of the recombinant MHV68-LMP2a, GCB cell proliferation occurred from 10 days to 17 days post infection as measured from the percentage of GCB cells in the spleen, which increased gradually for both recombinant MHV68-LMP2a and MHV68-WT. The proliferation of GCB cells typically peaks between 14- and 18-days post infection with latency still being observed in GCB cells 1-month post infection [Flaño et al. \(2002\)](#) and [Nealy et al. \(2010\)](#).

In experiments done with LC30 and CAR Balb/c mice in the later part of the project, when comparing recombinant MHV68-LMP2a and MHV68-NGFR in chronic infections of 2 months, percentages of GCB cells observed were at very low levels in comparison to that of 14 days post infection although viral genomic loads were at low undetectable levels. Levels of latency in the spleen have been shown to decrease by 3 to 4 weeks, with the bulk of the latency shifting to other cell populations such as in the memory cells or B1 cells [Willer & Speck \(2003\)](#) and [Rekow et al. \(2016\)](#).

Plasma cells, being sites of latency of all gHVs, showed elevated amounts in experiments conducted. The percentages of plasma cells in the spleens were higher and peaked at 14 days post infection for both virus infected mice. Liang and colleagues showed that gHVs driven plasma cell differentiation helps to regulate virus reactivation from latency and that majority of the cells that were reactivated were in fact, plasma cells [Liang et al. \(2009\)](#). Similar to this finding, we have shown that reactivation from latency was highest at 14 days post infection and this corresponded to the time point where the highest percentages of plasma cell differentiation also occurred.

## 6.3 INFECTION OF MHV68-LMP2A AND MHV68-NGFR IN CAR AND LC30 MICE

### 6.3.1 LOWER VIRAL GENOMIC LOAD LEVELS OF RECOMBINANT VIRUS COULD LIMIT EFFECTS STUDIED IN CHRONIC INFECTIONS

A major question for this project was in deciphering the effects of LMP2a protein when coupled to a constitutive CD30 signalling in vivo. The gHV EBV is able to transform normal human B cells eventually leading to lymphomas and cancer. EBV can undergo various different latency programs in which expression of different combinations of EBV viral proteins may determine the type of cancer or lymphoma that develops [Thorley-Lawson \(2005\)](#), [Price & Luftig \(2015\)](#) and [Thompson & Kurzrock \(2004\)](#). One such viral protein is that of the Latent Membrane Protein 2a (LMP2a) which mimics a constitutively active BCR signal, thus enabling LCL growth even if functional BCRs are lacking.

Furthermore, the BCR is essential for normal B cell development and many studies have shown that the signalling has been implicated in tumor formation [Niemann et al. \(2013\)](#). In order to investigate the effects of the EBV viral protein LMP2a, the gene segment was cloned into a murine gHV, the MHV68. This model as mentioned earlier, enables the investigation of the LMP2a gene and protein expression in vivo. LMP2a has been suggested to play a role mainly in activation, proliferation and survival of infected B cells early in in vitro infection however LMP2a does not influence the long term growth of immortalized cell lines [Wasil et al. \(2013\)](#). Results from our experiments showed that in chronic infections of 2 months, no significant differences were observed between the recombinant MHV68-LMP2a and the control MHV68-NGFR used. Furthermore, from viral genomic loads measured, the amount of viral load present as well as the reactivation from latency of the virus in splenocytes were at undetectable levels implying that much of the virus had been eliminated after two months. This could have caused the minimal effects of LMP2a during chronic infections in the experiments conducted.

### 6.3.2 LMP2A LEADS TO ENHANCED GCB CELL FORMATION AND PROLIFERATION

In the experiments conducted, MHV68-LMP2a infected mice displayed higher percentages of GCB cells compared to the control MHV68-NGFR. Thus, LMP2a expressed in the splenocytes and cervical lymph nodes drives proliferation of the GCB cells during the GC reaction. This is a key step in the formation of lymphomas because the GC is a structure within the follicle which is responsible and important for B cell differentiation into long lived plasma cells and memory cells [Fish & Longnecker \(2017\)](#). Several studies have also shown that LMP2a is able to accelerate tumorigenesis only in the presence of a second signal such as that of the c-MYC oncogene [Bultema et al. \(2009\)](#) and [Bieging et al. \(2009\)](#). Furthermore, for the case of EBV, which has various different latency programmes as mentioned earlier, it is the combination and different timing of the protein expressions that is important in development of different lymphomas [Price & Luftig \(2015\)](#). Nonetheless, we have shown that LMP2a expression did lead to proliferation of GCB cells which could play a role in the formation of lymphomas and tumors because most lymphomas occur in the GC and post GC reactions, where mutations are highly likely.

### 6.3.3 REPORTER POSITIVE CELLS REPRESENT CELLS THAT ORIGINATE FROM THE GCB CELL REACTION

In our experiments, LMP1/CD30  $\gamma 1$ cre mice as mentioned in [1.6](#) were used to produce mice that when immunized or infected, led to the constitutive signalling of the CD30. The cre recombinase segment is positioned on an immunoglobulin heavy chain constant region gene segment that is transcribed only in GCB cells [Casola et al. \(2006\)](#). Upon viral infection, the Cre recombinase protein

is expressed in GC cells resulting in deletion of the stop cassette upstream of the LMP1/CD30 gene. This leads to the expression of the LMP1/CD30 (LC30) gene together with the reporter gene hCD2 in LC30 mice and expression of the reporter gene CAR in CAR mice. Thus, a certain fraction of GC cells express the reporter gene. Most of the reporter positive non-GC cells stem most likely from cells that left the GC. Hence, if cells have a plasma cell phenotype but are still reporter positive, it suggests that these cells initially stemmed from the GC and differentiated to become the plasma cells. By looking in terms of reporter positive cells, an idea about where the origins of these cell can be made and hence enables us to indirectly track the different fates of the GCB under factors such as CD30 signalling.

Thus from data collected, even though percentages of B cells, T cells, plasma cells and memory cells did not significantly differ when compared between the two recombinant viruses used, differences were observed when dwelling into reporter positive cell results.

#### 6.3.4 CD30 DYSREGULATION IN LYMPHOMA DEVELOPMENT

In our experiments, it was seen that there were higher percentages of reporter positive cells within B cells in virus infected LC30 mice in comparison to virus infected CAR mice meaning to say that LMP1/CD30 had caused an expansion of B cells. Furthermore, in the GC an opposite result was obtained in which much lower percentages of reporter positive cells within GCB cells were observed. B cells that expressed LMP1/CD30 left the GC, thus contributing to higher percentages of reporter positive cells within B1a cells (at 2 months post infection), B1b cells and plasma cells in spleens, as well as B1a and B1b cells in the peritoneal cavity. Thus, constitutive CD30 signalling drives the differentiation of GCB cells to other non-GC cells. Interestingly, the constitutive CD30 signal led to a slower recovery from splenomegaly after 2 months infection, when compared with CAR mice. After viral infection, splenomegaly was present in all infected mice at 14 days post infection and this splenomegaly was attributed to the expansion of B cells and T cells. By 2 months post infection this splenomegaly was decreased in all mice but the rate of decrease was delayed in LC30 mice. Thus, CD30 here may have played a role in slowing down the rate of apoptosis and by increasing survival of these activated and proliferated cells. By slowing down the process of apoptosis through chronic infections, lymphomas may develop later when further mutations occur, such as in the GC reaction, or elsewhere, since tumor formation occurs through a process of many different mutations. For example, for the case of the CD30+ diffuse large B-cell lymphoma, certain STAT3 mutations have been found to occur simultaneously with CD30 expression [Ohgami et al. \(2014\)](#), and even in CD30+ anaplastic large cell B lymphoma, where somatic mutations occur in the IgH V gene regions [Kuze et al. \(1998\)](#). The higher percentages of reporter positive B cells in LC30 mice in comparison to controls suggests that constitutive CD30 signalling plays a role in tumorigenesis.

### 6.3.5 CONSTITUTIVE CD30 SIGNAL LEADS TO LARGER DIFFERENTIATION OF GCB CELLS TO B1 CELLS, ESPECIALLY THAT OF B1b IN PERITONEAL CAVITY, AS WELL AS PLASMA CELLS.

B1 cells are a subset of B cells that is found mainly in the peritoneal cavity. A small percentage is found in the spleens. They are already present in newborns and hence play a part in the innate and natural immunity rather than the adaptive immunity and may be divided into B1a and B1b cells [Graf et al. \(2019\)](#). B1 cell origins have been a matter of debate whether they are truly innate or may have developed from B2 cells through selection [Hardy \(2006\)](#). It was also discovered that gHVs establish latency not only in GCB or plasma cells but also in B1b cells found in the peritoneal cavity [Rekow et al. \(2016\)](#). This raises a suggestion that latency could have first developed in the GCB cells or plasma cells. These GCB cells or plasma cells later then differentiate or migrate into the peritoneal cavity as B1b cells. From our studies, we have shown that constitutive CD30 signalling in virus infected mice led to increased expansion of reporter positive B1 cells both in spleens and peritoneal cavity signifying that majority of these B1 cells originated from GCB cells. Furthermore, when looking in terms of the percentages of B1 cells that made up the fraction of reporter positive cells, higher percentages were found in LC30 mice indicating that the LMP1/CD30 expression leads to the expansion of B1 cells. Both in the spleen and in the peritoneal cavity, the percentage of B1b cells that made up the fraction of reporter positive cells was much higher in LC30 mice. These reporter positive cells stemmed from B1 cells, that have had their STOP cassette removed, thus proliferating as soon as they expressed the LMP1/CD30. This possible differentiation of GCB cells to B1 cells thus implies that the origins of B1 cells could be that of the GCB cells, as observed from our reporter positive cell studies, although it has been described that STOP cassette deletions in the  $\gamma$  cre mice did also occur not only in GCB cells, but in B1 cells but at very low percentages (lower than 1%) [Casola et al. \(2006\)](#). This implies that reporter positive B1 cells could have been cells that also originated from the B1 cell subset and not entirely from GCB cells. Despite this, it is unlikely that all the reporter positive B1 cells originated from the B1 due to extremely low STOP cassette deletions as mentioned by Casola and colleagues.

In summary, it can be said that the B1b cells in the peritoneal cavity arose as a result of migration from outside the peritoneal cavity from GCB cells or from B2 cells within the peritoneal cavity as described by Hardy [Hardy \(2006\)](#). Like that of the CD30+ primary effusion lymphoma (PEL), constitutive CD30 signalling here could play a role in driving differentiation of cells to B1 cells or B1-like cells as described [Sanchez-Martin et al. \(2017\)](#). Another possibility is that since the GC is the site of many mutations, a particular hypermutation could have occurred, causing the BCR to be polyreactive causing the GCB to differentiate to B1 cells thus giving them a B1-like phenotype. This dwells into the fact that the BCR plays a role in the differentiation of B cells into their various different

fates, one of them that of B1 cells [Hardy \(2006\)](#), [Graf et al. \(2019\)](#) and [Yam-Puc et al. \(2018\)](#).

When looking in terms of the plasma cells in spleens, although the percentage of the plasma cells that made up the fraction of reporter positive cells was not as high as that of the B1 cells, constitutive CD30 signalling led to larger percentages of plasma cells within the reporter positive cells compared to CAR mice. Thus, constitutive CD30 signalling led to increased plasma cell differentiation from the GCB cells, or increased proliferation of plasmablasts resulting in more plasma cells. A reversed pattern was observed in IgG1 memory cells, with percentage of the memory cells that make up the fraction of reporter positive cells being lower in LC30 mice than CAR mice. Hence, differentiation to plasma cells was favoured rather than differentiation to IgG1 memory cells.

In reaching plasma cells, the GCB cells undergo various stages that have been described as pre-plasmablasts and plasmablasts [Jourdan et al. \(2011\)](#). These cells, though short lived, undergo rapid proliferation [Sze et al. \(2000\)](#). These plasmablasts may in turn end up proliferating to produce a certain lymphomas the PEL, which is also a form of CD30+ B cell lymphoma [Küppers \(2005\)](#). Thus, our experiments give further evidence that a constitutive CD30 signalling may lead to the formation of lymphomas.

### 6.3.6 CONSTITUTIVE CD30 SIGNAL BLOCKS THE GC REACTION.

In our study, percentages of GCB cells were extremely low in LC30 mice only at chronic infections of 2 months in comparison to those of CAR mice. These percentages were also lower when compared to non-infected LC30 control mice. Not only that, but when looking in terms of reporter positive GCB cells, having the LC30 genotype also led to lower percentages of reporter positive GCB cells indicating that not all deletions occurred in the GCB cells but also elsewhere (as mentioned earlier, less than 1% did occur in B1 cells) or that LMP1/CD30 expression forced GCB cells to leave the GC thus losing their GC phenotype. Going into chronic infections of 2 months, the percentage of reporter positive GCB cells increased despite the decrease in the percentage of total GCB cells observed. In other words, GCB cells in LC30 mice that have undergone deletions of the STOP cassette, leading to constitutive CD30 signalling, leave the GC reaction and are unable to re-enter or undergo clonal expansion as GCB cells. Instead, they differentiate to other cell fates as observed from the decrease in percentage GCB cells within the fraction of reporter positive cells moving from 14 days to 2 months post infection. With low deletions occurring in LC30 mice at 14 days post infection, many GCB cells not stained as reporter positive were still present enabling them to re-enter the GC and undergo clonal expansion unlike the reporter positive GCB cells. Up to the point of chronic infections of 2 months, these GCB cells that were not reporter positive are now able to undergo deletion of the STOP cassette at some point, thus, giving rise to the increase in reporter positive GCB cells despite the drop in total percentages of GCB cells at 2 months.

This suggests that LC30 expression in the GCB cells blocks the GC reaction leading to a decreased proliferation. Studies have shown that CD30 did prevent the development of the GC [Fiedler \(2011\)](#) and in certain cases, disruption of secondary antibody production occurred in CD30 deficient mice [Gaspal et al. \(2005\)](#) and [Kennedy et al. \(2006\)](#).

# 7

## CONCLUSION & OUTLOOK

Many studies have focused on the role of LMP2a and CD30 dysregulation on tumorigenesis separately. Thus, in this project, we aimed to combine the effects of LMP2a expression and a dysregulated CD30 signalling (constitutive active) in GCB cells to see if the process of lymphoma formation and tumorigenesis is accelerated. However, from observations made, several problems arose that made it difficult for us to bring up a clear relationship, when the two effects were combined.

For these experiments, the PCMV (promoter of human cytomegalovirus) was used as a promoter for the transcription and expression of LMP2a. The PCMV was chosen in these experiments because the expression levels of the transgene, driven by this promoter, are maintained more stably during long-term cell cultures [Wang et al. \(2017\)](#). Despite this, it has been shown that expression level of the transgene of the PCMV decreases with extended times in culture due to transcriptional silencing [Hsu et al. \(2010\)](#). In choosing a promoter, it is important to select a promoter that enables both high expression levels and long-term stability. Several other promoters have been investigated that could be used for future experiments. For example, the Simian virus 40 (SV40), could be a possible candidate because despite having lower expression yield, proteins expressed are of higher stability than that of the PCMV. Combination with other cis-acting or enhancer elements could be introduced to further enhance the effects of the promoters and in the case of

SV40, when combined with MAR (matrix attachment region) elements, enabled high expression levels of protein of good stability [Hsu et al. \(2010\)](#). Nonetheless, many more studies would need to be done to characterise the different possible promoters used to determine which would be the most suitable.

The cloning of LMP2a into the MHV68 genome made it possible to introduce LMP2a in vitro in cells and in vivo in mice. Recombinant MHV68-LMP2a when tested, did not differ significantly from that of the MHV68-WT in terms of pathogenic properties such as lytic replication as well as virus growth in vitro. The only aspect was that, in vivo, the recombinant MHV68-LMP2a was eliminated at a higher rate compared to that of the MHV68-WT as observed from viral genomic loads measured. This is not surprising as several studies within our group, with other recombinant MHV68, gave a similar result. Thus, when infecting LC30 mice with the recombinant MHV68-LMP2a as well as another recombinant, MHV68-NGFR as the control, most of the effects seen were mainly due to the constitutive CD30 signalling. By chronic infection of 2 months, viral genomic loads were at low undetectable levels despite splenomegaly still being observed in the infected mice. This suggests that there were still very low levels of virus latently existing in the splenocytes.

Furthermore, staining the spleen slices to detect for the presence of LMP2a protein, as well as intracellular FACS staining of cells did not give rise to positive results indicating that LMP2a expression was minimal. This could be coupled to the fact that very little virus was present and even more, during the process of latency in the spleen, LMP2a expression was suppressed. Thus, in order to address the effects of LMP2a, perhaps another model could be used to justify certain claims that have been made in this project. The LMP2a gene could be cloned in the same way as the LMP1/CD30 genome on the Rosa26 site so that in the presence of immunization or infection, expression of the LMP2a with CD30, together with a reporter sequence downstream for easy detection, would occur indefinitely. This method that makes use of conditional expression of LMP2a as well as that of this project's CD30 constitutive expression, would eliminate the limitations of viral elimination in vivo. [Minamitani et. al.](#) did develop transgenic LMP1 and LMP2a mice as models that enabled conditional GCB cell LMP1 and LMP2a coexpression to decipher the effects that these two proteins had on each other. [Vrazo et. al](#) also managed to develop transgenic LMP1/2a mice from crossing LMP1 and LMP2a single transgenic mice [Vrazo et al. \(2012\)](#).

Other than this, since the formation of lymphoma has been described in immunocompetent mice, the effects of a dysregulated CD30 together with MHV68-LMP2a could be repeated in immunocompromised mice, such as knock out T and NK cell mice [Minamitani et al. \(2017\)](#). In doing so, elimination of the MHV68-LMP2a would also be reduced since T and NK cells play a huge role in the elimination of gHVs from the host. Another factor to consider is that lymphoma formation has been observed in longer time frames, so allowing infection for longer time periods from six months

to a year would enable the formation of lymphomas and tumors to be followed and better investigated. Next, in order to strengthen the results and conclusions obtained from this project, the *in vivo* experiments could be repeated with a greater sample size of CAR and LC30 mice for both the control and recombinant virus groups.

Lastly, various groups have made use of another recombinant virus, that of the MHV68-YFP where a yellow fluorescent protein gene is cloned into the MHV68 genome, the same way that the LMP2a gene was cloned [Collins & Speck \(2012\)](#). With this new recombinant virus introduced as a control virus in CD30 dysregulation studies, *in vivo*, additional questions regarding latency and phenotypic analysis of cell populations that are infected can be answered with respect to long term chronic infection experiments. With recombinant MHV68-YFP, it would be possible to track MHV68 infected cells and determine physical location of MHV68.

Nonetheless, we have shown that LMP2a with its role in mimicking a constitutive BCR signal, did play a role in the expansion of GCB cells. This could later lead to formation of lymphomas since in GC many mutations arise as a result of CSR and SHM. On the other hand, the constitutive dysregulated CD30 signal led to various prominent effects. Firstly, in the increased differentiation of GCB cells to plasma cells and the expansion of B1 cells. The constitutive CD30 signalling also led to a slowing down in the rate of decrease of splenomegaly suggesting that the rate of apoptosis was reduced and that cell survival was preserved. One other effect we observed was also LC30 genotype led to blocking of the GC reaction. All of these effects do play a role in lymphomagenesis but the combination of LMP2a expression and a constitutive dysregulated CD30 leading to accelerated tumorigenesis needs to be investigated in further studies.

# A

## RESTRICTION ENZYMES AND ADDITIONAL ENZYMES

Restriction enzymes and additional enzymes used, with their conditions are displayed in the **Table A.1** below.

Enzyme	Buffer	Temperature (°C)
AflIII	3	37
ApaLI	4	37
BamHI	2	37
BglIII	3	37
EcoRI	2	37
HindIII	2	37
HpaI	4	37
Klenow	dNTPs (2mmol)	30
Ligase T4	Buffer T4	16
MfeI	4	37
NdeI	Cut smart	37
PmlI	1	37
StuI	4	37
SacII	4	37
SspI	2	37
SfiI	2	50
SpeI	4	37
SmaI	4	25

Table A.1: List of restriction enzymes and other enzymes used with their conditions

## REFERENCES

Ackermann, M. (2006). Pathogenesis of gammaherpesvirus infections. *Veterinary microbiology*, 113(3-4), 211–222.

Adler, H., Messerle, M., & Koszinowski, U. H. (2001). Virus reconstituted from infectious bacterial artificial chromosome (bac)-cloned murine gammaherpesvirus 68 acquires wild-type properties in vivo only after excision of bac vector sequences. *Journal of Virology*, 75(12), 5692–5696.

Adler, H., Messerle, M., & Koszinowski, U. H. (2003). Cloning of herpesviral genomes as bacterial artificial chromosomes. *Reviews in Medical Virology*, 13(2), 111–121.

Adler, H., Messerle, M., Wagner, M., & Koszinowski, U. H. (2000). Cloning and mutagenesis of the murine gammaherpesvirus 68 genome as an infectious bacterial artificial chromosome. *Journal of Virology*, 74(15), 6964–6974.

Allman, D. & Pillai, S. (2008). Peripheral b cell subsets. *Current Opinion in Immunology*, 20(2), 149–157.

Alugupalli, K. R. & Gerstein, R. M. (2005). Divide and conquer: division of labor by b-1 b cells. *Immunity*, 23(1), 1–2.

Alugupalli, K. R., Leong, J. M., Woodland, R. T., Muramatsu, M., Honjo, T., & Gerstein, R. M. (2004). B1b lymphocytes confer t cell-independent long-lasting immunity. *Immunity*, 21(3), 379–390.

Arnon, T. I., Horton, R. M., Grigorova, I. L., & Cyster, J. G. (2012). Visualization of splenic marginal zone b-cell shuttling and follicular b-cell egress. *Nature*, 493(7434), 684–688.

Attanavanich, K. & Kearney, J. F. (2004). Marginal zone, but not follicular b cells, are potent activators of naive cd4 t cells. *The Journal of Immunology*, 172(2), 803–811.

Barton, E., Mandal, P., & Speck, S. H. (2011). Pathogenesis and host control of gammaherpesviruses: Lessons from the mouse. *Annual Review of Immunology*, 29(1), 351–397.

Bemark, M. (2015). Translating transitions—how to decipher peripheral human b cell development. *Journal of biomedical research*, 29(4), 264.

Bieging, K. T., Amick, A. C., & Longnecker, R. (2009). Epstein-barr virus Imp2a bypasses p53 inactivation in a myc model of lymphomagenesis. *Proceedings of the National Academy of Sciences*, 106(42), 17945–17950.

Bultema, R., Longnecker, R., & Swanson-Mungerson, M. (2009). Epsteinbarr virus Imp2a accelerates myc-induced lymphomagenesis. *Oncogene*, 28(11), 1471–1476.

Cancro, M. P. (2009). Signalling crosstalk in b cells: managing worth and need. *Nature Reviews Immunology*, 9(9), 657–661.

Cardin, R. D., Brooks, J. W., Sarawar, S. R., & Doherty, P. C. (1996). Progressive loss of cd8 t cell-mediated control of a gamma-herpesvirus in the absence of cd4 t cells. *Journal of Experimental Medicine*, 184(3), 863–871.

Carey, J. B., Moffatt-Blue, C. S., Watson, L. C., Gavin, A. L., & Feeney, A. J. (2008). Repertoire-based selection into the marginal zone compartment during b cell development. *Journal of Experimental Medicine*, 205(9), 2043–2052.

Casola, S., Cattoretti, G., Uyttersprot, N., Koralov, S. B., Seagal, J., Hao, Z., Waisman, A., Egert, A., Ghitza, D., & Rajewsky, K. (2006). Tracking germinal center b cells expressing germ-line immunoglobulin  $\gamma$ 1 transcripts by conditional gene targeting. *Proceedings of the National Academy of Sciences*, 103(19), 7396–7401.

Cerutti, A., Schaffer, A., Shah, S., Zan, H., Liou, H.-C., Goodwin, R. G., & Casali, P. (1998). Cd30 is a cd40-inducible molecule that negatively regulates cd40-mediated immunoglobulin class switching in non-antigen-selected human b cells. *Immunity*, 9(2), 247–256.

Chavez, J. C., Sahakian, E., & Pinilla-Ibarz, J. (2013). Ibrutinib: an evidence-based review of its potential in the treatment of advanced chronic lymphocytic leukemia. *Core evidence*, 8, 37.

Chen, Y., Rahemtullah, A., & Hochberg, E. (2007). Primary effusion lymphoma. *The Oncologist*, 12(5), 569–576.

Chen, Y., Sun, H., Liu, G., Wang, B., Wang, F., Sun, B., & Yao, K. (2009). Ebv Imp2a-specific t cell immune responses elicited by dendritic cells loaded with Imp2a protein. *Cellular Molecular Immunology*, 6(4), 269–276.

Chiarle, R., Podda, A., Prolla, G., Gong, J., Thorbecke, G., & Inghirami, G. (1999). Cd30 in normal and neoplastic cells. *Clinical Immunology*, 90(2), 157–164.

Collins, C. M. & Speck, S. H. (2012). Tracking murine gammaherpesvirus 68 infection of germinal center b cells in vivo. *PLoS ONE*, 7(3).

Evans, L. S. & Hancock, B. W. (2003). Non-hodgkin lymphoma. *The Lancet*, 362(9378), 139–146.

Fairfax, K. A., Kallies, A., Nutt, S. L., & Tarlinton, D. M. (2008). Plasma cell development: From b-cell subsets to long-term survival niches. *Seminars in Immunology*, 20(1), 49–58.

Feldman, E. R., Kara, M., Oko, L. M., Grau, K. R., Krueger, B. J., Zhang, J., Feng, P., Dyk, L. F. V., Renne, R., Tibbetts, S. A., & et al. (2016). A gammaherpesvirus noncoding rna is essential for hematogenous dissemination and establishment of peripheral latency. *mSphere*, 1(2).

Fiedler, P. (2011). *Die Expression von LMP1, LMP2A und CD30 in B-Zellen zur Analyse physiologischer und pathogener Effekte*. PhD thesis, Imu.

Fish, K. & Longnecker, R. (2017). Ebv germinates lymphoma from the germinal center in a battle with t and nk cells. *Proceedings of the National Academy of Sciences*, 114(18), 4571–4573.

Flaño, E., Kim, I.-J., Woodland, D. L., & Blackman, M. A. (2002).  $\gamma$ -herpesvirus latency is preferentially maintained in splenic germinal center and memory b cells. *The Journal of experimental medicine*, 196(10), 1363–1372.

Franzoso, G., Carlson, L., Poljak, L., Shores, E. W., Epstein, S., Leonardi, A., Grinberg, A., Tran, T., Scharton-Kersten, T., Anver, M., et al. (1998). Mice deficient in nuclear factor (nf)- $\kappa$ b/p52 present with defects in humoral responses, germinal center reactions, and splenic microarchitecture. *The Journal of experimental medicine*, 187(2), 147–159.

Gaspal, F. M. C., Kim, M.-Y., Mcconnell, F. M., Raykundalia, C., Bekiaris, V., & Lane, P. J. L. (2005). Mice deficient in ox40 and cd30 signals lack memory antibody responses because of deficient cd4 t cell memory. *The Journal of Immunology*, 174(7), 3891–3896.

Graf, R., Seagal, J., Otipoby, K. L., Lam, K.-P., Ayoub, S., Zhang, B., Sander, S., Chu, V. T., & Rajewsky, K. (2019). Bcr-dependent lineage plasticity in mature b cells. *Science*, 363(6428), 748–753.

Gredmark-Russ, S., Cheung, E. J., Isaacson, M. K., Ploegh, H. L., & Grotenbreg, G. M. (2008). The cd8 t-cell response against murine gammaherpesvirus 68 is directed toward a broad repertoire of epitopes from both early and late antigens. *Journal of Virology*, 82(24), 12205–12212.

Grywalska, E. & Rolinski, J. (2015). Epstein-barr virusassociated lymphomas. *Seminars in Oncology*, 42(2), 291–303.

Haas, K. M., Poe, J. C., Steeber, D. A., & Tedder, T. F. (2005). B-1a and b-1b cells exhibit distinct developmental requirements and have unique functional roles in innate and adaptive immunity to s. pneumoniae. *Immunity*, 23(1), 7–18.

Hardy, R. R. (2006). B-1 b cell development. *The Journal of Immunology*, 177(5), 2749–2754.

Hatton, O., Strauss-Albee, D. M., Zhao, N. Q., Haggadone, M. D., Pelpola, J. S., Krams, S. M., Martinez, O. M., & Blish, C. A. (2016). Nkg2a-expressing natural killer cells dominate the response to autologous lymphoblastoid cells infected with epstein-barr virus. *Frontiers in immunology*, 7, 607.

Hsu, C.-C., Li, H.-P., Hung, Y.-H., Leu, Y.-W., Wu, W.-H., Wang, F.-S., Lee, K.-D., Chang, P.-J., Wu, C.-S., Lu, Y.-J., & et al. (2010). Targeted methylation of cmv and e1a viral promoters. *Biochemical and Biophysical Research Communications*, 402(2), 228–234.

Hussain, A. R., Ahmed, S. O., Ahmed, M., Khan, O. S., Abdulmohsen, S. A., Plataniolas, L. C., Al-Kuraya, K. S., & Uddin, S. (2012). Cross-talk between nfkb and the pi3-kinase/akt pathway can be targeted in primary effusion lymphoma (pel) cell lines for efficient apoptosis. *PLoS ONE*, 7(6).

Jost, P. J. & Jurgen, R. (2006). Aberrant nf-b signaling in lymphoma: mechanisms, consequences, and therapeutic implications. *Blood*, 109(7), 2700–2707.

Jourdan, M., Caraux, A., Caron, G., Robert, N., Fiol, G., Rème, T., Bolloré, K., Vendrell, J.-P., Le Gal-Iou, S., Mourcin, F., et al. (2011). Characterization of a transitional preplasmablast population in the process of human b cell to plasma cell differentiation. *The Journal of Immunology*, 187(8), 3931–3941.

Kantor, A. (1993). Origin of murine b cell lineages. *Annual Review of Immunology*, 11(1), 501–538.

Kennedy, M. K., Willis, C. R., & Armitage, R. J. (2006). Deciphering cd30 ligand biology and its role in humoral immunity. *Immunology*, 118(2), 143–152.

Klein, U. & Dalla-Favera, R. (2008). Germinal centres: role in b-cell physiology and malignancy. *Nature Reviews Immunology*, 8(1), 22–33.

Knipe, D. M. & Howley, P. (2013). *Fields Virology; Chapter 61 EBV*, (pp. 1898–1954). Lippincott Williams & Wilkins.

Küppers, R. (2005). Mechanisms of b-cell lymphoma pathogenesis. *Nature Reviews Cancer*, 5(4), 251–262.

Küppers, R. (2009). The biology of hodgkin's lymphoma. *Nature Reviews Cancer*, 9(1), 15–27.

Küppers, R., Kanzler, H., Hansmann, M.-L., & Rajewsky, K. (1996). Immunoglobulin v genes in reed-sternberg cells. *The New England journal of medicine*, 334(6), 404–406.

Kuze, T., Nakamura, N., Hashimoto, Y., & Abe, M. (1998). Most of cd30 anaplastic large cell lymphoma of b cell type show a somatic mutation in the igh v region genes. *Leukemia*, 12(5), 753–757.

Lentz, V. M. & Manser, T. (2001). Cutting edge: Germinal centers can be induced in the absence of t cells. *The Journal of Immunology*, 167(1), 15–20.

Leval, L. D. & Gaulard, P. (2010). Cd30 lymphoproliferative disorders. *Haematologica*, 95(10), 1627–1630.

Liang, X., Collins, C. M., Mendel, J. B., Iwakoshi, N. N., & Speck, S. H. (2009). Gammaherpesvirus-driven plasma cell differentiation regulates virus reactivation from latently infected b lymphocytes. *PLoS Pathogens*, 5(11).

Lin, A. & Karin, M. (2003). Nf- $\kappa$ b in cancer: a marked target. *Seminars in Cancer Biology*, 13(2), 107–114.

Macias-Garcia, A., Heizmann, B., Sellars, M., Marchal, P., Dali, H., Pasquali, J.-L., Muller, S., Kastner, P., & Chan, S. (2016). Ikaros is a negative regulator of b1 cell development and function. *Journal of Biological Chemistry*, 291(17), 9073–9086.

Mack, A. A. & Sugden, B. (2008). Ebv is necessary for proliferation of dually infected primary effusion lymphoma cells. *Cancer Research*, 68(17), 6963–6968.

Madrid, L. V., Wang, C.-Y., Guttridge, D. C., Schottelius, A. J. G., Baldwin, A. S., & Mayo, M. W. (2000). Akt suppresses apoptosis by stimulating the transactivation potential of the rela/p65 sub-unit of nf- $\kappa$ b. *Molecular and Cellular Biology*, 20(5), 1626–1638.

Martin, F., Oliver, A. M., & Kearney, J. F. (2001). Marginal zone and b1 b cells unite in the early response against t-independent blood-borne particulate antigens. *Immunity*, 14(5), 617–629.

Mebius, R. E. & Kraal, G. (2005). Structure and function of the spleen. *Nature Reviews Immunology*, 5(8), 606–616.

Meffre, E. & Wardemann, H. (2008). B-cell tolerance checkpoints in health and autoimmunity. *Current Opinion in Immunology*, 20(6), 632–638.

Melchers, F. (2006). Anergic b cells caught in the act. *Immunity*, 25(6), 864–867.

Minamitani, T., Ma, Y., Zhou, H., Kida, H., Tsai, C.-Y., Obana, M., Okuzaki, D., Fujio, Y., Kumanogoh, A., Zhao, B., & et al. (2017). Mouse model of epsteinbarr virus lmp1- and lmp2a-driven germinal center b-cell lymphoproliferative disease. *Proceedings of the National Academy of Sciences*, 114(18), 4751–4756.

Münz, C. (2017). Humanized mouse models for epstein barr virus infection. *Current opinion in virology*, 25, 113–118.

Murphy, K., Weaver, C. T., Mowat, A., & Janeway, C. A. J. (2017). *Janeways immunobiology*. Garland Science.

Nealy, M. S., Coleman, C. B., Li, H., & Tibbetts, S. A. (2010). Use of a virus-encoded enzymatic marker reveals that a stable fraction of memory b cells expresses latency-associated nuclear antigen throughout chronic gammaherpesvirus infection. *Journal of virology*, 84(15), 7523–7534.

Niemann, U., C., Wiestner, & Adrian (2013). B-cell receptor signaling as a driver of lymphoma development and evolution. *Seminars in Cancer Biology*, 23(6A), 410–421.

Obukhanych, T. V. & Nussenzweig, M. C. (2006). T-independent type ii immune responses generate memory b cells. *Journal of Experimental Medicine*, 203(2), 305–310.

Ohgami, R. S., Ma, L., Monabati, A., Zehnder, J. L., & Arber, D. A. (2014). Stat3 mutations are present in aggressive b-cell lymphomas including a subset of diffuse large b-cell lymphomas with cd30 expression. *Haematologica*, 99(7), e105–e107.

Pillai, S. & Cariappa, A. (2009). The follicular versus marginal zone b lymphocyte cell fate decision. *Nature Reviews Immunology*, 9(11), 767–777.

Price, A. M. & Luftig, M. A. (2015). To be or not iib: A multi-step process for epstein-barr virus latency establishment and consequences for b cell tumorigenesis. *PLOS Pathogens*, 11(3), e1004656.

Rekow, M. M., Darrah, E. J., Mboko, W. P., Lange, P. T., & Tarakanova, V. L. (2016). Gammaherpesvirus targets peritoneal b-1 b cells for long-term latency. *Virology*, 492, 140–144.

Roth, D. B. (2014). V(d)j recombination: Mechanism, errors, and fidelity. *Microbiology spectrum*, 2(6).

Rowland, S. L., Leahy, K. F., Halverson, R., Torres, R. M., & Pelanda, R. (2010). Baff receptor signaling aids the differentiation of immature b cells into transitional b cells following tonic bcr signaling. *The Journal of Immunology*, 185(8), 4570–4581.

Sanchez-Martin, D., Uldrick, T. S., Kwak, H., Ohnuki, H., Polizzotto, M. N., Annunziata, C. M., Raffeld, M., Wyvill, K. M., Aleman, K., Wang, V., & et al. (2017). Evidence for a mesothelial origin of body cavity effusion lymphomas. *Journal of the National Cancer Institute*, 109(9).

Sasaki, Y., Derudder, E., Hobeika, E., Pelanda, R., Reth, M., Rajewsky, K., & Schmidt-Suprian, M. (2006). Canonical nf-b activity, dispensable for b cell development, replaces baff-receptor signals and promotes b cell proliferation upon activation. *Immunity*, 24(6), 729–739.

Scanlon, S. T. (2019). B1 or b2? the bcr decides. *Science*, 363(6428), 703.

Schneider, C. & Hübinger, G. (2002). Pleiotropic signal transduction mediated by human cd30: A member of the tumor necrosis factor receptor (tnfr) family. *Leukemia amp; Lymphoma*, 43(7), 1355–1366.

Senftleben, U. (2001). Activation by ikkalpha of a second, evolutionary conserved, nf-kappa b signaling pathway. *Science*, 293(5534), 1495–1499.

Sha, W. C., Liou, H.-C., Tuomanen, E. I., & Baltimore, D. (1995). Targeted disruption of the p50 subunit of nf- $\kappa$ b leads to multifocal defects in immune responses. *Cell*, 80(2), 321–330.

Silva, S. R. D. & Oliveira, D. E. D. (2011). Hiv, ebv and kshv: Viral cooperation in the pathogenesis of human malignancies. *Cancer Letters*, 305(2), 175–185.

Simas, J. P. & Efthathiou, S. (1998). Murine gammaherpesvirus 68: a model for the study of gamma-herpesvirus pathogenesis. *Trends in Microbiology*, 6, 276–282.

Sohn, D.-H., Sohn, H.-J., Lee, H.-J., Lee, S.-D., Kim, S., Hyun, S.-J., Cho, H.-I., Cho, S.-G., Lee, S.-K., Kim, T.-G., & et al. (2015). Measurement of cd8 and cd4 t cell frequencies specific for ebv lmp1 and lmp2a using mrna-transfected dcs. *PLoS one*, 10(5), e0127899.

Sotomayor, E. M., Young, K. H., & Younes, A. (2014). Clinical roundtable monograph: Cd30 in lymphoma: its role in biology, diagnostic testing, and targeted therapy. *Clinical advances in hematology and oncology*, 12(4 Suppl 10), 1–22.

Sperling, S., Fiedler, P., Lechner, M., Pollithy, A., Ehrenberg, S., Schiefer, A.-I., Kenner, L., Feuchtinger, A., Kühn, R., Swinerd, G., et al. (2019). Chronic cd30 signaling in b cells results in lymphomagenesis by driving the expansion of plasmablasts and b1 cells. *Blood, The Journal of the American Society of Hematology*, 133(24), 2597–2609.

Srivastava, B., Lindsley, R. C., Nikbakht, N., & Allman, D. (2005). Models for peripheral b cell development and homeostasis. *Seminars in Immunology*, 17(3), 175–182.

Stevenson, Belz, G., Altman, J., & Doherty (1999). Changing patterns of dominance in the cd8+ t cell response during acute and persistent murine gamma-herpesvirus infection. *European Journal of Immunology*, 29(4), 1059–1067.

Suárez, A. L. & van Dyk, L. F. (2008). Endothelial cells support persistent gammaherpesvirus 68 infection. *PLoS pathogens*, 4(9), e1000152.

Sunil-Chandra, N. P., Arno, J., Fazakerley, J., & Nash, A. A. (1994). Lymphoproliferative disease in mice infected with murine gammaherpesvirus 68. *The American journal of pathology*, 145(4), 818–826.

Sunil-Chandra, N. P., Efstathiou, S., Arno, J., & Nash, A. A. (1992). Virological and pathological features of mice infected with murine gammaherpesvirus 68. *Journal of General Virology*, 73(9), 2347–2356.

Sze, D. M.-Y., Toellner, K.-M., Vinuesa, C. G. D., Taylor, D. R., & Maclennan, I. C. (2000). Intrinsic constraint on plasmablast growth and extrinsic limits of plasma cell survival. *The Journal of Experimental Medicine*, 192(6), 813–822.

Taylor, G. S. & Blackbourn, D. J. (2011). Infectious agents in human cancers: Lessons in immunity and immunomodulation from gammaherpesviruses ebv and kshv. *Cancer Letters*, 305(2), 263–278.

Thompson, M. P. & Kurzrock, R. (2004). Epstein-barr virus and cancer. *Clinical Cancer Research*, 10(3), 803–821.

Thorley-Lawson, D. A. (2005). Ebv the prototypical human tumor virus just how bad is it? *Journal of Allergy and Clinical Immunology*, 116(2), 251–261.

Usherwood, E. J., Stewart, J. P., Robertson, K., Allen, D. J., & Nash, A. A. (1996). Absence of splenic latency in murine gammaherpesvirus 68-infected b cell-deficient mice. *Journal of General Virology*, 77(11), 28192825.

Virgin, H. W., Latreille, P., Wamsley, P., Hallsworth, K., Weck, K. E., Canto, A. J. D., & Speck, S. H. (1997). Complete sequence and genomic analysis of murine gammaherpesvirus 68. *Journal of virology*, 71(8), 5894–5904.

Vrazo, A. C., Chauchard, M., Raab-Traub, N., & Longnecker, R. (2012). Epstein-barr virus Imp2a reduces hyperactivation induced by Imp1 to restore normal b cell phenotype in transgenic mice. *PLoS Pathogens*, 8(4), e1002662.

Wang, W., Jia, Y.-L., Li, Y.-C., Jing, C.-Q., Guo, X., Shang, X.-F., Zhao, C.-P., & Wang, T.-Y. (2017). Retracted article: Impact of different promoters, promoter mutation, and an enhancer on recombinant protein expression in cho cells. *Scientific Reports*, 7(1), 10416.

Wardemann, H. (2003). Predominant autoantibody production by early human b cell precursors. *Science*, 301(5638), 1374–1377.

Wasil, L. R., Tomaszewski, M. J., Hoji, A., & Rowe, D. T. (2013). The effect of epstein-barr virus latent membrane protein 2 expression on the kinetics of early b cell infection. *PLOS ONE*, 8(1), e54010.

Willer, D. O. & Speck, S. H. (2003). Long-term latent murine gammaherpesvirus 68 infection is preferentially found within the surface immunoglobulin d-negative subset of splenic b cells in vivo. *Journal of virology*, 77(15), 8310–8321.

Wirtz, T., Weber, T., Kracker, S., Sommermann, T., Rajewsky, K., & Yasuda, T. (2016). Mouse model for acute epstein-barr virus infection. *Proceedings of the National Academy of Sciences of the United States of America*, 13(48), 13821–13826.

Woyach, J. A., Johnson, A. J., & Byrd, J. C. (2012). The b-cell receptor signaling pathway as a therapeutic target in cll. *Blood*, 120(6), 1175–1184.

Yam-Puc, J. C., Zhang, L., Zhang, Y., & Toellner, K.-M. (2018). Role of b-cell receptors for b-cell development and antigen-induced differentiation. *F1000Research*, 7, 429.



## Eidesstattliche Versicherung

---

Name, Vorname

Ich erkläre hiermit an Eides statt,  
dass ich die vorliegende Dissertation mit dem Titel

selbständig verfasst, mich außer der angegebenen keiner weiteren Hilfsmittel bedient und alle Erkenntnisse, die aus dem Schrifttum ganz oder annähernd übernommen sind, als solche kenntlich gemacht und nach ihrer Herkunft unter Bezeichnung der Fundstelle einzeln nachgewiesen habe.

Ich erkläre des Weiteren, dass die hier vorgelegte Dissertation nicht in gleicher oder in ähnlicher Form bei einer anderen Stelle zur Erlangung eines akademischen Grades eingereicht wurde.

Chew, Zakir Hassan

---

Ort, Datum

---

Unterschrift Doktorandin bzw. Doktorand